THE UNIVERSITY *of* EDINBURGH

The Role of Filaggrin in Skin Barrier Function and Atopic Dermatitis

Roland Poh Cheong Chu

Thesis submitted for the Degree of Doctor of Philosophy

The University of Edinburgh

2011

To Tammy and my parents

Declaration

I declare that the work presented in this thesis is the result of my own work unless otherwise stated. This work has also not been previously submitted, in whole or in part, for any other degree or personal qualification.

Roland Poh Cheong Chu

Acknowledgements

First and foremost, I would like to thank Dr Richard Weller (Department of Dermatology) and Dr Perdita Barran (School of Chemistry), both at the University of Edinburgh, for their supervision, patience and invaluable help during my PhD studies. Their guidance and support have been vital to the very completion of this thesis.

I would also like to thank Professor Sarah Howie, Dr Simon Brown and Dr Paul Fitch at the Queen's Medical Research Institute (University of Edinburgh) for their assistance in developing a novel filaggrin ELISA system. I am also very grateful to Dr Martin Wear and his team at the Edinburgh Protein Production Facility, who have been instrumental in helping me refine the purification of filaggrin using HPLC techniques. I am also indebted to Mr Mark Butterworth who kindly allowed me to approach his surgical patients to obtain skin tissues for filaggrin extraction. Dr Logan MacKay and the team at SIRCAMS (School of Chemistry, University of Edinburgh) have provided invaluable help and guidance in the structural study in this thesis. In particular, I am truly grateful to Dr Stefan Weidt at SIRCAMS for his indispensible help in the HCT experiments. I am also indebted to Dr Sharizan Ghaffar, Dr Lit Hiang Lee and Dr Nayani Madarasingha for their help in the functional study in this thesis. Dr Sharizan Ghaffar was very much involved in every aspect of that study and for that I am truly grateful. I would also like to thank Professor Irwin McLean and his team at the University of Dundee, who not only genotyped my study subjects but have also been generous with their advice and support. Finally, everyone in the Barran research group has my gratitude for welcoming me into their midst and patiently taught me about mass spectrometry.

The Medical Research Council has funded this PhD study, for which I am truly grateful.

Abstract

Loss-of-function mutations in the filaggrin gene (*FLG*) have recently been shown to be strongly associated with atopic dermatitis (AD). The overall aim of this study was to explore the role of filaggrin in skin barrier function and AD.

There were two main focuses in this study. The first was a functional study whose primary objective was to determine if *FLG* mutations correlated with skin barrier dysfunction in AD. Fifty-five mild to moderate AD individuals were recruited, genotyped and had their skin barrier assessed using three different measures - transepidermal water loss (TEWL), skin capacitance and the number of tape strips required to abrogate skin barrier. A secondary aim of this functional study was to test the hypothesis that corneocytes were less adherent to one another in filaggrin-related AD compared to wild-type AD skin.

The second main focus of this thesis was a structural study aimed at interrogating the structure-function relationship of filaggrin. Filaggrin protein was extracted and purified from a total of 21 AD and non-AD subjects and analysed using mass spectrometric techniques. Specifically, matrix assisted laser desorption/ionisation time-of-flight (MALDI-TOF) mass spectrometry (MS) and nano liquid chromatography tandem MS (LC-MS/MS) were utilised. Part of this structural study also involved developing and optimising the extraction and purification of filaggrin protein, including a novel way of extracting filaggrin from skin using tape stripping. In addition, a novel filaggrin-specific enzyme-linked immunosorbant assay (ELISA) was also developed, which could serve as a useful screening test for the protein.

In this study, *FLG* mutations were found to correlate with higher TEWL and fewer number of tape strips required to abrogate skin barrier, but not with skin capacitance. *FLG* mutations were also not shown to correlate with AD severity. The mean amount of protein extracted from filaggrin-related AD skin

was also significantly higher compared to wild-type AD skin, supporting the hypothesis that corneocytes were less adherent to one another (and therefore, densely packed) in filaggrin-related AD skin. MS analysis of filaggrin confirmed the heterogeneic nature of filaggrin protein, even within a single individual. Interestingly, this structural study also showed that filaggrin was only minimally expressed in the skin of all the AD individuals studied, whether or not they possessed any *FLG* mutation. Due to the limited amount of filaggrin extracted from AD skin, it was not possible to conduct comparative structural analysis between filaggrin from AD and non-AD skin.

Table of Contents

List of Figures

List of Tables

Abbreviations

3D	3-dimensional
Å	Angstrom (1 Å = 1 x 10^{-10} metre)
AA	Alopecia areata
ACHC	α-cyano-4-hydroxycinnamic acid
AD	Atopic dermatitis
API	Atmospheric pressure ionisation
BCA	Bicinchoninic acid
BSA	Bovine serum albumin
C-terminal	Carboxyl-terminal
CE	Cornified cell envelope
CI	Chemical ionisation
CID	Collision-induced dissociation
cm	Centimetre
CV	Column volume
^{o}C	Degrees Centigrade
Da	Dalton
DHB	2,5-dihydroxybenzoic acid
DTT	Dithiothreitol
EDC	Epidermal differentiation complex
EDTA	Ethylenediaminetetraacetic acid
EI	Electron impact ionisation
EIA	Enzyme immunoassay
ELISA	Enzyme-linked immunosorbant assay
ESI	Electrospray ionisation
FLG	Filaggrin gene
g	Gram
g	Standard gravity
GaF	Goat anti-filaggrin antibody
h	Hour
HCT	High capacity trap
HPLC	High-pressure liquid chromatography
HRP	Horseradish peroxidase
i.d.	Internal diameter
IV	Ichthyosis vulgaris
K	Lysine amino acid
kDa	Kilo dalton
L	Litre
LC	Liquid chromatography
LC-MS/MS	Liquid chromatography tandem mass spectrometry
LDI	Laser/desorption ionisation
LOD	Logarithm of the odds (to the base of 10)
M	Molar
µl	Microlitre

µg	Microgram
µm	Micrometre
MaF	Mouse anti-filaggrin antibody
MALDI	Matrix assisted laser desorption/ionisation
min	Minute
ml	Millilitre
mg	Milligram
MGF	Mascot Generic Format
mm	Millimetre
mM	Millimolar
MOPS	3-(N-morpholino)propanesulfonic acid
MS	Mass spectrometry
MS/MS	Tandem mass spectrometry
m/z	Mass to charge ratio
N	Normal
N-terminal	Amino-terminal
NaCl	Sodium chloride
Nd:YAG	Neodymium:yttrium aluminium garnet
nESI	Nanoelectrospray ionisation
ng	Nanogram
nm	Nanometre
o.d.	Outer diameter
OD	Optical density
PADs	Peptidylarginine deiminases
PCR	Polymerase chain reaction
pg	Picogram
PMF	Peptide mass fingerprinting
PMSF	Phenylmethylsulfonyl fluoride
pI	Isoelectric point
PPase	Protein phosphatase
PVDF	Polyvinyl difluoride
R	Arginine amino acid
RaF	Rabbit anti-filaggrin antibody
RF	Radio frequency
rpm	Revolutions per minute
s	Second
SC	Stratum corneum
SDS	Sodium dodecyl sulfate
SDS-PAGE	SDS-polyacrylamide gel electrophoresis
SDTB	Semi-dry transfer buffer
STS	Steroid sulfatase gene
TBS	Tris buffered saline
TBST	0.05 % (v/v) Tween 20 in TBS
TEWL	Transepidermal water loss
T_H2	Type 2 helper T cells
TMB	3,3,5 tetramethylbenzidine

TOF	Time-of-flight
UV	Ultraviolet
V	Volt
V_t	Total bed volume (= the total volume of an LC column)
XLI	X-linked ichthyosis

Chapter 1 Introduction

1.0 INTRODUCTION

The skin is one of the largest organs in the human body, and serves multiple functions. As it is the main interface between an individual and the environment, its primary role is that of a protective barrier between the environment and the internal milieu, minimising water loss outwards (inside-outside barrier) while preventing entry of allergens, irritants and pathogens (outside-inside barrier). During terminal differentiation, the keratinocytes (the predominant cell type of the epidermis) undergo a series of well-defined morphological and biochemical changes during which actively dividing basal cells differentiate through the spinous and granular cell layers to eventually form the uppermost (cornified) layer of the epidermis, or stratum corneum (SC) [1]. This layer consists of anucleated squame cells, and together with lipid-enriched intercellular domain, form the main permeability barrier of the skin. (Figure 1.1)

Diseases of the skin are very common, with atopic dermatitis (AD) being one of the commonest in developed countries. AD is a chronic skin disease characterised by pruritus and inflammation. It affects up to 20 % of children and up to 10 % of adults [2] and therefore represents an enormous burden on health care, particularly when its prevalence appears to be increasing in recent decades [3].

The predisposition of AD is known to be highly heritable, as evidenced by twin studies showing concordance rates of 0.72-0.86 for monozygotic versus 0.21-0.23 for dizygotic twins [4-7]. AD, as well as the other features of atopy, also shows clustering within families [8]. Genome-wide association studies have identified several hot spots, but due to poor replication of these studies, it is believed that a complex interplay for different genes and environmental stimuli underlies the disease [9]. Nonetheless, Cookson *et al* identified statistically significant genetic linkage with polymorphic markers within the epidermal

differentiation complex (EDC) on chromosome 1q21 [10], where the *FLG* gene is located.

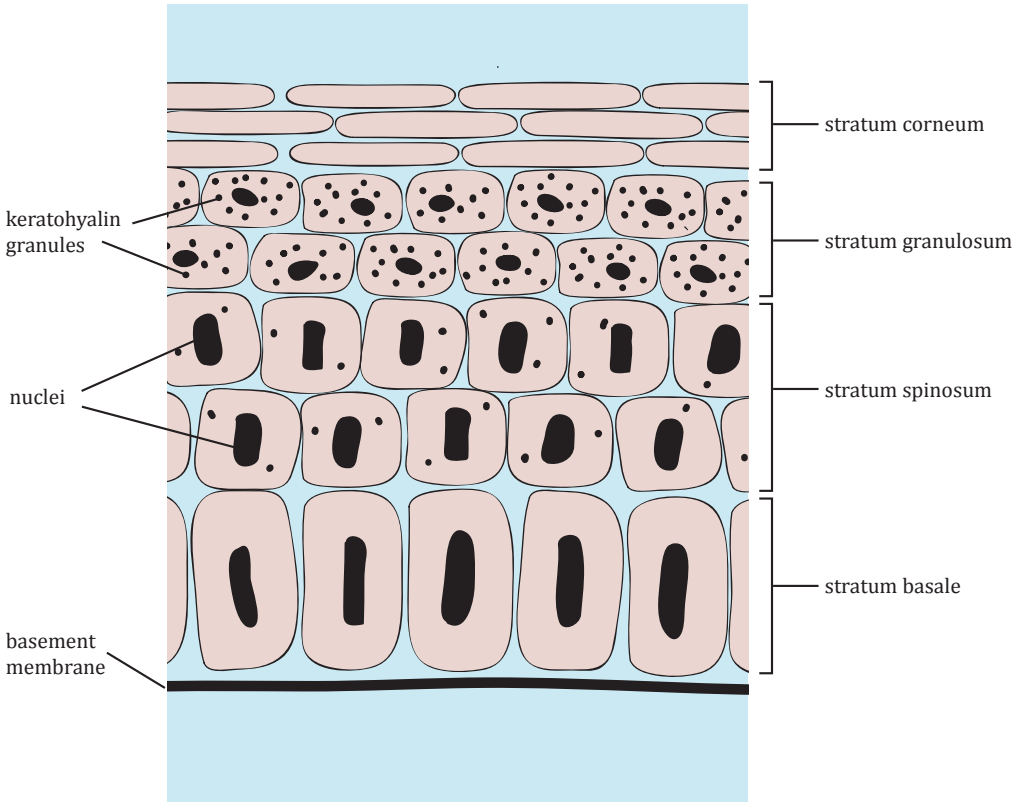

Figure 1.1 Diagram showing keratinocytes through the different stages of epidermal differentiation. Actively proliferating keratinocytes in the stratum basale differentiate and move upwards through the spinous and granular layers to eventually form the anucleated squame cells of the stratum corneum.

A consistent feature of AD is a T_H2-dominated cytokine milieu [11-13]. As such, particularly in view of the marked inflammation of the disease, most studies on AD pathogenesis have focused on the putative role of the immune response. At the same time, there is evidence for many years that a defective skin barrier is present in AD. Evidence of this is shown in increased transepidermal water loss [14-16], increased permeability to exogenous substances [17-19] and decreased skin hydration [15, 20, 21]. However, the most important evidence for barrier dysfunction having a role in AD

pathogenesis came in 2006, when McLean's group at the University of Dundee showed a strong association of loss-of-function mutations in the gene encoding filaggrin with AD [22, 23]. The group had initially studied ichthyosis vulgaris (IV), and showed that this relatively common genodermatosis affecting approximately one in 250 people was caused by mutation in the profilaggrin gene, *FLG*. A link between IV and profilaggrin has long been suspected [24], but the *FLG* gene had been technically too difficult to sequence until the McLean's group's success in comprehensively analysing the gene. They showed that IV is caused by two loss-of-function mutations in the *FLG* gene (R501X and 2282del4). The first is a nonsense mutation (where an arginine was replaced by a stop codon), while the second is a frameshift mutation with a 4-base pair deletion at position 2282 resulting in a premature stop codon [25]. Due to the semi-dominant inheritance pattern of the gene, individuals who are either homozygous or compound heterozygous for the gene fail to express detectable filaggrin protein in the epidermis, while single heterozygotes will express a reduced amount of the protein. Given the common co-occurrence of IV with AD, the group also subsequently showed that *FLG* gene mutations are a major predisposing factor for AD, as well as asthma developing in association with AD [22].

The McLean group initially studied a cohort of Irish children with AD and found that the combined allele frequency for the two prevalent loss-of-function *FLG* mutations (R501X and 2282del4) in the AD subgroup was 0.330 compared to 0.042 in an unselected Irish control population. The LOD score (to the base 10) was estimated to be 3.08 – 3.27 [22]. This association has since been independently reproduced in more than 25 studies in European populations [23, 26-35], with odds ratios between 2.8 and 13.4. Only one Italian study had so far fail to show an association, but the cohort studied had unusually low frequencies of *FLG* mutations, thereby limiting it statistical power to detect an association [36]. To date, more than 20 loss-of-function *FLG* mutations (Figure 1.2) have been identified [22, 37-41].

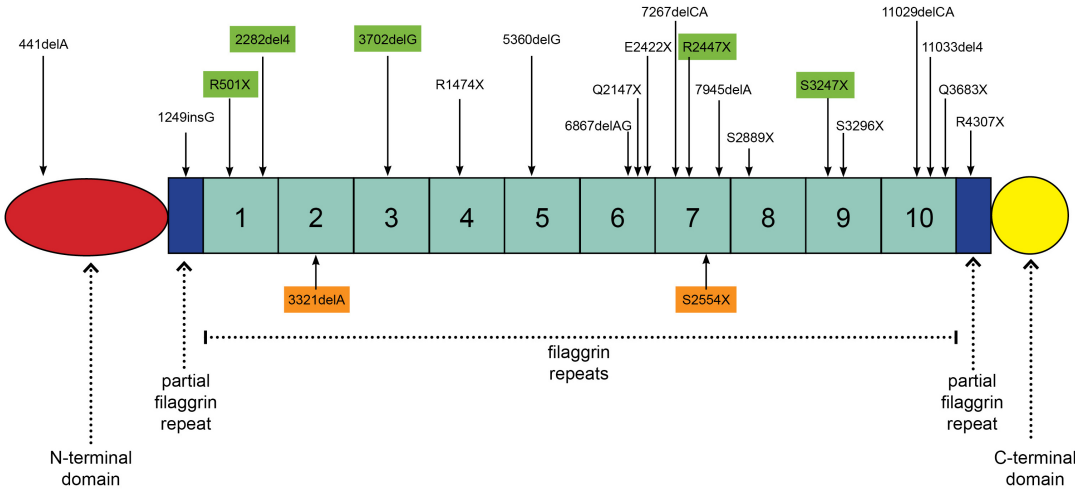

Figure 1.2 Schematic representation of the profilaggrin molecule illustrating the N-terminal domain, two partial filaggrin repeat domains flanking 10 almost identical filaggrin repeat domains, as well as the C-terminal domain. The locations of the loss-of-function *FLG* mutations identified to date are shown, all of which are either nonsense or out-of-frame deletion mutations. Variants highlighted in green are prevalent in European populations, while those in orange are common in individuals of Oriental ancestry [30].

Reviewing the original Irish AD cohort in light of these additional mutations showed that 47% carried a filaggrin null allele [38]. In cohorts where eczema was milder, there was evidence that although the association was less strong, *FLG* gene mutations were still a significant risk factor [42-44]. Therefore, it appeared that filaggrin-related AD had an earlier onset, was more persistent, and was strongly associated with atopic features such as asthma [31, 35, 45].

Non-European populations had also been shown to carry *FLG* mutations, although these were different variants to the common European ones (Figure 1.2). Studies looking at these populations similarly showed significant association between *FLG* mutations and AD [37, 39, 40, 46, 47]

1.1 Profilaggrin structure and function

The EDC on chromosome 1q21 consists of three gene families that are expressed late in human epidermal differentiation [48]. They encode precursor proteins of the cornified cell envelope (CE), calcium-binding proteins and intermediate filament-associated proteins [49, 50]. Profilaggrin is one of the intermediate filament-associated precursor proteins [24, 51, 52], and is the main constituent of the keratohyalin granules in the epidermis [53-56]. The *FLG* gene, together with genes encoding trichohyalin, repetin and hornerin, belongs to the 'fused' gene family which characteristically have variable number of internal tandem repeats.

The *FLG* gene (Figure 1.3) comprises of three exons and two introns [57, 58], with the initiation codon for translation located in Exon 2 while most of the profilaggrin is encoded in Exon 3.

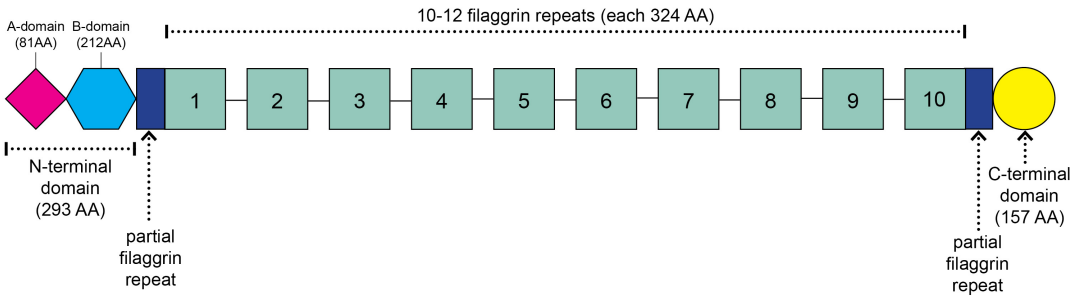

Figure 1.3 Schematic representation of the *FLG* gene showing the N-terminal domain (that contains a calcium-binding A-domain and a B-domain), two partial filaggrin repeats flanking 10 almost identical filaggrin repeat (joined by short linker segments), and a C-terminal domain. The number of filaggrin repeat domains varies from 10 to 12 between individuals (with duplication of the 8th or 10th domain, or both). Each filaggrin repeat in humans is identical in size (324 amino-acid long), but polymorphic in sequence.

Profilaggrin is a large (around 400 kDa), highly phosphorylated, insoluble protein consisting of 10 - 12 filaggrin units in humans (20 or more in rodents). There are no introns within the filaggrin portion of the coding region although the filaggrin repeats are joined by short linker segments [57, 59-62]. Each filaggrin repeat in humans is 324 amino-acid long (972 bp), each identical in size but polymorphic in sequence [59, 61]. The length of tandemly-arranged filaggrin repeats are flanked by two partial filaggrin repeats and an amino- and carboxyl-terminal domains. Subsequent to profilaggrin synthesis in the epidermal granular layer, it is rapidly phosphorylated and accumulates in keratohyalin granules [53-56]. It is believed that this sequestration of the phosphoprotein prevents premature and hence deleterious aggregation between filaggrin and keratin [63-65].

1.1.1 Profilaggrin amino-terminal domain

The profilaggrin N-terminal domain is 293 amino-acid long and consists of a conserved A-domain (81 amino-acid long) and less conserved cationic B domain (212 amino-acid long) [57, 58, 66]. The A-domain contains two calcium-binding S100-like EF-hands that each binds a Ca^{2+} ion [67]. Like other S100 proteins, calcium binding brings about a conformational change to the N-terminal domain [67], suggesting that calcium plays a key role in profilaggrin processing.

The B-domain contains functional bipartite nuclear localisation sequences (bNLSs) that facilitate nuclear translocation of the N-terminal domain [68, 69]. At the nucleus, Ishida-Yamamoto *et al* proposed that the N-terminal domain promotes keratinocyte denucleation [68].

It is postulated that the first N-terminal processing event during terminal differentiation involves the release of a peptide (50 kDa) containing the N-terminal domain and a partial filaggrin repeat. Further calcium-dependent

processing frees the N-terminal domain (32 kDa) [70]. This two-stage mechanism is thought to allow for fine control of filaggrin functions: cleavage of the N-terminal filaggrin peptide, coupled with dephosphorylation, leaves the polyfilaggrin region available for proteolytic processing to filaggrin monomers; while subsequent removal of the partial filaggrin repeat frees the N-terminal domain to translocate to the nucleus.

In summary, the N-terminal domain is thought to have two main roles. First, it regulates profilaggrin-filaggrin processing (which is likely to be calcium-dependent) and hence regulates the keratin-aggregation of filaggrin. Second, it is possibly involved in terminal differentiation processes such as keratinocyte denucleation.

1.1.2 Profilaggrin carboxyl-terminal domain

The C-terminal domain, like the N-terminal domain, has little homology with the filaggrin repeats (only around 17%). There is limited literature on its structure and function. There is considerable species variation in length, with humans having a 157 amino acid-long domain, but rats and mice having 23 and 26 respectively [71, 72]. Nonetheless, the last 15 amino acids of all three species share 53-60% sequence identity [57].

Although the function of the C-terminal domain is thus far uncertain, Sandilands *et al* showed that in humans who carry *FLG* mutations that express a truncated profilaggrin species (up to 10 filaggrin repeats but not the C-terminus) are unable to process these into filaggrin monomers [23]. This suggests that the C-terminal domain plays an essential role in profilaggrin to filaggrin processing. Further evidence to support this is seen in studies on the flaky tail mouse which showed that a similarly truncated profilaggrin does not form normal keratohyalin granules, is present only at low levels in the epidermis, and is not subsequently processed to filaggrin [73].

In summary, it appears that the C-terminal domain plays a role in keratohyalin formation and the normal proteolytic processing of profilaggrin into filaggrin.

1.1.3 Processing of profilaggrin to filaggrin

1.1.3.1 Dephosphorylation

Profilaggrin is extensively phosphorylated following its synthesis, and since only dephosphorylated filaggrin monomers are able to aggregate keratin 1 and 10 and other intermediate filaments, it is believed that this phosphorylation process is to control premature aggregation [74].

The processing of profilaggrin into individual filaggrin monomers is a highly regulated process involving multiple molecular events (Fig 1.4). This process is better understood in rodents, although it is believed to be very similar in humans. Dephosphorylation has been shown to be an early processing step (preceding proteolysis) as no phosphorylated intermediate species are detected [75]. Several protein phosphatases (PPase) have been shown to possibly play a role, such as the protein phosphatase PP2A (a member of the protein phosphatase 2A family) [76] and another phosphatase purified by Ohno *et al* called PPase: EC 3.1.3.2 [77]. Work done on the former showed a reverse relationship between the phosphatase activity and NaCl concentration, which suggests that the reduction in sodium concentration characteristically found in granular cells may be a regulatory mechanism for this enzyme. Other possible regulatory mechanisms postulated for this dephosphorylation process are the release of highly basic histones as granular cells degranulate, enhancing the activity of PPases and filaggrin (which is also highly basic) and activating PPases themselves in a positive feedback manner [76, 78].

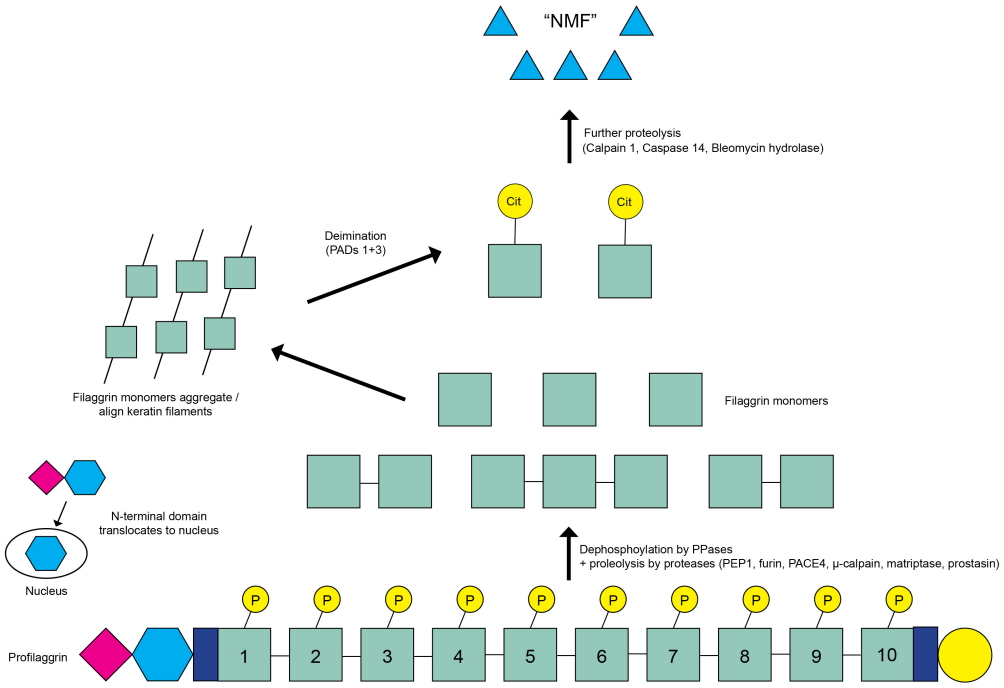

Figure 1.4 Model of profilaggrin and filaggrin processing. During terminal differentiation, the phosphorylated profilaggrin is dephosphorylated (probably involving the activity of one or more PPases) and then proteolytically cleaved to individual filaggrin monomers. Several proteases such as PEP1 and matriptase are thought to be involved in the proteolysis process. The cleaved N-terminal domain is then translocated to the nucleus. Within the SC, the filaggrin monomers aggregate and align keratin filaments to form macrofibrils. This results in compaction of the cytoskeleton and cross-linking of keratin intermediate filaments by transglutaminases and modification by peptidylarginine deiminases (PADs) to form a highly insoluble keratin matrix (a major component of the SC). The filaggrin monomers are subsequently degraded by various proteases into hydrophilic amino acids and derivatives, which are the natural moisturising factor (NMF) that contributes to skin hydration.

1.1.3.2 Proteolytic cleavage

Once again, the proteolytic processing of profilaggrin is best characterised in mouse profilaggrin. Resing *et al* studied this process in C57/Bl6 mice and identified two types of linker segments that differed in the residues following the carboxyl terminus of filaggrin [75]. One type has Tyr-Tyr-Tyr (Type A), while the other has Phe-Tyr-Pro-Val- Tyr-Tyr-Tyr (Type B). Hence, it was predicted that two different proteases cleaved the different linker segment

types. A previous study by the same group found two transient profilaggrin intermediates (containing two and three filaggrin domains) during processing, and these were subsequently found to only have Type B linker segment [75]. Hence the authors proposed that profilaggrin processing occurred in two distinct stages. The first stage involved the cleaving of Type A linker segment by one protease, while the second stage involved the cleaving of Type B linker segment by another protease to release individual filaggrin monomers.

In addition to mice, transient profilaggrin intermediates are also observed in other species, such as humans [56], rabbit [79], rat and guinea pig [80]. This suggests a common multi-stage processing mechanism in all mammals. However, an important difference in humans profilaggrin compared to other mammals studied is the presence of only one type of linker segments [59]. Therefore, it is presently uncertain if human profilaggrin is similarly processed.

Several proteases are thought to possibly play a role in proteolytically cleaving profilaggrin into filaggrin monomers. These include profilaggrin endopeptidase 1 (PEP1) which is a chymotrypsin-like protease [81], the proprotein convertases furin and PACE4 [82, 83] and μ-calpain [84, 85]. In addition, studies on mouse knockout models have also uncovered other possible enzymes involved in profilaggrin processing, such as the serine proteases matriptase [86], prostasin [87], inhibitors such as lympho-epithelial Kazal type inhibitor (LEKTI), which is encoded by the *Spink5* gene [88, 89] and 12R lipoxygenase (a dioxygenase that is preferentially expressed in the epidermis and catalyse the dioxygenation of fatty acid substrates [90, 91].

1.2 Filaggrin structure and function

1.2.1 Filaggrin processing

As seen in Figure 1.4, the proteolytic cleavage of profilaggrin results in individual filaggrin monomers. Filaggrin has been shown, *in vitro*, to aggregate keratin filaments into macrofibrils, hence its name (*fil*ament *aggr*egating prote*in*) [74, 92]. Under *in vitro* conditions, when keratin filaments and filaggrin were combined, they were shown to form a characteristic structural form similar to the 'keratin pattern' of SC cells [92-94]. Support of this role *in vivo* came from a study using immuno-electron microscopy on affected epidermis of ichthyosis vulgaris patients. This showed that localisation of filaggrin in lower cornified cells (albeit greatly reduced in IV compared to normal epidermis) correlated precisely with the formation of aggregated keratin filaments, while the absence of filaggrin in upper cornified cells correlated with disarrayed keratin filaments [55]. As filaggrin binds to keratin filaments with simple ionic and/or hydrogen-bonding interactions (the 'ionic zipper hypothesis') [95], these aggregate into macrofibrils which results in compaction of the cytoskeleton and cross-linking of keratin intermediate filaments by transglutaminases and modification by peptidylarginine deiminases (PADs) to form a highly insoluble keratin matrix. Together with lipids and other cornified envelope proteins, this protein scaffolding forms the SC, which is the primary skin barrier. Specifically, filaggrin aggregates keratin 1, keratin 10 and other intermediate filaments [55], and this collapses the keratin cytoskeleton during cornification and a form of programmed cell death [96]. A study by Presland *et al* also provided evidence that filaggrin is a major component of the cornified cell envelope [97].

Finally, within the SC, the filaggrin monomers are progressively degraded into hydrophilic amino acids and derivatives, including urocanic acid and pyrrolidone carboxylic acid. These make up the natural moisturising factor (NMF) which contributes to skin hydration [98]. The degradation of filaggrin is

fairly rapid – its half-life is estimated to be about 6 h [75]. However, this has been shown to be variable, being dependent on the SC hydration and external humidity [80, 98, 99]. Post-translational enzymes are involved in this degradation process, including peptidylarginine deiminases (PAD1 and PAD3), which are thought to be involved in the deimination of filaggrin [100-102]. Ishida-Yamamoto *et al* postulated that as the deimination of filaggrin converts its net charge from basic to almost neutral, this disturbs the ionic binding between filaggrin and keratin and hence encourages further filaggrin degradation [103]. Enzymes shown to cleave deiminated filaggrin monomers include caspase-14, an aspartate-specific proteinase whose expression is almost entirely restricted to the upper epidermis [104], calpain 1 and bleomycin hydrolase [105].

NMF compounds are abundant within corneocytes and represents up to 30% of the dry weight of the SC [105]. It is highly hygroscopic and is important in maintaining hydration of the skin, particularly in dry environmental conditions [98]. In addition, NMF is also thought to facilitate important biochemical events within the SC such as regulating protease activity and maintaining skin pH, and possibly also have a role in cutaneous antimicrobial defence [106].

1.2.2 Heterogeneity of filaggrin

Filaggrin monomers are found to be polymorphic. Even within a single individual, functional filaggrin consists of a heterogeneous population of molecules. Although all monomers are of the same length (324 amino acids), there is considerable variation in charge and sequence, with adjacent repeats showing as much as 20 % sequence variation [59, 61]. In the study by Gan *et al*, the authors found that most of the identified variations merely resulted in conservative changes to the molecule [59], thereby leaving the structural properties of the protein largely unaltered. Thus, the human filaggrin system is

doubly polymorphic: profilaggrin contains a variable numbers of filaggrin repeats, with functional filaggrin monomers showing sequence heterogeneity.

In contrast to human filaggrin monomers, mouse and rat filaggrin sequences seem to be highly conserved although this could merely be due to the rodent protein being obtained from inbred strains [62, 84].

1.2.3 Filaggrin mutations

As mentioned previously, there are more than 20 loss-of-function mutations found within the *FLG* gene to date. Five are prevalent in European populations with non-European populations having other population-specific mutations [38]. All these mutations are nonsense or frameshift mutations, resulting in a truncated form of profilaggrin protein. Sandilands *et al* showed that none of these truncated profilaggrin species can be processed properly into functional filaggrin monomers [23]. Hence, the effect of a mutation near the N-terminal domain of profilaggrin is similar to that of a mutation near the C-terminal domain, with both resulting in a reduction or complete absence of filaggrin [45]. Due to this equivalence of effect, several studies have used a 'combined null genotype' in their statistical analysis, which groups individuals with any one or any combination of two *FLG* mutations instead of analysing each mutation separately [107].

A noteworthy observation arising from genetic studies of the *FLG* gene is that the loss-of-function mutations are extremely common in the general population, with the R501X and 2282del4 mutations being carried by around 9% of the Irish population [22]. This high prevalence suggests a possible evolutionary heterozygote advantage. Irvine and McLean postulated that this mildly perturbed skin barrier in heterozygotes might be a form of 'natural vaccination' against bacterial antigens, conferring some survival advantage

during the great plagues and other ancient epidemics [29]. It is presently unknown when these *FLG* mutations arose in human history.

1.3 Relevance of filaggrin to human diseases

The recent discovery of filaggrin mutation as the cause of IV, and in particular the subsequent discovery of its strong association with AD, has renewed interest in this gene. In addition to these two common skin conditions, *FLG* genetics is also generating new insight into AD-related asthma, as well as providing possible disease mechanisms for systemic allergies.

1.3.1 Ichthyosis vulgaris

IV is a very common autosomal dominant skin disease, with an incidence of one in 250 people [108]. It is characterised by generalised xerosis with scaling particularly on the lower legs, keratosis pilaris and palmar hyperlinearity. There is also an association with atopy. Early clues suggested filaggrin's role in IV; for example, histopathological studies of IV had shown abnormal keratohyalin granules within the granular layer, and reduced or absent expression of filaggrin in patients' skin [24, 109, 110]. Zhong *et al* also mapped several pedigrees of IV to the EDC on chromosome 1q21, providing further evidence of filaggrin's role [111].

Previous attempts to sequence the *FLG* gene were hampered by the repetitive nature of the sequence, due primarily to the tandem repeats of the filaggrin domains. However, recent improvements in sequencing technology and the use of single nucleotide polymorphisms to aid sequence-specific PCR amplification have finally enabled the comprehensive analysis of the *FLG* gene [23]. This allowed Smith *et al* to study 15 pedigrees of IV and ascertain that IV is caused by loss-of-function mutations in the *FLG* gene [25]. They determined

that IV is inherited in a semi-dominant manner with incomplete penetrance (around 90 % in homozygotes). Therefore, heterozygotes display mild or no phenotype, whereas homozygotes or compound heterozygotes have a severe form of IV.

Initially, two premature termination codon-causing mutations, R501X and 2282del4, were identified. Subsequently, other novel mutations were demonstrated both in European and non-European populations [23, 26, 37, 38, 40, 46, 47, 112].

1.3.2 Atopic dermatitis

The clinical association between IV and AD is well recognised. As mentioned previously, AD is a genetically complex disease with a strong environmental component. Previous studies have provided some evidence of filaggrin's role in the genetic susceptibility of AD. For instance, Seguchi *et al* demonstrated that filaggrin expression is suppressed in the skin of AD patients [113]. Additionally, previous genome-wide association studies had linked AD to a locus on 1q21 [10], and an association had also been reported between specific profilaggrin allelotypes and dry skin [114]. Thus, it was perhaps not entirely surprising that having ascertained filaggrin's role in IV, Palmer *et al* subsequently demonstrated the strong association between *FLG* gene mutations with AD. What was surprising, however, was the strength of this association. In a trait as complex as AD, an estimated LOD score of 3.08 – 3.27 [22] (with an LOD score ≥ 3 indicating significant linkage) was remarkable.

Despite this strong association, it is certain the *FLG* mutations alone do not account for all cases of AD. Only up to half of all AD cases can be explained by the presence of at least one *FLG* null allele. It is known that AD is typically associated with increased expression of T_H2 cytokines (such as IL-4 and IL-13), both of which have been shown to reduce filaggrin gene and protein expression

[115]. It is likely, therefore, that a defect in filaggrin expression may be acquired in a subgroup of AD that is due to other inherited or acquired primary abnormalities [116].

1.3.3 Asthma

Asthma is part of the atopic disease complex, together with AD and allergic rhinitis. As mentioned earlier, *FLG* mutations have been shown to be associated with asthma, but only with asthma that is coexistent with AD and not asthma alone [22, 29, 117]. This suggests a casual relationship between AD and asthma. This has led to the hypothesis that asthma present in AD individuals is due to a primary defect in the epidermal barrier which allows allergens to penetrate the skin to make contact with Langerhans cells (the antigen-presenting cells in the skin) [118] leading to sensitisation and asthma [116]. There are several lines of evidence for this. These include the lack of filaggrin in bronchial mucosa [119], the association of *FLG*-positive AD with high serum IgE and allergic sensitisation [120], and the association between *FLG* mutations and greater asthma severity [117].

1.3.4 Genetic modifier in other diseases

Recently, *FLG* mutations are emerging as a genetic modifier in certain dermatological conditions. One of these conditions is alopecia areata (AA). This condition, which affects nearly 2 % of the population [121], presents with patchy hair loss and is thought be to a autoimmune disease directed against the hair follicle. An association of AA with atopic disease had been reported previously [122-125] and hence it was reasonable to search for a possible role of filaggrin in AA. Betz *et al* analysed a large cohort of AD patients and found no significant association between the two commonest null *FLG* mutations (R501X and 2282del4) with AA [126]. However, these mutations were significantly

associated with AA in those patients who also had AD. In addition, the group found that AA with concomitant *FLG*-associated AD was more likely to be more severe.

Another condition that *FLG* mutations may act as genetic modifiers is X-linked ichthyosis (XLI), which is caused by mutations in the steroid sulfatase gene (*STS*) located on the X chromosome [127]. Liao *et al* studied two brothers with the condition. One had a mild phenotype with fine scales, whereas the other was more severely affected. Both carried the same *STS* missense mutation T165I but the more severely affected brother was also a heterozygous carrier of *FLG* mutation R501X. This suggests that the degree of filaggrin expression is possibly a genetic modifier in XLI. It also suggests that especially in genodermatoses with known defects in epidermal differentiation, *FLG* mutations may similarly act as genetic modifiers [127].

1.4 Biophysical measures of skin barrier function

Several non-invasive biophysical measures have been used in cutaneous research to assess the function of the skin barrier. Of these, three of the most commonly used measures are transepidermal water loss (TEWL), SC hydration, and the number of tape strips required to induce a predefined level of barrier disruption.

TEWL is one of the most important parameters in the assessment of skin barrier function, and is particularly sensitive in assessing irritant effect on barrier function [128]. It is a measure of water evaporation from the skin surface, thus a measure of how 'leaky' the skin barrier is. Intact skin, therefore, has a low TEWL [129], while an impaired skin barrier characteristically shows increased TEWL [130, 131]. Its use as a reliable measure of skin barrier function has been extensively validated [129, 132-136]. Although it is a very quick and easy parameter to measure experimentally, there have been concerns about the

standardisation and reproducibility of TEWL measurements, since it is known that factors such as the type of instrument used, site and environmental factors affect TEWL measurements [137-139]. Hence, it is important during TEWL measurements to note these factors and keep them constant.

Skin barrier function can also be assessed by measuring the water content of the SC. SC hydration has been shown to affect permeability and flexibility, as well as the enzymatic activity of normal SC desquamation [140, 141]. Hence, impaired skin barrier is associated with low SC hydration [142, 143]. There are many techniques to measure SC hydration, with the most common being an indirect measurement of SC hydration by measuring skin capacitance. Skin capacitance is determined by the dielectric nature of the epidermis, which varies depending on the amount of moisture in the skin. Therefore, skin with different amount of hydration will have different dielectric constants, thus giving different capacitance values. Factors that affect TEWL measurements also affect skin hydration. Hence, these need to be kept constant for accurate comparison [144].

In addition to TEWL and skin capacitance, another measure of skin barrier function is by using tape stripping, which is a technique further described in Chapter 1.5. Specifically, the number of tape strips required to achieve TEWL > 20 $g/m^2/h$ (which is generally accepted as the level where the SC is abrogated) can be used as a functional measure of skin barrier [145-147]. Therefore, in skin with an impaired barrier, fewer number of tape strips will be required to achieve TEWL > 20 $g/m^2/h$.

1.5 Tape stripping in skin research

Since it was first described by Pinkus in 1951, adhesive tape stripping has become a widely used technique in dermatological research [148-158]. It is a simple, validated, minimally invasive method and is used in a broad range of

applications. These include evaluating the bioavailability and dermatopharmacokinetics of topically-applied drugs [159-162], obtaining SC cells for analysis [146, 163, 164], studying various aspects of skin permeability [165-170], and analysing skin barrier function [146, 156, 171].

There are several commercially available adhesive tapes used, with the D-Squame tape strips (Cuderm Corporation) being the most commonly used. The technique itself is easy to perform [172]. Pieces of tape strips are consecutively pressed onto the surface of the skin and then removed. The superficial layers of the SC will adhere to the tapes and are available for further analysis. If necessary, the amount of SC collected can either be determined gravimetrically (that is, weighing the tape strips) or by protein determination [149, 173, 174].

It is, however, well documented that many factors affect the amount of SC removed, including the anatomical site [175, 176], intensity and duration of the pressure applied [174, 175], sex and age [176], material of the tapes used [175], ambient temperature [177, 178], and skin hydration [179]. Hence, it is important that these test conditions are well defined for standardisation.

1.6 Mass spectrometry

Mass spectrometry (MS) is an analytical tool used to measure the mass of molecules and atoms expressed as their mass-charge (m/z) ratio. There are numerous types of mass spectrometers but all consist of three fundamental parts: an ion source, a mass analyser, and a detector (Figure 1.5). In order for MS analysis, the sample molecules need to be converted by the ion source into gas-phase ionic species. These ionic analytes are then extracted into the mass analyser where they are separated according to their m/z ratios. Finally, the ion current due to the separated ionic analytes is detected by a suitable detector where their relative abundance is displayed in the form of a mass spectrum.

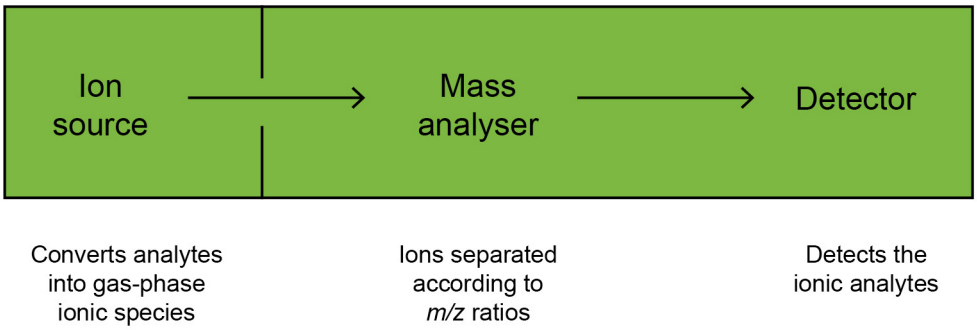

Figure 1.5 Diagram of a generic mass spectrometer. There are three fundamental parts: an ion source that converts sample molecules into gas-phase ionic species, a mass analyser that separates the ions according to the *m/z* ratios, and finally a detector that detects the separated ionic analytes.

Over the last 20 years, biological MS has made huge advances, largely due to the development in the 1980s of 'soft ionisation' methods - electrospray ionisation (ESI) [180-182] and matrix assisted laser desorption/ionisation (MALDI) [183]. These methods allow for the routine and general formation of molecular ions of intact biomolecules, and are instrumental in driving the design and manufacture of smaller and cheaper instruments with increased mass range, higher routine resolution and mass accuracy [184]. Today, MS is the most sensitive method for structural characterisation of biomolecules. For instance, proteins that are separated by gel electrophoresis can be identified at the picomole level and below [185, 186], while neuropeptides can even be detected at the zeptomole (10^{-21}) level [187].

1.6.1 Ionisation methods

In order to allow for MS analysis, the sample must first be ionised and vaporised. Until the development of the 'soft ionisation' methods, samples were

usually ionised by electron-impact (EI) or chemical-ionisation (CI) methods, both of which require a vaporised sample. Hence, for a long time, MS was restricted to small and thermostable compounds. This was because most biomolecules, being polar and thermally labile, would be excessively fragmented by EI and CI methods. The 'soft ionisation' methods (MALDI and ESI), on the other hand, allow for the ionised biomolecules to be transferred from the condensed phase into the gas phase without excessive fragmentation [188]. In this thesis, both MALDI and ESI are employed.

1.6.1.1 Matrix-assisted laser desorption/ionisation

The term matrix-assisted laser desorption ionisation was first coined in 1985 by Franz Hillenkamp, Michael Karas and their colleagues [189]. There are essentially two steps in MALDI. First, the sample is pre-mixed with a highly absorbing matrix compound. This mixture is dried, resulting in a 'solid solution' with the analyte molecules isolated and embedded throughout the matrix. The second step occurs in a vacuum within the source of the mass spectrometer, where portions of the solid solution are bombarded with a high-energy laser over a short duration. Although the exact mechanism of the MALDI process is still not completely understood [190, 191], it is generally thought that the rapid heating by the laser causes localised sublimation of the matrix crystals and expansion of the matrix into the gas phase while encapsulating intact analyte in the expanding matrix plume [192]. The ionisation of the analyte in MALDI is also incompletely understood [193]. The widely accepted view is that the analyte molecules are ionised by acid-base proton transfer reactions with the protonated matrix ions in a dense phase just above the surface of the matrix [192] (Figure 1.6). The ions in the gas phase are then accelerated towards the mass analyser by an electrostatic field.

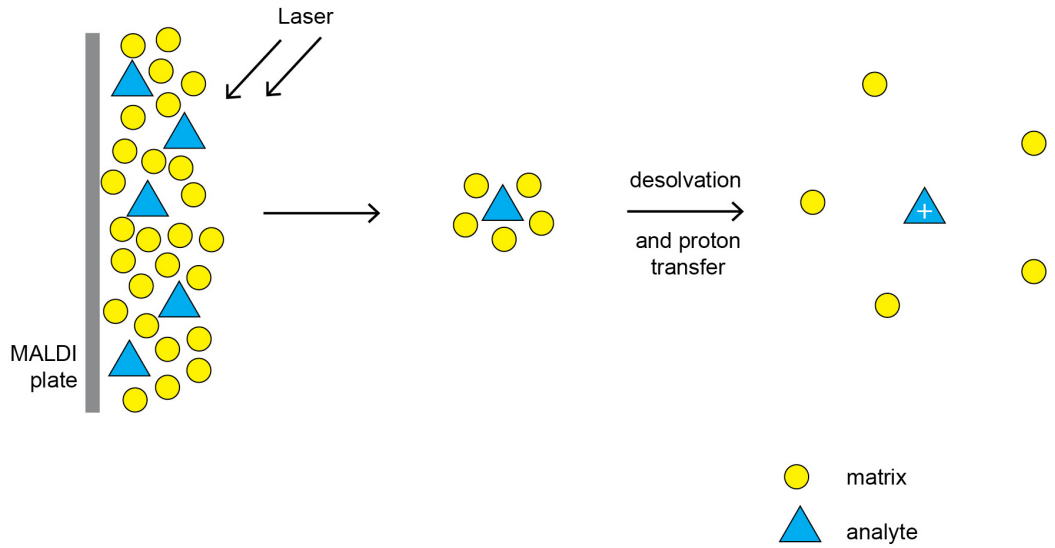

Figure. 1.6 Desorption and ionisation in MALDI. The 'solid solution' containing the analyte molecules is bombarded with a high-energy laser, which causes sublimation of the matrix crystals and while encapsulating intact analyte in the expanding matrix plume. It is thought that the analyte molecules are subsequently ionised by acid-base proton transfer reactions with the protonated matrix ions in a dense phase just above the surface of the matrix.

Early mass spectrometers used lasers that were applied directly to the sample. This direct mode of application of laser (termed laser/desorption ionisation, LDI) often resulted in excessive fragmentation of the sample. Hence, LDI restricted MS analysis to only small organic molecules with molecular mass less than 1000 Da. In MALDI, the use of a matrix with the sample has revolutionised the analysis of large, non-volatile and thermally labile compounds such as proteins, oligonucleotides, polymers and large inorganic molecules. Indeed, in the field of protein chemistry, it is arguably the most efficient method of ionising peptides [184]. Other advantages of MALDI include the tolerance for contaminants and buffers, high sensitivity, uncomplicated mass spectra (since most ions are singly charged) and rapid analysis [194].

The use of a matrix, which provides for both desorption and ionisation, is crucial to the success of this ionisation method [195]. The most important

function of the matrix is to rapidly and efficiently absorb energy from the laser and transform this into excitation energy for the sample, which brings about the ionisation of the sample (and matrix). More importantly, this spares the sample from excessive and direct energy that may otherwise result in thermal decomposition. To allow for the matrix to achieve this function, it needs to have strong optical absorption at the wavelength of the laser radiation [196].

Other characteristics required of an effective matrix include: 1) a fairly low molecular weight to be sublimable yet large enough so as not to evaporate during sample preparation; 2) vacuum stability; 3) ability to promote ionisation of the analyte; 4) solubility in solvents compatible with the analyte and bring about homogenous co-crystallisation; 5) lack of chemical reactivity and 6) ability to separate the analyte molecules to prevent analyte aggregation [195, 197].

Most present day MALDI mass spectrometers use ultraviolet lasers because of their ease of operation and low cost. Among these, nitrogen lasers with a wavelength of 337 nm are considered the standard, but others used include frequency-tripled and quadrupled Nd:YAG (neodymium:yttrium aluminium garnet) lasers, with wavelengths 355 nm and 266 nm respectively.

A range of compounds is suitable for use as matrices, but the three most commonly used are 3,5-dimethoxy-4-hydroxycinnamic acid (sinapinic acid), α-cyano-4-hydroxycinnamic acid (ACHC) and 2,5-dihydroxybenzoic acid (DHB). A solution of the matrix in purified water generally also includes an organic solvent (such as acetonitrile to solubilise hydrophobic molecules) and trifluoroacetic acid (to act as a proton source to encourage ionisation of the analyte).

MALDI is most commonly coupled to time-of-flight (TOF) mass analysers [198]. There are two main reasons for this. First, TOF has the capability of analysing ions over a wide mass range; thus it is able to analyse the high-mass

ions generated by MALDI. Second, both MALDI and TOF mass analysis are pulsed rather than continuous events [184, 195]. MALDI-TOF instruments typically have an 'ion mirror' that doubles the ion flight path and increase the resolution of the *m/z* measurements.

In protein chemistry, MALDI-TOF is particularly useful in peptide mass fingerprinting (PMF), where digested peptides are mass-analysed and compared against protein databases to identify the parent protein [199-203]. Protein identification by PMF is further described in Chapter 1.6.4.

The MALDI mass spectra of proteins and peptides typically include mainly the singly protonated molecular species and their oligomeric ions (e.g. $[M+H]^+$, $[2M+H]^+$). Additionally, Na^+ and K^+ adducts are also common features of these MALDI spectra.

1.6.2.2 Electrospray ionisation

The widespread use of ESI was started by the work of Fenn *et al* when they obtained multiply charged ions from proteins and determined their molecular weights using mass spectrometers of modest *m/z* range [180, 204]. ESI is a type of atmospheric pressure ionisation (API), which allows the analysis of non-volatile samples without first converting them to the gaseous phase. The most important advantage of API sources is the simplicity for the direct on-line coupling of separation techniques such as high-pressure liquid chromatography (HPLC) to the mass spectrometer [195].

During standard ESI, the sample is dissolved in an organic solvent that is continuously pumped through a narrow stainless steel capillary tube at a flow rate of 1 - 1000 μL/min). A potential difference of 3 – 4 kV between the tip of the capillary and the walls of the surrounding atmospheric pressure region produces an electrostatic field of sufficient strength to disperse the emerging

sample in a fine mist of charged droplets. This process is aided by a co-axially introduced nebulising gas (usually nitrogen) flowing around the outside of the capillary tube, which helps to direct the spray emerging from the capillary tip towards the mass analyser. The charged droplets are gradually stripped of the solvent molecules as they flows through a region containing a drying gas (usually warm nitrogen) before the charged sample ions (free from solvent) are directed through a sample cone or orifice into an low-pressure transport region before finally entering the mass analyser that is held under high vacuum (Figure 1.7).

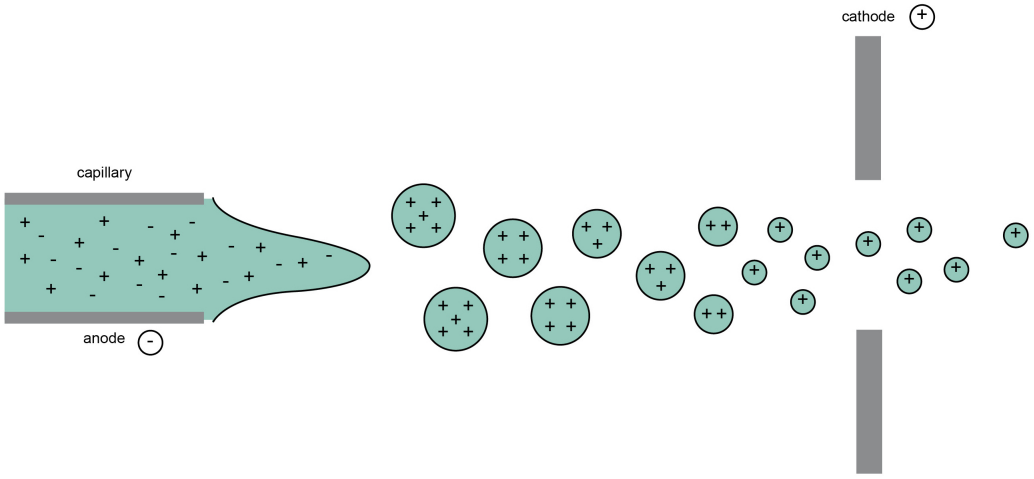

Figure 1.7 Standard ESI process. Dissolved sample is continuously pumped through narrow stainless steel capillary tube. The electrostatic field brought about by the potential difference between the tip of the capillary and the walls of the surrounding atmospheric pressure region disperses the emerging sample in a fine mist of charged droplets. This process is aided by a co-axially introduced nebulising gas, which also helps to direct the emerging spray towards the mass analyser. The charged droplets are gradually desolvated as they flows through a drying gas before the charged sample ions are directed through a sample cone or orifice into a low-pressure transport region before entering the mass analyser held under high vacuum.

Thus, there are three main stages in ESI: droplet formation, droplet shrinkage, and gaseous ion formation. Microscopic examination of the nascent drop forming at the tip of the capillary shows that when the applied voltage is low, the drop is almost spherical. With increasing voltage, the drop elongates, eventually adopting the form of a Taylor cone [205, 206] just before small

droplets are released, creating the spray [207, 208]. As the droplets travelled through the drying gas, they become desolvated and reduced in size until surface-coulombic forces overcome surface-tension forces and the droplets break up further into even smaller droplets [209, 210]. This continues until either an ion desorbs from a droplet (Ion-Desorption Model) or the solvent is completely removed (Charge Residue Model) [211, 212]. There is still considerable debate as to the exact mechanism of ion formation, and is likely that different mechanisms occur under different scenarios [213-215].

Nanoelectrospray ionisation (nESI) is a modification of the standard ESI developed by Wilm and Mann [186, 216]. It has proven to be enormously important in the analysis of biochemical and pharmaceutical samples since much smaller quantities of analytes are required [217]. With nESI, the capillary tip used is much smaller, and the flow rate reduced to 30 – 1000 nL/min. Thus, not only is far less sample consumed, a small volume of sample also lasts for several minutes, allowing multiple analyses to be performed. This is particularly advantageous in tandem mass spectrometric (MS/MS) amino acid sequencing. In this study, samples are first passed through a liquid chromatography (LC) column before nESI and MS/MS, in a set up known as nano LC-MS/MS.

1.6.3 Mass analysers

1.6.3.1 Time-of-flight mass analysers

The TOF mass spectrometer is one of the simplest mass analysing devices. It separates ions according to their velocities when they drift in a free-field region that is called a flight tube. The charged ions generated at the ion source (e.g. MALDI) are accelerated towards the flight tube by a potential difference between an electrode and the extraction grid [195]. Since all the ions acquire the same kinetic energy (equal to zV_s, where z is the charge of the ion and V_s the accelerating potential), ions travel at velocities v that are an inverse

function of the square root of their *m/z* values (Equation 1.1). That is, the velocity of lighter ions will be higher and hence will arrive at the detector at the end of the flight tube faster than heavier ions.

Equation 1.1:

$$v = \left(\frac{2zeV_s}{m} \right)^{1/2}$$

The time *t* needed to cover the length of the flight tube *L* is given by Equation 1.2.

Equation 1.2:

$$t = \frac{L}{v}$$

Therefore, replacing *v* by its value in Equation 1.2 gives Equation 1.3.

Equation 1.3:

$$t^2 = \frac{m}{z}\left(\frac{L^2}{2eV_s} \right)$$

Thus, the *m/z* of an ion entering that flight tube can be calculated from its time of arrival at the detector. The conversion of the flight times measured to mass values involves a simple mass calibration using the flight times of two different known mass ions [195]. Apart from this ease of mass calibration, other advantages of the TOF analyser include its (theoretical) unlimited upper mass range, high sensitivity and rapid speed of analysis [218-221].

The recent renewed interest in TOF is largely attributed to its natural coupling to the MALDI ion source. In the past, TOF analysers suffered from poor mass resolution. One main factor that restricted resolution in early TOF analysers was the variation of the kinetic energy distribution of the ion beam, resulting in ions with higher initial energy arriving at the detector sooner those with the same mass but with lower initial energy. There are two main ways to improve mass resolution. First, the initial burst of ions can be allowed to

equilibrate and dissipate before they are accelerated into the flight tube. This mode of operation is known as 'delayed pulsed extraction', which helps to overcome the kinetic energy spread among ions with the same *m/z* leaving the source [222]. Another way of improving mass resolution is the use of a reflectron. This is an electrostatic mirror consisting of a series of electric lenses with increasing repelling potential that reflects the ion beam back to the detector. In principle, ions with more kinetic energy (therefore higher velocity) will travel deeper into the reflectron compared to less energetic ions. Since the faster ions spend more time in the reflectron, they will arrive back at the detector at the same time as slower ions with the same *m/z* [223].

1.6.3.2 Three-dimensional (3D) ion trap mass analysers

The quadrupole ion trap was first described in 1960 [224], although only modified to a useful mass spectrometer in the 1980s by Stafford *et al* [225]. The 3D ion trap is a device that traps ions in a radio frequency (RF) quadrupolar field, in a space defined by a ring electrode between two endcap electrodes. A high voltage RF potential is applied to the ring, while the endcaps are held at ground. The oscillating potential difference between the ring and endcap electrodes forms a substantially quadrupolar field. Depending on the RF voltage level, the field can trap ions of a particular mass range. An auxiliary voltage is also fed to the exit endcap, which is used for various purposes during precursor ion isolation, fragmentation, and mass analysis phases of the scan sequence. (Figure 1.8)

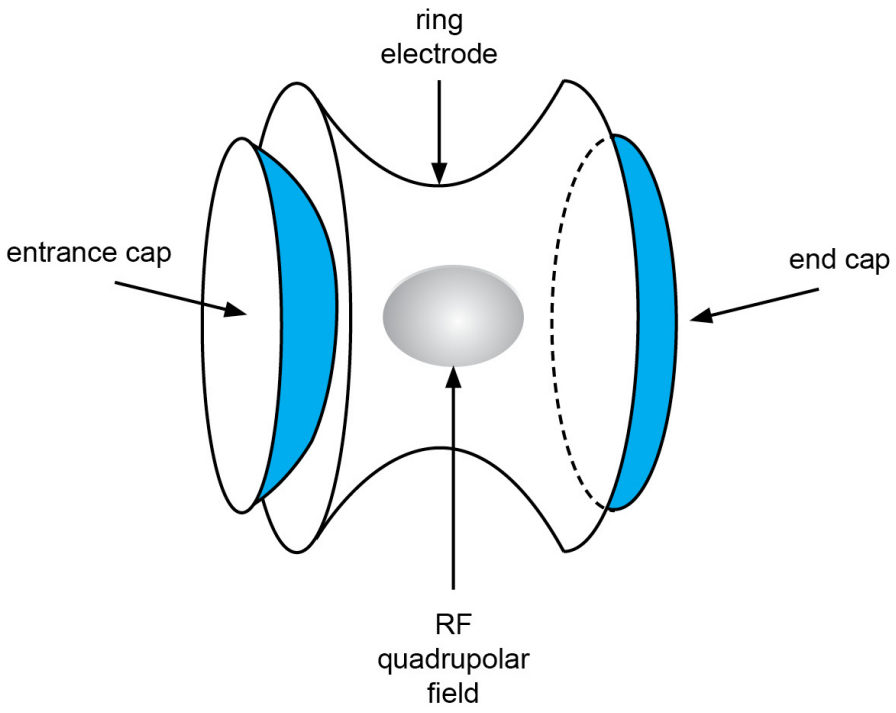

Figure 1.8 The 3D ion trap geometry. A high voltage RF potential is applied to the ring electrode, while the endcap electrodes are held at ground. The oscillating potential difference between the ring and endcap electrodes form an RF quadrupolar field where ions are trapped.

In order to reduce ion losses in the trap, a collision gas (helium) is present in the trap to extract energy from the ion beam and cause retention of at least a certain portion of the ions entering the trap. Other parameters that affect trapping efficiency include the ion injection directions, initial phase of the RF voltage, energy of the incoming ion beam, and the *m/z* value and mass of the ion [226].

There are various ways of analysing the ions according to their mass, but the most commonly used is the mass instability mode. Here, there is a stability limit (determined by the RF potential) within which the orbit of ions with a certain mass is stable while those with lower masses are unstable and ejected. As the RF potential is ramped, ions of higher masses become sequentially unstable and are ejected.

Although having a mainly quadrupolar field, the high capacity trap (HCT) as used in this work is really a 'multipole-superimposed' ion trap in which the quadrupolar field has contributions from hexapolar, octopolar and even higher-order fields. This induces non-linear resonances that cause energy to be rapidly taken up in the ion motion. The ions, by taking up energy very quickly, can then leave the ion trap without becoming unstable in the field. This ultimately allows for fast data acquisition without compromising mass resolution. The sequential mass ejection of the ions is then detected by the ion detector to produce a mass spectrum [227].

1.6.4 Protein identification by peptide mass fingerprinting

In PMF, a protein is first digested into peptides using a sequence-specific protease. The masses of this group of peptides are then matched against the theoretical masses of peptides from *in silico* digested proteins (using the same protease) in a database [201, 203]. It is called peptide mass fingerprinting because a protein digested by a sequence-specific protease generates predictable masses that are generally unique to the protein (hence a 'mass fingerprint'). Trypsin is the most commonly used protease, cleaving proteins at the C-termini of arginine (R) and lysine (K) residues. Although it is known as peptide *mass* fingerprinting, MS analysis of peptides actually provides a list of *m/z* ratios. This experimentally obtained *m/z* ratios of peptides is then matched using an algorithm to compare with theoretically predicted peptide *m/z* ratios of proteins in a database. Scores are assigned according to the number of matches obtained, as well as the quality of the matches. PMF is generally performed using MALDI-TOF mass spectrometers [201].

1.6.5 Protein identification using tandem mass spectrometry

MS/MS involves at least two stages of mass analysis. In the most common MS/MS experiment, a first analyser isolates a precursor ion, which is focused into a collision region where it undergoes fragmentation (spontaneously or by some activation) to yield product ions. These product ions are then analysed by a second analyser [195].

MS/MS for the structural characterisation of organic molecules was first utilised by Beynon and colleagues [228]. It is particularly in protein chemistry that MS/MS has become most widely utilised [185, 186, 229-232]. In fact, it has largely replaced PMF as the main protein identification approach. There are various ways by which peptide ions can be fragmented, which is largely dependent on the type of mass spectrometer used. This in turn determines where in the peptide backbone the peptides are fragmented [233]. An inert gas is generally introduced into the collision region to enable collision between the precursor ion and inert gas atoms or molecules. The result of this is a population of excited peptide ions that decompose to product ions in a process known as 'collision-induced dissociation' (CID) which is the decomposition process used in triple quadrupole, ion trap and quadrupole-time of flight (QTOF) hybrids mass spectrometers [234]. The process of CID on each of the peptide ions can be automated with various protocols developed to allow for specific precursor ions to be selected for CID. For instance, in data-dependent acquisition MS/MS, the most abundant ion is selected first for CID with the next most abundant ion analysed next, and so forth [235].

Low-energy CID generally results in the cleavage of the amide bond of peptides. Hence the majority of the product ions formed are b and y ions (Figure 1.9). A b ion is formed when the positive charge associated with the parent peptide ion is retained by the N-terminal fragment side, while a y ion is when the charge is retained by the C-terminal fragment of the cleaved amide bond [230].

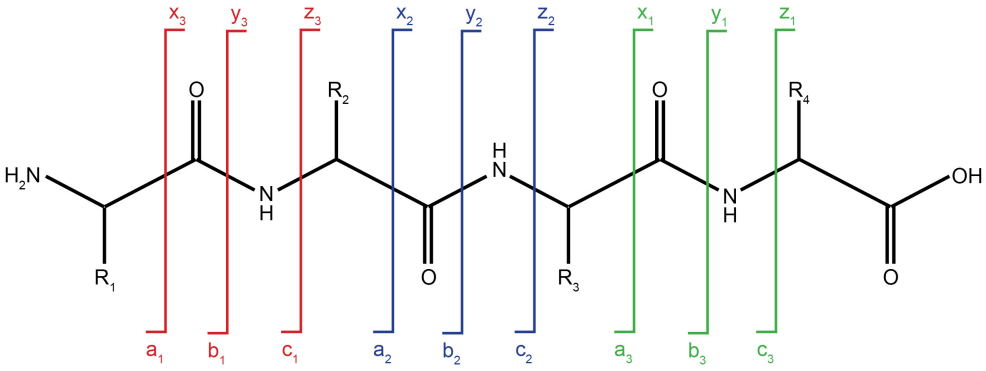

Figure 1.9 Roepstorff-Fohlmann-Biemann nomenclature of fragment ions that can be generated following gas phase fragmentation [230]. Peptide fragmentation through collision with residue gas generally leads to the generation of b and y ions. Schematic adapted from Faull [236].

From the peptide fragmentation spectra obtained from MS/MS, proteins can be identified using two methods. The first method is known as *de novo* sequencing which is based on the principle that each peptide fragment in a series differs from its neighbour by one amino acid. Therefore, in principle, it is possible to determine the amino acid sequence by mass difference between neighbouring peaks in a series [237]. The main advantage of *de novo* sequencing is that peptide sequencing is not restricted to peptides contained in a database. However, there are significant difficulties with this method, which primarily stems from the fact that information in MS/MS is often incomplete and intervening peaks, which may or may not belong to a peptide series, can make analysis very difficult [238]. Although attempts have been made to automate this process, it is still a time-consuming and difficult task [239].

The second method of protein identification is to compare the *m/z* peaks in the CID spectra with theoretical *in silico* generated MS/MS CID spectra. In contrast to *de novo* sequencing, this is easily automated and is the more commonly used method. The reason database searching is easier than *de novo*

sequencing is that only a minute fraction of the possible peptide amino acid sequences actually occur naturally. Thus, even if a peptide fragmentation spectrum is inadequate for complete amino acid sequencing, it may still contain sufficient information for it to be uniquely matched to a peptide sequence in a database on the basis of the observed and expected fragment ions [231, 240, 241].

1.7 Objectives of this study

There were two main focuses in the study described in this thesis. The first was a functional study whose primary objective was to determine whether *FLG* mutations correlated with altered skin barrier function in AD subjects. A correlation between *FLG* mutations and AD has been well established [23, 26, 33, 35], and it has also been shown that skin barrier dysfunction is a feature of AD skin [15, 242]. However, there is at present limited evidence for a defective skin barrier function in filaggrin-related AD, with the few studies that had attempted to analyse this reporting inconsistent results [243, 244]. For this functional study (as detailed in Chapter 5), a cohort of AD subjects was recruited and genotyped for the *FLG* gene. The skin barrier function of these individuals was assessed by three different measures, and analysed to see if they correlated with the presence of *FLG* mutations. There was also a secondary aim in this functional study, which was to test the hypothesis that corneocytes were less adherent to one another in filaggrin-related AD compared to wild-type AD skin. This hypothesis was developed from an unexpected finding reported by Nemoto-Hasebe *et al* [244], who showed that SC thickness was greater in the skin of filaggrin-related AD.

The second focus of this study aimed to interrogate the structure-function relationship of filaggrin, by comparing filaggrin protein extracted from AD and non-AD skin. Although *FLG* mutations are strongly associated with AD, only up to about half of AD individuals possess these mutations while the rest

have the wild-type genotype [38]. Genetics, of course, cannot completely inform about cell physiology. For instance, there may be post-translational modifications, or dynamic processes of protein maturation and degradation can alter the structure and function of the final active protein [245]. Therefore, the aim of this structural study was to analyse filaggrin protein directly using MS techniques, specifically MALDI MS and nano LC-MS/MS. Any structural differences noted in filaggrin between AD and non-AD skin would hopefully provide further insight into its role in AD. This structural study is detailed in Chapter 6.

In order to analyse filaggrin using MS techniques, a sufficient amount of the protein had to be extracted and purified. Traditionally, discarded skin from procedures such as breast reduction surgery and abdominoplasty is used in skin research that requires a large amount of skin cells. Indeed, breast reduction skin was collected from several healthy non-AD individuals for use in the development of the filaggrin extraction and purification, but it would have been impractical to recruit only subjects who underwent breast reduction surgeries or abdominoplasties. As such, tape stripping was used for the first time as a minimally-invasive method of extracting filaggrin from subjects' skin. Chapter 3 describes the development of tape strip extraction and purification of filaggrin.

Soon after commencing this study, it became clear that there were practical benefits to having a relatively quick screening test to detect and quantify filaggrin in the skin. This was primarily because *FLG* genotyping was time-consuming and expensive, and also because the detection of filaggrin in significant quantity in skin samples should make genotyping these samples unnecessary, as reasoned in Chapter 4. In the absence of any commercially-available filaggrin-specific ELISA at that time, attempts were made to develop a novel one, the process of which is detailed in Chapter 4.

Chapter 2 Materials and Methods

2.0 MATERIALS AND METHODS

2.1 Recruitment of subjects

Subjects with AD, as well as non-AD control subjects, were recruited from the general dermatology outpatient and patch test clinics at the Royal Infirmary of Edinburgh. Additionally, in order to recruit AD subjects with a wide range of AD severity (since AD individuals who attend dermatology clinics tend to have more severe disease), advertisements about the study were also placed on student notice boards throughout the University of Edinburgh.

Informed written consent was obtained from all subjects. The study had received prior approval by the Lothian Research Ethics Committee.

2.1.1 Entry criteria of atopic dermatitis

All subjects were of Western European descent since different filaggrin mutations are prevalent in different populations. Most of the AD subjects were already diagnosed with the condition by their dermatologists or general practitioners. Nonetheless, every subject was interviewed and examined at the start of recruitment to ensure fulfilment of the UK Working Party's diagnostic criteria of AD [246]. These criteria are shown in Table 2.1. Similarly, these criteria were also used to ensure that non-AD control subjects did not have the condition.

Diagnosis of AD requires the presence of an **itchy** skin condition plus **3 or more** of the following:

1. Visible flexural dermatitis
2. Personal history of flexural dermatitis
3. Personal history of dry skin in the last 12 months
4. Personal history of asthma or hay fever
5. Childhood eczema

Table 2.1 UK Working Party's diagnostic criteria for the diagnosis of AD [246]. All subjects in the AD group had to fulfil these criteria at the point of recruitment.

2.1.2 Exclusion criteria

Subjects who had active inflammation or infection on the flexural surfaces of the forearms (where skin barrier function tests were performed) were excluded, as were those who did not discontinue topical treatment for their AD on the test areas at least 1 week prior to skin barrier assessment.

2.2 Clinical assessment of atopic dermatitis severity

The Six Area Six Sign Atopic Dermatitis (SASSAD) severity score was chosen as the measure of AD severity in this study because it is a validated, simple and effective system to record and monitor disease activity [247]. The score is obtained by grading six signs (erythema, exudation, excoriation, dryness, cracking and lichenification) on a scale of 0 (absent) to 3 (severe) at each of six anatomical sites (Table 2.2).

During the initial interview, subjects were also asked about the past and present treatment for their AD, including any previous inpatient treatment, in

order to fully characterise their disease severity. Additional information noted was the presence a personal or family history of atopy.

Six clinical signs		Six anatomical sites	
1.	Erythema	1.	Head and neck
2.	Exudation	2.	Trunk
3.	Excoriation	3.	Hands
4.	Dryness	4.	Feet
5.	Cracking	5.	Arms
6.	Lichenification	6.	Legs

Table 2.2 The Six Area Six Sign Atopic Dermatitis Severity (SASSAD) score. The six signs are graded on a scale of 0 (absent), 1 (mild), 2 (moderate), or 3 (severe) at six anatomical sites. The maximum score is 108.

2.3 Genotyping

All AD subjects were screened for *FLG* mutations, with the genotyping performed at the Molecular Medicine Unit at the University of Dundee. Specifically, the four *FLG* mutations that were most prevalent in Western European populations (2282del4, R501X, R2247X and S3247X) were screened for. Together, these mutations had been shown to account for up to 95% of the known *FLG* mutations in European populations [248]. Genotyping was performed using a TAQMAN-based allelic discrimination assay (Applied Biosystems) on an Applied Biosystems 7900HT sequence detection system. Details of the assay, including the probes and primers used, were previously described by Sergeant *et al* [249].

2.4 Serum IgE level

All subjects had their total serum IgE levels (IU/ml) measured at the start of the study. Blood samples were analysed by the Blood Transfusion Service at the Royal Infirmary of Edinburgh.

2.5 Skin barrier function tests

To objectively assess the function of the skin barrier, three different measures were performed: 1) TEWL, 2) skin capacitance (as a measure of SC hydration), and 3) the number of tape strips required to abrogate the skin barrier.

2.5.1 TEWL and skin capacitance

TEWL and skin capacitance were measured on all subjects according to the European Society of Contact Dermatitis guidelines [137].

TEWL was measured with a Tewlameter TM300 (Courage and Khazaka) using an open chamber probe that contained a hygrometer. This measures the humidity of the incoming and outgoing air passing through the test area, with the TEWL being the difference between the two values. Since TEWL is a measure of the amount of water loss from the skin surface, it is therefore essentially a measure of how effective the skin barrier is at keeping moisture within.

Skin capacitance was measured with a Corneometer CM825 (Courage and Khazaka). Skin capacitance is determined by the dielectric nature of the epidermis, which varies depending on the amount of moisture in the skin.

Therefore, skin with different amount of hydration will have different dielectric constants, thus giving different capacitance values.

One week prior to the TEWL and skin capacitance measurements, all subjects were asked to discontinue the use of emollients, topical steroids and any other treatment for their AD. Subjects were rested for at least 15 min prior to measurements being taken from the flexural surface of the forearm (4 cm below the antecubital fossa) that was free from any eczematous rash or infection. The room temperature was kept between 20-22 ^{o}C and humidity between 40–60 %. Additionally, both tests were performed in an open-topped box to limit convection currents and condensation. These standardised conditions were taken to minimise variability in the measurements. Three measurements were obtained for each test from each subject, with the average of the three measurements used for subsequent analysis.

2.5.2 Tape stripping

In addition to being used as a method of protein extraction (as described in Chapter 3), tape stripping was also used as a measure of skin barrier function. Specifically, the number of tape strips required to abrogate the permeability barrier (defined as TEWL > 20 g/m^2/h) had been shown to be a good indicator of skin barrier [145-147]. D-Squame tape discs (14 mm and 22 mm diameter tape discs, CuDerm Corporation), which were specifically designed for SC cell sampling, were used. Each tape was placed on a marked site on the forearm before a spring-loaded device delivering a fixed pressure of 225 g/cm^2 was applied over it for 10 s. The tape was then peeled off unidirectionally using a forceps. Consistency in the applied pressure and tape stripping procedures were maintained to optimise the removal of a consistent amount of SC cells in each tape [250].

2.6 Bicinchoninic acid (BCA) protein assay

The Pierce BCA protein assay kit (Thermo Scientific) was used for all protein quantification. A working reagent was first prepared by mixing 50 parts of BCA Reagent A to 1 part of BCA Reagent B. Bovine serum albumin (BSA) standards ranging from 25-2000 μg/ml were prepared in water. To 200 ul of working reagent was pipetted 10 ul of unknown sample or standard. The resultant solution was then incubated at 37 ^{o}C for 30 min before its absorbance was determined at 562 nm with a BioPhotometer (Fisher Scientific). A standard curve was generated from the BSA standards from which sample concentrations were determined.

2.7 SDS-polyacrylamide gel electrophoresis (SDS-PAGE) and immunoblotting

2.7.1 SDS-PAGE

2 x SDS Sample Buffer

20 mM NaH_2PO_4

0.2 M DTT

2 % (v/v) glycerol

2 % (w/v) SDS

0.001 % bromophenol blue

SDS Running Buffer

30 mM MOPS

60 mM Tris-base

6 mM $NaHSO_3$

0.1 % (w/v) SDS

10 ul of SDS Sample Buffer was mixed with 10 ul of protein samples. These were heated at 100 °C for 2 min before they were loaded onto a 4-20 % RunBlue precast gel (Expedeon). The samples were resolved by electrophoresis in the SDS Running Buffer on a BioRad gel apparatus at 150 V for 40-45 min.

2.7.2 Detection of separated protein

2.7.2.1 Staining with InstantBlue

Staining of the protein bands was performed using InstantBlue protein gel stain (Expedeon), which is a Coomassie-based stain. The SDS-PAGE gel was immersed in approximately 20 ml of InstantBlue and stained for at least 1 h.

2.7.2.2 Immunoblotting

Semi-dry transfer buffer (SDTB)
48 mM Tris
39 mM glycine
20 % (v/v) ethanol

Ponceau S stain
0.1 % (w/v) Ponceau S in 5 % acetic acid

Tris Buffered Saline (TBS)
20 mM Tris
150 mM NaCl
(pH adjusted to 7.5 using HCl)

TBS-tween (TBST)
0.05 % (v/v) Tween 20 (Sigma-Aldrich) in TBS

Blocking Buffer

5 % (w/v) ovalbumin (Sigma-Aldrich) in TBST

Dilution Buffer

1 % (w/v) ovalbumin (Sigma-Aldrich) in TBST

***SuperSignal West Femto Maximum Sensitivity Substrate Working Solution* (Thermo Scientific)**

Substrate components 1 and 2 in equal amount

Immediately following electrophoresis, the SDS-PAGE gel was washed in SDTB for 15 min. Resolved protein bands were transferred onto a Hybond-P PVDF membrane (Amersham) in SDTB at 20 V for 50 min, in a Trans-Blot SD Transfer Cell (Bio-Rad). Following transfer, the membrane was stained briefly with Ponceau S stain to allow visualisation of successful transfer of the protein bands. After washing the stain off with water, the membrane was blocked in Blocking Buffer for 1 h before being incubated with a primary antibody (see Table 2.3) in Dilution Buffer for 1 h at room temperature or overnight at 4 ^{o}C. The blot was then washed three times (5 min each time) in TBST before being incubated in a horseradish peroxidise (HRP)-coupled secondary antibody in Dilution Buffer for 1 h at room temperature. After the blot was washed twice with TBST (5 min each time) and once with TBS (5 min), it was incubated for 5 min in 500 µl of SuperSignal West Femto Maximum Sensitivity Substrate. Specific bands were digitally captured using the VersaDoc Imaging System (Bio-Rad).

Primary antibodies	Species/Description	Dilutions	Company
ab24584	Rabbit polyclonal	1:1000	Abcam
AKH1	Mouse monoclonal	1:200	Santa Cruz
G-20	Goat polyclonal	1:200	Santa Cruz
ab17808	Mouse monoclonal	1:200	Abcam
HRP-coupled secondary antibodies	**Species/Description**	**Dilutions**	**Company**
P0448	Polyclonal goat anti-rabbit	1:10,000	Dako
P0447	Polyclonal goat anti-mouse	1:10,000	Dako
P0449	Polyclonal rabbit anti-goat	1:10,000	Dako

Table 2.3 Primary anti-filaggrin antibodies and HRP-coupled secondary antibodies used in immunoblotting, with their corresponding dilutions used.

2.8 One-way filaggrin-specific enzyme-linked immunosorbant assay (ELISA)

Carbonate-bicarbonate Buffer

One carbonate-bicarbonate buffer capsule (Sigma-Aldrich) in 100 ml distilled water

Tris Buffered Saline (TBS)

20 mM Tris

150 mM NaCl

(pH adjusted to 7.5 using HCl)

TBS-tween (TBST)

0.05 % (v/v) Tween 20 (Sigma-Aldrich) in TBS

Blocking Buffer

1 % (w/v) ovalbumin (Sigma-Aldrich) in TBST

Dilution Buffer

0.1 % (w/v) ovalbumin (Sigma-Aldrich) in TBST

In this novel ELISA system (further discussed in Chapter 4), filaggrin was quantified using two antibodies: a mouse monoclonal IgG_1 anti-filaggrin antibody (ab17808, Abcam), and a biotinylated rat anti-mouse-IgG_1 antibody (550331, BD Pharmingen).

Filaggrin-containing samples were bound to high-binding enzyme immunoassay (EIA) plates (Corning-Costar) with a 1:1 dilution in Carbonate-bicarbonate Buffer (Sigma-Aldrich). These were measured against an 8-point standard curve generated by sequential dilutions of pooled purified filaggrin (200, 100, 50, 25, 12.5, 6.25, 3.125, 0 ng/ml). Samples and standards were analysed in duplicates, loaded in 50 µl volumes per well. The plates were then incubated at 37 ^{o}C for 2 h. Unless stated otherwise, all subsequent steps were separated by five wash steps (full-well volumes) using TBST, where the final wash was forcefully blotted onto absorbent paper towels on a flat surface.

After washing, the plates were then blocked with the Blocking Buffer (200 µl per well) for 2 h at room temperature. Following another wash, ab17808 was added (50 µl per well) at 1:250 dilution before an overnight incubation at 4 ^{o}C. The plates were washed again before 50 µl of the biotinylated rat anti-mouse-IgG_1 antibody was added to each well at 1:2000 dilution. The plates were then incubated at 37 ^{o}C for 2 h. After washing, the biotinylated signal was developed and visualised using a streptavidin/substrate system. This involved adding 50 µl of streptavidin (R&D) at 1:200 dilution into each well and incubating at room temperature for 30 min. After washing, 50 µl of 3,3,5 tetramethylbenzidine (TMB, Sigma-Aldrich) was added to each well for about

30 min at room temperature. Colour development was stopped (without any washing step) with the addition of 25 µl of 2 N H_2SO_4 (Sigma-Aldrich).

All ELISA data were collected on a Synergy HT Multi-Detection Microplate Reader using Gen 5 Microplate Data Collection and Analysis Software (both BioTek Instruments) at a wavelength of 450 nm, with a subtracted reference at 650 nm.

2.9 Mass spectrometry

2.9.1 In-gel digestion of protein

Destaining Solution

50 % (v/v) acetonitrile

Reducing Solution

10 mM DTT

0.2 % (w/v) EDTA

100 mM NH_4HCO_3

Alkylating Solution

50 mM iodoacetamide

100 mM NH_4HCO_3

Trypsin Solution

0.1 µg/µl sequencing grade modified trypsin (Promega) in 50 mM NH_4HCO_3

Peptide Extraction Solution

5 % (v/v) trifluoroacetic acid

50 % (v/v) acetonitrile

Protein bands on SDS-PAGE gels were excised using a disposable scalpel before being further cut into smaller cubes (approximately 1 x 1 mm in size). These were transferred into a microcentrifuge tube containing 200 ul of Destaining Solution and incubated at room temperature for 5 min. The destaining step was then repeated before excess liquid was removed and the gel pieces dried in a Gyrovap for 15 min. Next, the gel pieces were incubated at 56 ^{o}C for 30 min in 15 ul Reduction Solution and cooled to room temperature. Any excess Reduction Solution was then removed before the gel pieces was incubated at room temperature, in the dark for 30 min, with 10-50 µl of Alkylating Solution. The Alkylating Solution was removed and the gel pieces washed with 200 ul of 100 mM NH_4HCO_3 for 10 min. The solution was removed before dehydrating the gel pieces with 200 ul neat acetonitrile for 10 min. The washing and dehydration process was repeated prior to drying the gel pieces in a Gyrovap for 15 min. Next, 5 ul of Trypsin Solution was added to the gel pieces, which were then incubated at 37 ^{o}C for 15 min. To the gel pieces was added 10-15 ul of 50 mM NH_4HCO_3 before they were incubated at 37 ^{o}C overnight. The digestion liquid was removed and transferred to a new microcentrifuge tube. Enough Peptide Extraction Solution was then added to immerse the gel pieces, which were shaken at room temperature for 30 min. The extraction solution was then pooled with the digestion liquid from the previous step and dried in a Gyrovap. The dried peptides were resuspended in 10 ul of 0.1 % formic acid prior to analysis by mass spectrometry.

2.9.2 In-solution digestion of protein

Resuspension Solution

50 mM NH_4HCO_3

Reducing Stock Solution

200 mM DTT

100 mM NH_4HCO_3

Alkylating Stock Solution

1 M iodoacetamide

100 mM NH_4HCO_3

Trypsin Solution

0.1 µg/ul sequencing grade modified trypsin (Promega) in 200 µL acetic acid

Purified protein was dried in a Gyrovap before being resuspended in 100 µl of 50 mM NH_4HCO_3. The sample was then reduced by adding 5 µl of Reducing Stock Solution and heating at 56 ^oC for 30 min. Next, 4 µl of the Alkylating Stock Solution was added to the sample and incubated at room temperature in the dark for 1 h. The alkylation was stopped by adding 20 µl of the Reducing Stock Solution and incubating the sample at room temperature for 1 h. Next, enough Trypsin Solution was added to give a ratio of trypsin to sample of 1 µg trypsin to 20 µg protein. The sample was incubated overnight at 37 ^oC before digestion was terminated by the addition of 1 % formic acid.

2.9.3 Zip tipping

Wash Buffer

0.1 % (v/v) formic acid

Elution Buffer

0.1 % (v/v) formic acid

50 % (v/v) acetonitrile

$ZipTip_{18}$ and $ZipTip_4$ (Millipore) were used to desalt and concentrate samples prior to MALDI-TOF analysis. The former was used for tryptic-digests while the latter was used for intact protein samples. Protein samples (both

intact and tryptic-digests) were dried in a Gyrovap before being resuspended in 20 µl of Wash Buffer. A new ZipTip was first equilibrated by aspirating 10 ul of Elution Buffer onto the tip before dispensing the buffer. This was repeated twice before the tip was washed three times with the Wash Buffer. The sample was then loaded onto the tip by aspirating and dispensing the sample 10-15 times for maximal binding. The tip was then washed three times with the Wash Buffer. Finally, 10 ul of the Elution Buffer was aspirated and dispensed 3-5 times to elute the sample.

2.9.4 MALDI-TOF MS

Matrix for peptide digest analysis

10 mg/ml α-cyano-4-hydroxycinnamic acid
50 % (v/v) acetonitrile
0.05 % (v/v) formic acid

Matrix for intact protein analysis

10 mg/ml sinnapinic acid
50 % (v/v) acetonitrile
0.05% (v/v) formic acid

0.5 µl of sample (tryptic-digest or intact protein) was spotted onto a 96-well MALDI plate before an equal volume of the appropriate matrix was added to it. These were then air-dried before analysis with a MALDI De-STR (ABI) mass spectrometer. Data were collected in positive reflectron mode using a 337 nm nitrogen laser. Each spectrum obtained was an average of 200 spectra (200 laser shots per spot). For intact protein analysis, a summation of at least three average spectra was performed. All spectra were batch processed in Data Explorer with default settings of advanced background correction, noise filter and de-isotoping.

2.9.5 Online nano LC-MS/MS

Solvent A

0.1 % (v/v) formic acid

2 % (v/v) acetonitrile

98 % (v/v) distilled water

Solvent B

0.1 % (v/v) formic acid

20 % (v/v) acetonitrile

80 % distilled water

Tryptic-digests (in-gel or in-solution) were separated online by reversed-phase nano LC. This was performed on an UltiMate 3000 (Dionex) equipped with a C18 PepMap100 trap (C18, 300 µm i.d. x 5 mm; 5 µm, 100 Å, Dionex) and C18 PepMap100 analytical column (C18, 75 µm i.d. x 15 cm; 3 µm, 100 Å, Dionex). The protein concentration in the samples was adjusted to approximately 25 µg/ml. Each analysis was then performed by injecting 5 µl of this diluted solution, and subsequently repeated with 10 µl. The trap column was loaded and washed with 0.1 % trifluoroacetic acid (TFA) at a flow rate of 30 µl/min. Analytical flow rate was 0.35 µl/min with the column temperature maintained at 40 ^{o}C. An increasing gradient of 4-90 % of Solvent B across 35 min was applied to elute the peptides. This was followed by a 5-min washout phase using 100 % Solvent B, before the column was re-equilibrated for 5 min with 95 % Solvent A/4 % Solvent B.

The eluent was electrosprayed directly into the High Capacity Trap mass spectrometer (HCT Ultra, Bruker) through a non-coated picotip (360 µm o.d., 20 µm i.d., 10 µm i.d. tip, New Objective, MA) mounted on an online nanospray source (Agilent).

The HCT ion trap was operated in positive ion mode, and ions with a mass range of 300–1500 *m/z* were accumulated in the ion trap for a maximum of 200 ms. The Auto MS/MS function was used for alternating precursor ion scanning and the MS/MS of three precursor ions fragmented by CID. Any ion from which a spectrum was collected was added to an exclusion list for 2 min.

Raw data from the HCT was processed using DataAnalysis and Biotools (both from Bruker). Peak lists in Mascot Generic Format (MGF) were submitted to Mascot using an in-house MASCOT service (Matrix Science)

2.10 Statistical analysis

Statistical analysis was performed using PASW Statistics 18.0. Depending on whether the data were normally distributed, either the t-test or the Mann-Whitney U-test was used to compare the variables between the two AD subgroups. For the comparison of categorical data between the AD subgroups, either the chi-square test or the Fisher's exact test was used. *P*-values of < 0.05 were taken to be significant.

Chapter 3 Development and Optimisation of Filaggrin Extraction and Purification

3.0 DEVELOPMENT AND OPTIMISATION OF FILAGGRIN EXTRACTION AND PURIFICATION

To allow for accurate structural studies of filaggrin using mass spectrometry, an adequate amount of filaggrin had to be extracted and purified from individuals. To date, only three laboratories had described the extraction and purification of filaggrin: Dale/Steinert/Walsh's group at the University of Washington, von Essen's group at the University of Helsinki and Serre's group at the University of Toulouse. The methods described by the first two groups [92, 251] involved using a denaturing extraction buffer while Serre's group used a Tris/EDTA buffer [252]. Interestingly, the final purified filaggrin from each group had different molecular weights as seen on SDS-PAGE. Also, while the purified filaggrin from the University of Washington group was strongly basic, that from Serre's group produced an acidic/neutral isoform of the protein (pI of 5.8-7.4). The Helsinki's group provided no pI information for their protein.

In all these papers, filaggrin was extracted from either human foreskins or breast reduction tissues. To date, no one has attempted to extract filaggrin by tape stripping.

All the extraction and purification methods described had common features. First, the epidermal layer was removed by either heating the skin tissue alone, or immediately plunging the skin into ice water after the application of heat. The aim was to separate the epidermal layer from the underlying skin. Next, some form of homogenisation was performed to solubilise the protein extracted. The subsequent purification of filaggrin involved the use of LC, primarily to separate out keratin which is the most abundant protein found in the epidermis.

There were considerable difficulties encountered while attempting to replicate the filaggrin extraction and purification procedures published to date. One reason was the absence of sufficient details; another was the use of

reagents (e.g. 1,1,2-trichloro-trifluoro-ethane) that were no longer commercially available. Additionally, the use of tape stripping to extract filaggrin from skin also meant that further modifications were required in order to optimise the purification process. The procedures described were, nonetheless, mostly based on that described by Thulin and Walsh [253].

3.1 Extraction of filaggrin

3.1.1 Extraction from human breast tissues

In the initial stages of developing and refining the extraction and purification of filaggrin, skin from human breast tissues was used. Filaggrin thus extracted was also used in the development of the filaggrin-specific ELISA.

Discarded breast tissues from patients who underwent breast reduction procedures performed by a local plastic surgeon were collected. Informed and written consent were obtained prior to surgery. None of these volunteers had AD and were therefore presumed to have wild-type *FLG*, although none were genotyped.

The breast tissues were heated at 55 ^{o}C in a 15 mM EDTA, 85% PBS solution for 5 min. This allowed the epidermis to be peeled off. About 1 g wet weight of epidermis was generally obtained from a bilateral breast reduction procedure and was used for each purification procedure. The epidermis obtained was then roughly divided and placed into 10 Precellys CK14 ceramic beads tubes (Bertin Technologies).

800 µl of a buffer containing 9 M urea and 50 mM Tris (pH 8), and several crystals of phenylmethylsulfonyl fluoride (PMSF) were also added into each tube. The tubes were then placed into a Precellys 24 homogeniser (Bertin Technologies) and subjected to two sessions of homogenisation. Each session

consisted of three cycles of 20-s homogenisation at 5,500 rpm, with a 30-s pause between each cycle. The tubes were then initially centrifuged at 12,000 *g* for 10 min at 4 ^{o}C. The supernatant from each tube was combined before further centrifugation at 50,000 *g* for 1 h. The combined supernatant was then sequentially filtered through a 5 μm and 0.22 μm syringe filters to remove any particulates prior to purification.

3.1.2 Extraction using tape stripping

The use of tape stripping to extract filaggrin from skin is a method first described in this study. Tape stripping has the advantages of being minimally-invasive, relatively pain-free and quick. As described earlier, D-Squame tapes (CuDerm) were used, with 100 tapes collected from four to six sites on the medial aspect of each subject's forearm for each preparation. These were placed in a conical flask containing 30 ml of extraction buffer (9 M urea and 50 mM Tris, pH 8) and shaken at 250 rpm in a shaking incubator at 20 ^{o}C for two days. The tapes were then manually rubbed to optimise the removal of the material adherent to them. The extract was then sequentially filtered through a 5 μm and a 0.45 μm filter prior to purification.

3.2 Comparison of various homogenisation methods

In order to extract and purify filaggrin from skin tissues, the protein needs to be solubilised in an extraction buffer. Full thickness skin poses a challenge for homogenisation mainly because of the elastic nature of the skin tissue. The best homogenisation method is one that produces uniform homogenisation with minimal loss of skin sample. Several homogenisation methods are generally used in the extraction of protein from skin tissues. These include the Dounce homogeniser, grinding with sand, using a rotator/stator

type tissue homogeniser and homogenising with tubes containing ceramic beads.

3.2.1 Dounce homogeniser

This is essentially a round glass pestle that is manually and repeated driven into a glass tube containing the skin tissues and extraction buffer. The number of strokes and the force administered are obviously important in determining its effectiveness in homogenising the sample. For the breast tissue samples, 50 strokes were administered. There were always residual bits of unhomogenised epidermis, even when up to 200 strokes were administered. Also, there was significant loss of sample during the homogenisation process due to the transfer of sample into and out of the glass tube, as well as those adhering to and precipitating on the glass tube walls. None of the purification process using the Dounce homogeniser produced detectable amount of filaggrin.

3.2.2 Rotor/stator type homogeniser

The tissue tearor (Biospec Products) is a rotor/stator type tissue homogeniser that is supposed to have the capability of rapidly homogenising, dispersing and emulsifying samples. It has a rotor that turns at 5-30,000 rpm. However, significant problems were encountered while using this method of homogenisation. First, the epidermis had to be cut up into bits small enough to get through the protective outer casing around the rotor blade. Second, even when the epidermal tissues were small enough to get through the protective outer casing, they were still frequently stuck between this casing and the rotor. Finally, even after 30 minutes of vigorous homogenisation, there were still visible unhomogenised epidermal tissues. Once again, purification of epidermal

extracts homogenised this way did not produce sufficient filaggrin protein for identification.

3.2.3 Precellys 24 tissue homogeniser (Bertin Technologies)

Epidermal tissues were placed into single-use Precellys CK14 tubes containing ceramic beads (Bertin Technologies). High-speed whirl mixing in a 'figure of eight' motion resulted in the rapid, uniform homogenisation of the samples. The final extract is homogenous and milky-white, with no residual tissue fragments visible. The effective homogenisation of epidermal tissues required two sessions of homogenisation with a 3-min break between each. Each session consisted of three cycles of 20-s homogenisation at 5,500 rpm, with a 30-s pause between each cycle. Twenty-four samples can be processed at any one time. The obvious advantages of the Precellys homogeniser were the speed of homogenisation, minimal loss of the skin tissues, and most importantly, effective homogenisation since it was the only method tried that produced sufficient filaggrin after purification to allow for identification using mass spectrometry.

3.3 Purification of filaggrin

3.3.1 Weak anionic exchange liquid chromatography

Buffer A (pH 8.0)
9 M urea
50 mM Tris-base

Buffer B (pH 8.0)

9 M urea

50 mM Tris-base

1 M NaCl

A previous study on mouse epidermis showed that extraction with a denaturing buffer dissolved about 95 % of the tissue proteins, of which about 60% consisted of keratin subunits with much of the remainder being filaggrin [254]. So the main aim during purification was the removal of keratin from the initial protein extract.

Filaggrin has a strongly cationic charge [92], and so can be separated easily from the anionic keratin subunits using ion exchange chromatography. Most LC protein purification generally starts with an anion exchange chromatography. In this study, a DEAE Sepharose FF (GE Healthcare) column (V_t 5 ml, 1.6 x 2.5 cm) attached onto an AKTAexplorer system (GE Healthcare) was used. After an initial wash of 2 column volume (CV) with Buffer A, the filtered extract was pumped into the weak anionic exchange column at 5 ml/min and the flow-through collected in 1 ml fractions. The bound keratin was subsequently eluted from the column with 5 CV of Buffer B (Figure 3.1).

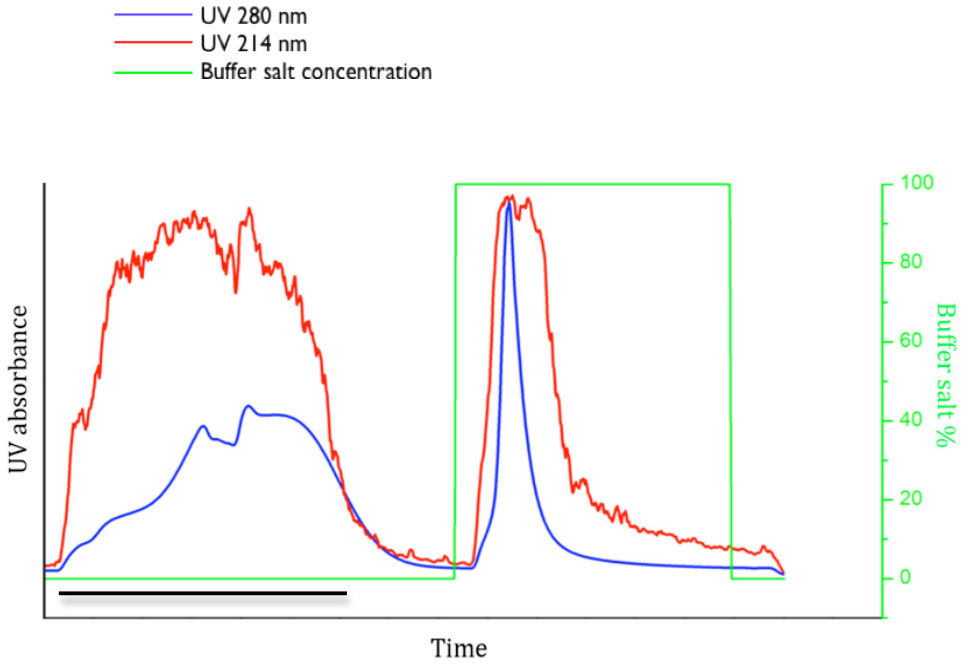

Figure 3.1 Typical chromatogram from the DEAE sepharose purification step. The blue and red curves are the UV traces at 280 nm and 214 nm, respectively. UV at 280 nm wavelength detects aromatic groups of protein side chains, while UV at 214 nm wavelength is about 10 times more sensitive as it detects peptide bonds. However, the latter is also less specific because it also picks up nucleotides, certain metabolites and buffer salts. The green curve indicates the ionic strength of the elution buffer. Fractions were collected during the run, and the flow-through fractions corresponding to that under the broad peak (indicated by the horizontal black line) were pooled for further purification.

3.3.2 Acetone precipitation

Resuspension buffer

47 mM Tris (pH 8.0)

5 mM EDTA (pH 7)

1 mM PMSF

The flow-through fractions containing filaggrin were pooled and precipitated by adding 3 volume of ice-cold acetone and kept in ice for 10 min. This allowed the protein to be concentrated, as well as the removal of salt and lipid-soluble contaminants. The main disadvantage was that invariably, some of the precipitated protein would fail to resuspend, resulting in a loss of protein. After centrifugation for 20 min at 12,000 *g*, the supernatant was discarded and

the precipitate resuspended in 10 ml of Resuspension Buffer. The suspension was centrifuged at 12,000 *g* for another 20 min and the supernatant collected.

In the case of filaggrin extraction using tape stripping, this acetone precipitation step was replaced by a desalting step using a gel filtration column instead. This was because the amount of protein extracted by tape stripping was much less compared to using homogenised epidermis and therefore only a very small amount of precipitate was formed following acetone precipitation, with significant loss of protein upon resuspension of the precipitate. Additionally, since tape stripping was a 'cleaner' extraction method without the substantial lipidaceous contaminants present in full epidermis, there was even less reason for this precipitation process. Nonetheless, prior to the subsequent purification steps, there was still the need to exchange the initial urea-based buffer to the Resuspension Buffer.

3.3.3 Buffer exchange with gel filtration chromatography

For the purification of filaggrin extract from tape stripping, a HiPrep 26/10 (GE Healthcare) gel filtration column (V_t ~53 ml, 2.6 x 10 cm) was used to replace the initial urea buffer to the Resuspension Buffer. Pooled fractions containing filaggrin from the DEAE-Sepharose column flow-through were applied to the column pre-equilibrated in Resuspension Buffer, at a flow rate of 8 ml/min. Fractions under the protein peak from the chromatogram was collected for further purification.

3.3.4 Strong cation exchange liquid chromatography

Buffer A

100 mM NaH_2PO_4 (pH 3.5)

Buffer B

100 mM NaH_2PO_4 (pH 3.5)

1.5 M NaCl

To further purify the protein extract, a strong cation exchange column was used. The aim of this was to bind the strongly cationic filaggrin to the column matrix, which would then be eluted and collected subsequently. The final supernatant from the acetone precipitation step (for breast tissue extracts), or the pooled fractions from the desalting step (for tape strip extracts) was applied to a POROS S/10 (Applied Biosystems) strong cation exchange column (V_t 1.7 ml, 4.6 x 100 mm). A chromatogram was developed at a flow rate of 10 ml/min as follows: After an initial wash of 2 CV in 100 mM NaH_2PO_4 buffer (pH 3.5), and a further 2 CV wash with 66 % Buffer A/33 % Buffer B, a gradient to 33 % Buffer A/66 % Buffer B was developed over 10 CV. After this, there was a step up to 100 % Buffer B. Fractions of 1 ml volume were collected and analysed by immunoblotting to identify fractions containing filaggrin (Figure 3.2).

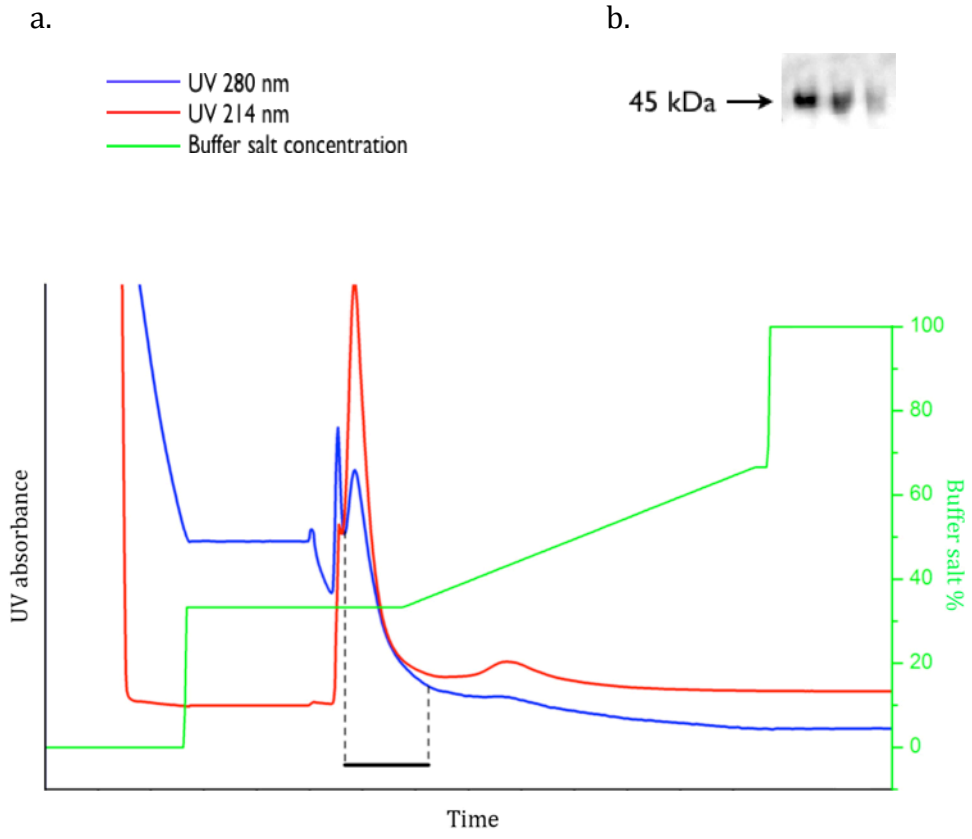

Figure 3.2 (a) Typical chromatogram from the POROS S/10 strong cation exchange column purification step. The blue and red curves are the UV traces at 280 nm and 214 nm, respectively. The green curve indicates the ionic strength of the elution buffer. Fractions were collected during the run, and those corresponding to that under the main peak (indicated by the horizontal black line) were pooled. (b) Immunoblotting of these fractions using a monoclonal mouse filaggrin antibody confirmed filaggrin bands at around 45 kDa.

3.3.5 Desalting step using reversed-phase chromatography

Finally, in order to desalt the buffer prior to MS analysis, the pooled fractions from the previous purification step were applied to a POROS R1 (Applied Biosystems) reversed-phase column (V_t 0.1 ml, 2.1 x 30 mm). A step gradient is developed from 0 to 80 % acetonitrile in 0.05 % TFA. Fractions under the sharp protein peak were collected for MS analysis (Figure 3.3).

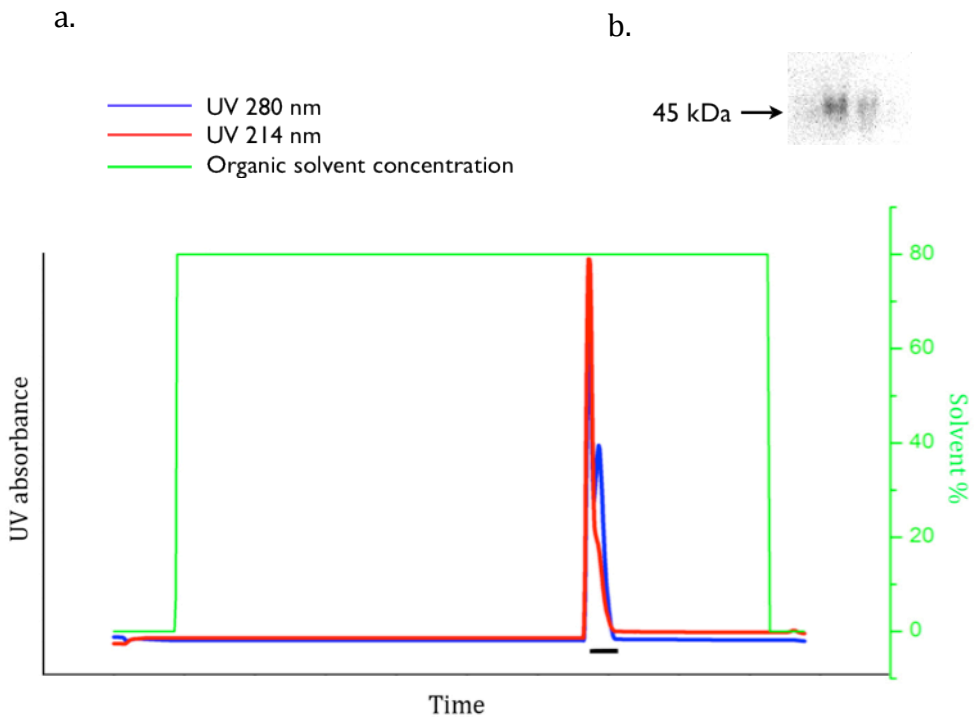

Figure 3.3 (a) Typical chromatogram from the POROS R1 reversed-phase column desalting step. The blue and red curves are the UV traces at 280 nm and 214 nm, respectively. The green curve indicates the concentration of the organic solvent. Fractions under the sharp peak (indicated by the horizontal black line) were pooled. (b) Immunoblotting of these fractions using a monoclonal mouse filaggrin antibody confirmed filaggrin bands at around 45 kDa.

3.4 Modifications made to extraction and purification process

Various modifications to the extraction and purification of filaggrin were attempted during this study in the hope of increasing the yield of the final purified filaggrin. These included increasing the size of the tape strips used (by replacing the 14 mm-diameter tapes with larger 22 mm-diameter ones), extending the extraction time (from one day to two days) and replacing the acetone protein precipitation step with an LC desalting step to reduce protein loss. A flow chart detailing these modifications is shown in Figure 3.4.

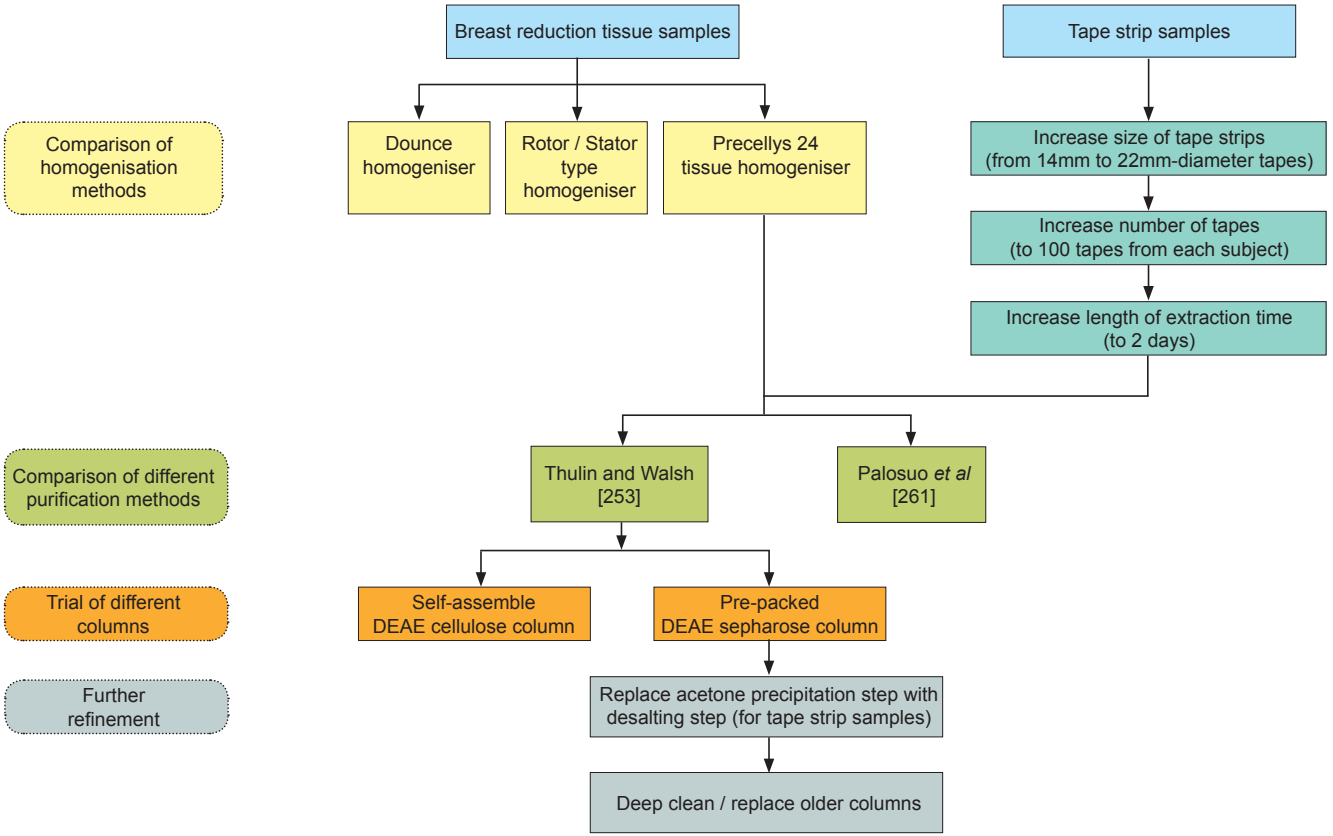

Figure 3.4 Flowchart of modifications made to the filaggrin extraction and purification process

Chapter 4 Development of a Filaggrin-specific ELISA

4.0 DEVELOPMENT OF A FILAGGRIN-SPECIFIC ELISA

Genotyping of the *FLG* gene is technically difficult due to its size and repetitive nature of the filaggrin subunits within the gene. Hence this is currently only routinely performed by a few genetics departments in the country, and is consequently time-consuming and expensive. There are, therefore, obvious practical benefits to having a quick screening test (e.g. an ELISA system) to detect and quantify filaggrin in the skin. Previous biochemical and immunohistochemical studies have shown that any null mutation in the *FLG* allele result in an absence of filaggrin expression, which means that individuals who are homozygous or compound heterozygous for the *FLG* mutation do not express filaggrin in their skin, and that individuals who are *FLG* heterozygous express less filaggrin [23, 73, 255]. Therefore, if a relatively large amount of filaggrin protein is detected in an individual's skin, it is likely that that individual will have a wild-type *FLG* genotype and hence will not require genotyping. Conversely, if filaggrin is found to be relatively reduced or absent in the skin, then it may infer the presence of a *FLG* mutation. Confining genotyping to this latter group would therefore save resources.

The aim of the work described in this chapter was to develop a filaggrin-specific ELISA system. There are two common ELISA formats - 'one way' and 'sandwich' ELISAs. The 'one way' ELISA involves coating a 96-well plate with filaggrin-containing samples before the addition of filaggrin-specific antibodies to detect and quantify the amount of the filaggrin. The 'sandwich' ELISA involves pre-coating the wells with one anti-filaggrin antibody prior to sample addition, before a different detecting filaggrin antibody was added. As the latter has the advantage of better sensitivity and specificity, developing a filaggrin-specific 'sandwich' ELISA was the initial focus of this study.

4.1 Development of a filaggrin-specific 'sandwich' ELISA

The 'sandwich' ELISA involved pre-coating a high-binding EIA plate with an anti-filaggrin antibody as a 'capture' layer, followed by a protein-rich blocking step to reduce subsequent non-specific binding. The filaggrin-containing sample was then added before another anti-filaggrin antibody (different from that used as the capture antibody) was used as the 'primary detection antibody'. Next, the relevant biotinylated antibody ('secondary detection antibody') against the primary detection antibody was added for subsequent streptavidin/substrate detection, which was a colourimetric development system used by many commercial ELISA systems.

At the start of developing this ELISA, there were only a limited number of filaggrin antibodies commercially available. Three were initially obtained: a rabbit (RaF) polyclonal (ab24584, Abcam), a mouse (MaF) monoclonal (AKH1, Santa Cruz Biotechnology), and a goat (GaF) polyclonal (G-20, Santa Cruz Biotechnology). Details of these antibodies are shown in Table 4.1.

Antibodies	Species/Description	Immunogen	Company
ab24584	Rabbit polyclonal	DSQVHSGVQVEGRRGH (corresponding to amino acids 24-39 of filaggrin)	Abcam
AKH1	Mouse monoclonal	Purified filaggrin of foreskin of human origin	Santa Cruz
G-20	Goat polyclonal	Peptide mapping within an internal region of filaggrin of human origin	Santa Cruz

Table 4.1 Details of the three anti-filaggrin antibodies assessed for suitability for 'sandwich' ELISA development. All three antibodies detected filaggrin as shown in Figure 4.1.

Immunoblot analysis confirmed that all three detected filaggrin (Figure 4.1). Initial experiments utilised the antibodies (all at 0.1 μg/well) in three different orientations: 1) RaF as capture/MaF as primary detection, 2) MaF as capture/GaF as primary detection, and 3) GaF as capture/RaF as primary detection. Skin extracts from two healthy control subjects (A and B) were analysed. The concentrations of the biotinylated secondary detection antibodies were those suggested by the manufacturers. Results (shown in Figure 4.2) indicated that the last orientation (GaF/RaF) was the most promising, with fairly linear optical density (OD) readings, although detection was saturated with high readings from the control wells. This orientation was therefore further investigated.

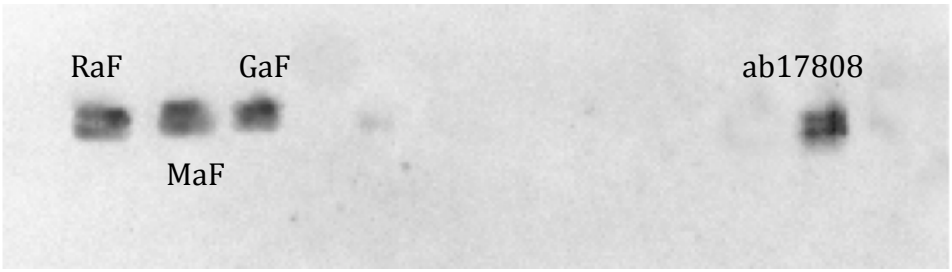

Figure 4.1 Immunoblot confirming that the three anti-filaggrin antibodies (RaF, MaF and GaF) used in the development of the 'sandwich' ELISA detected filaggrin. Also shown is filaggrin detected using the mouse monoclonal anti-filaggrin antibody (ab17808) used in the development of the 'one way' ELISA (Chapter 4.2).

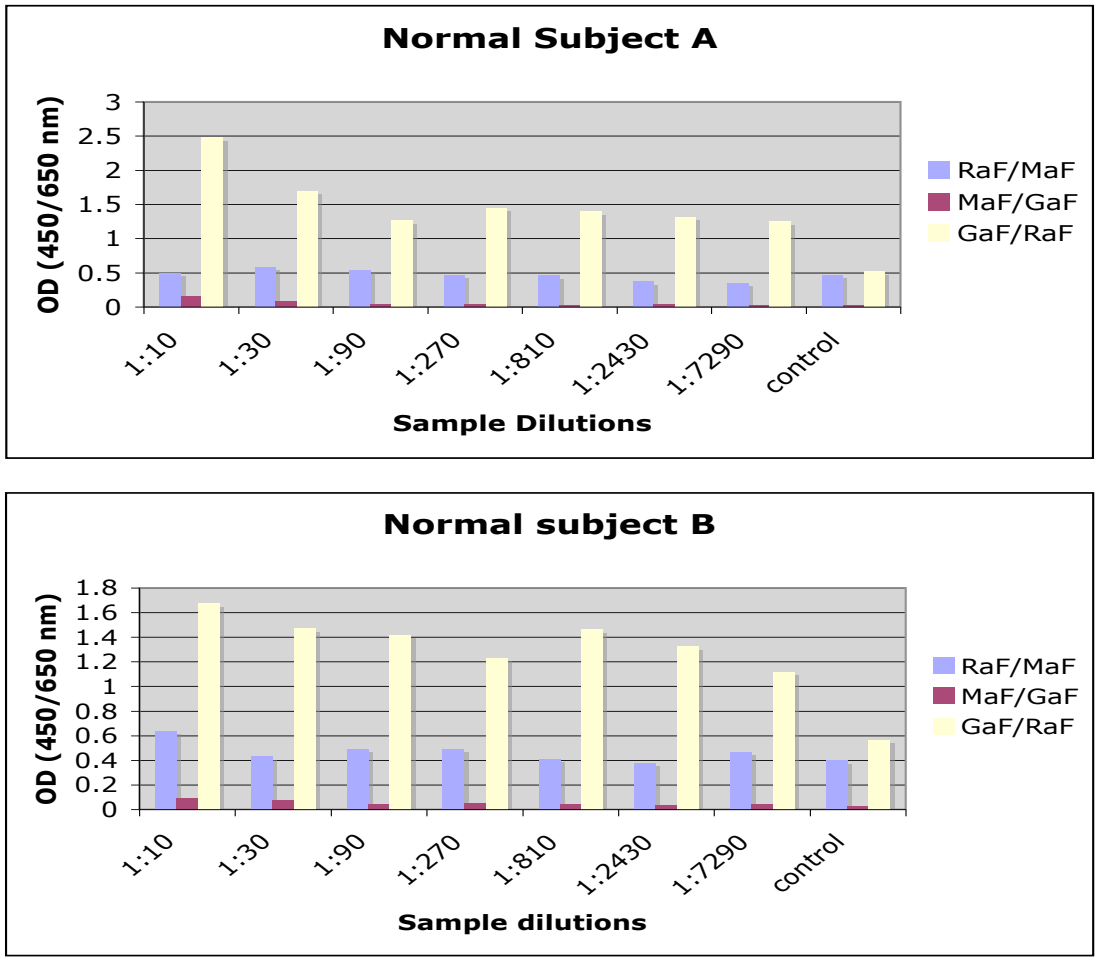

Figure 4.2 Results of ELISA experiments using three anti-filaggrin antibodies in three different orientations. Skin extracts from two healthy normal subjects (A and B) were analysed, with the samples sequentially diluted as shown. The concentration of the three anti-filaggrin antibodies was 0.1 μg/ml, while those of the biotinylated secondary detection antibodies were as per manufacturers' recommendations. The last orientation (GaF/RaF) appeared the most promising with fairly linear OD readings. However, OD readings from the control wells were high. This high background was investigated further (see Section 4.1).

In an attempt to reduce the detection saturation, the concentration of the RaF capture antibody was variably reduced (0.1, 0.03, 0.01 µg/well) in a subsequent experiment. This showed that 0.01 µg/well of RaF was sufficient to detect filaggrin, although the detection was still too saturated with the OD signals from the control wells giving unacceptably high readings. Hence, the concentration of the GaF primary detection antibody was reduced while the concentration of the RaF capture antibody as fixed at 0.01 µg/well. This showed

that GaF at a concentration of 0.01 µg/well was sufficient to give good detection, although the high OD signals in the control wells persisted.

In subsequent experiments, one or more of the antibodies were omitted in the negative control wells in order to study the nature of any non-specific binding that was the likely cause of the high OD signals in the control wells. Table 4.2 shows the antibodies added to the control wells in these experiments.

Experiments	Antibodies within the control wells	Results
1	RaF, GaF and secondary detection antibody	High OD signals
2	RaF and secondary detection antibody	Low OD signals
3	Secondary detection antibody only	Low OD signals

Table 4.2. Experiments to study the nature of possible non-specific binding. One or more of the antibodies were omitted in the control wells. The secondary detection antibody used was a polyclonal rabbit anti-goat biotinylated antibody (E0466, DakoCytomation). Results suggest non-specific binding between RaF and GaF.

The results of these experiments suggested the presence of non-specific binding between RaF and GaF. Subsequent experiments included the use of GaF that was pre-incubated overnight at 4 ^{0}C with rabbit serum, as well as the addition of rabbit serum in the blocking and dilution buffers. Unfortunately, these alterations did not affect non-specific signals. Finally, to exclude the possibility that the blocking step was inefficient, BSA was replaced with ovalbumin as the blocking agent. This brought about a dramatic general reduction in the OD signals, not just in the control wells but also in the sample wells. Various alterations to the protocol were subsequently implemented in an attempt to increase the sample OD signals while keeping 'blank' signals low. These included testing other orientations of the antibodies with ovalbumin as

the blocking agent, as well as increasing the concentration of the various antibodies. However, none of these were successful in eradicating non-specific signal.

It was eventually decided that the ‘sandwich’ ELISA was not sufficiently specific with these three anti-filaggrin antibodies in any orientation. Hence, efforts were subsequently focussed on just developing a 'one way' ELISA.

4.2 Development of a filaggrin-specific 'one way' ELISA

The 'one way' ELISA involved coating a high-binding EIA plate with a filaggrin-containing sample. This was followed by a protein-rich blocking step to minimise subsequent non-specific binding before an anti-filaggrin antibody was added as a ‘primary detection’ antibody. A biotinylated antibody raised against the relevant species of the primary antibody was then added to detect the bound anti-filaggrin antibody (‘secondary detection step’). Biotinylated binding was then quantified with the addition of Streptavidin-HRP/substrate.

At the time when the decision was made to focus on developing a 'one way' ELISA, several more anti-filaggrin antibodies became available commercially while others that were previously available (such as RaF, ab24584) were no longer sold. A new mouse monoclonal antibody (ab17808, Abcam) raised against a recombinant full-length filaggrin was purchased for the purpose of developing this assay. Again, immunoblot analysis confirmed that it detected filaggrin (Figure 4.1). Initial experiments aimed to determine the detection sensitivity of ab17808, with the EIA plate coated with serial 10-fold dilutions of filaggrin standards ranging from 1000 ng/ml to 1 pg/ml. The wells were then blocked with ovalbumin, before ab17808 (at 1:250 dilution) was added as the primary detection antibody. Following this, a biotinylated rat anti-mouse-IgG_1 antibody (550331, BD Pharmingen) was added as the secondary detection antibody (1:2000 dilution) before streptavidin/substrate

visualisation. Antibodies concentrations were selected either on the basis of previous chequerboard titres, or as per manufacturers' recommendations. This experiment demonstrated that, at these antibodies concentrations, filaggrin was detected from 1000 to 10 ng/ml. In order to increase detectable colourimetric signal, the substrate development duration was extended from 10 minutes to 30 minutes, which resulted in good standard curves with a linear profile between 200 to 25 ng/ml. Figure 4.2 shows a typical standard curve.

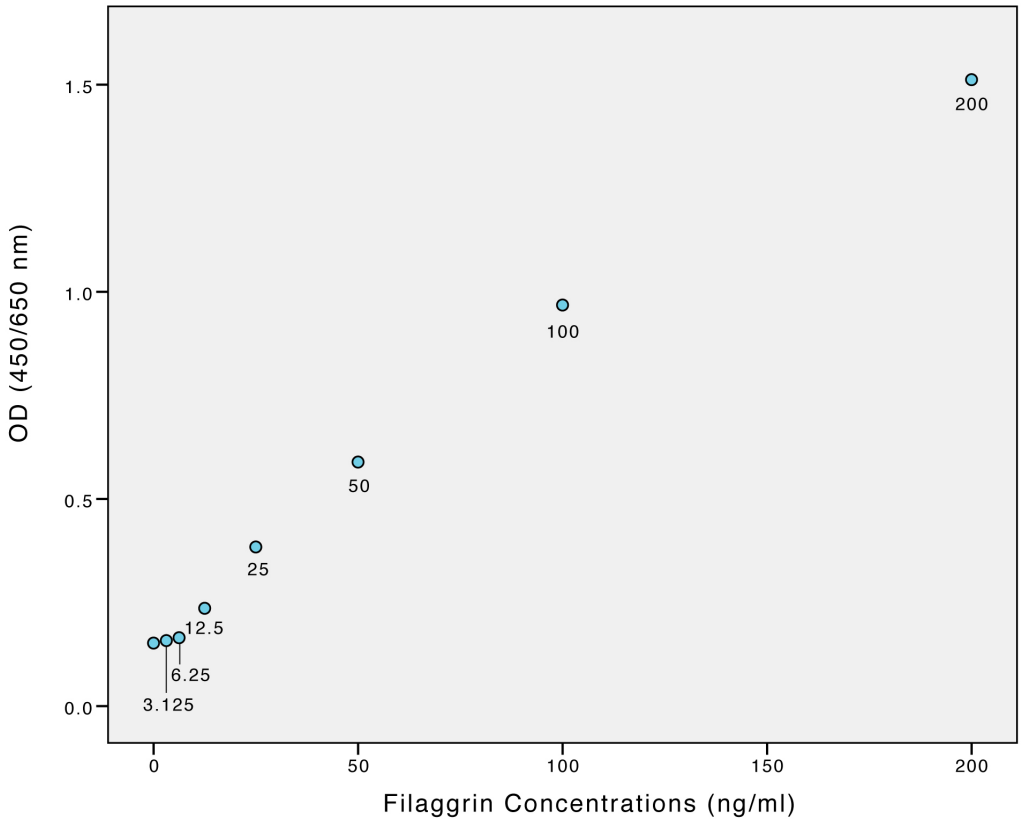

Figure 4.3 A typical standard curve obtained with the 'one way' filaggrin ELISA, showing good linearity between concentrations 200 to 25 ng/ml. The full protocol for the ELISA is detailed in Chapter 2.9.

In summary, this chapter describes the development of a novel ELISA that can quantify filaggrin with a detection sensitivity of approximately 30 ng/ml. Given more time and resources, newer anti-filaggrin antibodies could have been purchased and tested to refine the 'sandwich' ELISA that was limited by non-specific binding. Recently, a filaggrin-specific 'sandwich' ELISA has, in fact, been marketed by UCSN Life Science (Wuhan, China). According to the assay's documentation, it is capable of detecting human filaggrin from tissue homogenates and biological fluids, with a detection lower limit of 312 pg/ml. If validated, this would be much more sensitive than the one-way filaggrin ELISA described in this chapter.

Chapter 5 Correlation of *FLG* variants with AD and skin barrier dysfunction

5.0 CORRELATION OF *FLG* VARIANTS WITH AD AND SKIN BARRIER DYSFUNCTION

FLG loss-of-function mutations are associated with early onset, and persistent AD [31]. In the presence of AD, they also predispose towards asthma and hay fever [42]. It has previously been shown that skin barrier dysfunction is a feature of AD skin, as demonstrated by raised TEWL and reduced SC hydration [15, 242]. However, the few studies that have looked at these measures in relation to *FLG* status have reported inconsistent results [243, 244].

Although there is an unequivocal correlation between *FLG* mutations and atopic disease, there is less evidence for a defective skin barrier function in filaggrin-related AD. The primary aim of this functional study, therefore, was to determine whether *FLG* mutations correlated with altered skin barrier function in AD subjects. Skin barrier function was assessed using three functional measures, specifically TEWL, skin capacitance (which measures SC hydration), and the number of tape strips required to achieve TEWL >20 $g/m^2/h$. In addition, the amount of protein extracted with tape strips was also quantified in eight of these subjects (four from the filaggrin-related AD group and four from the wild-type AD group). This was to test a hypothesis developed from an unexpected finding reported by Nemoto-Hasebe *et al* [244], who showed that SC thickness was greater in filaggrin-related AD compared to wild-type AD skin. To possibly explain this finding, it was hypothesised in this study that corneocytes in filaggrin-related AD skin were less adherent to one another and therefore less densely packed, which should translate to more corneocytes (and therefore more protein) being removed by each tape strip. Testing this hypothesis was the secondary aim of this study.

The cohort in this functional study consisted of only mild and moderate AD subjects, which were representative of the majority of AD sufferers. As the

main objective was to study the effects of *FLG* mutations on the AD phenotype, non-AD subjects were not included.

5.1 Correlation between *FLG* variants and the presence and severity of AD

A total of 55 mild to moderate AD subjects of Western European ancestry were recruited. All were screened for the four *FLG* null mutations most commonly found in European populations (2282del4, R501X, R2247X and S3247X).

Forty-two of the subjects were labelled 'wild-type AD' (that is, they did not possess any of the four *FLG* mutations screened for). The remaining 13 were labelled 'filaggrin-related AD'. Among this latter group, 12 were *FLG* heterozygotes (of which 10 had the 2282del4 mutation, three had the R501X mutation, one had the S3247X mutation, and one was a compound heterozygote [2282del4/R501X]). Only one subject was found to be homozygous for the *FLG* mutation (R501X).

The demographic and clinical data of these subjects are shown in Table 5.1. Notably age, sex, a history of asthma, a family history of atopy and mean IgE level were similar between the filaggrin-related AD and wild-type AD groups. On the other hand, the prevalence of hay fever was found to be significantly higher in the filaggrin-related AD group (85% versus 53%, $p < 0.05$). The severity of AD in the two groups was also similar, as demonstrated by the similar SASSAD scores.

	Filaggrin-related AD	Wild-type AD
Number of subjects	13 (24%)	42 (76%)
Mean age ± SEM	36.0 ± 3.5	36.2 ± 2.1
Male	5 (39%)	14 (33%)
Asthma	5 (39%)	17 (40%)
Hay fever*	11 (85%)	22 (52%)
Family history of atopy	11 (85%)	32 (75%)
Mean total IgE (IU) ± SEM	420.1 ± 238.0	731.3 ± 220.3
Mean SASSAD score ± SEM	11.4 ± 2.1	12.4 ± 1.4

Table 5.1 Demographic and clinical data of the filaggrin-related AD and wild-type AD groups. Age, sex, a history of asthma, a family history of atopy and mean IgE level were similar between the two groups. However there was a significantly higher prevalence of hay fever in the filaggrin-related AD group compared to the wild-type AD group (85% vs 53%, $p < 0.05$). The SASSAD score (which measured AD severity) was found to be similar between the two groups (11.4 ± 2.1 vs 12.4 ± 1.4).

5.2 Correlation between *FLG* variants and skin barrier dysfunction

Table 5.2 compares the three measures of skin barrier function between the filaggrin-related AD and wild-type AD groups. Using the Mann-Whitney U-test, TEWL was found to be higher in the filaggrin-related AD group compared to the wild-type AD group (mean 8.4 ± 2.0 g/m^2/h vs 8.1 ± 5.9 g/m^2/h). The distribution in the two groups differed significantly (Mann-Whitney $U = 163.0$, $p = 0.029$ two-tailed). The number of tape strips required to achieve TEWL > 20 g/m^2/h was lower in the filaggrin-related AD group compared to the wild-type AD group (mean 11.3 ± 1.9 vs 14.1 ± 5.5), which was also statistically significant ($p = 0.007$). There was, however, no significant difference in capacitance between the two groups (mean 58.3 ± 17.7 vs 58.2 ± 17.9 i.u.).

Four randomly selected subjects in each group also had the total amount of protein extracted from their tape strips quantified. The mean protein amount extracted from the tape strips was found to be almost twice as much in the filaggrin-related AD subjects (33.4 ± 8.1 μg/cm^2) as in the wild-type AD subjects (18.6 ± 6.4 μg/cm^2). This difference was statistically significant (p = 0.028).

	Filaggrin-related AD	**Wild-type AD**
Median TEWL (g/m^2/h)*	7.9 (IQR 7.1-9.7)	6.8 (IQR 5.5-8.7)
Mean capacitance (i.u.) ± SEM	58.3 ± 4.9	58.2 ± 2.8
Mean number of tape strips required to achieve TEWL > 20 g/m^2/h ± SEM*	11.3 ± 0.5	14.1 ± 0.8
Mean protein amount (μg/cm^2) in tape strips (n=4 in each group) ± SEM *	33.4 ± 2.2	18.6 ± 1.0

Table 5.2 Comparison of skin barrier function and mean amount of protein extracted between the filaggrin-related AD and wild-type AD groups. TEWL was significantly higher in the filaggrin-related AD group (8.4 ± 2.0 g/m^2/h) compared to the wild-type AD group (8.1 ± 5.9 g/m^2/h) while the number of tape strips required to achieve TEWL > 20 g/m^2/h was found to be significantly lower in the filaggrin-related AD group (11.3 ± 0.5) compared to the wild-type AD group (14.1 ± 0.8). No significant difference was found in skin capacitance between the two groups. The mean amount of protein extracted from the tape strips was also determined and was found to be significantly higher in the filaggrin-related AD compared to the wild-type AD group (33.4 ± 2.2 vs 18.6 ± 1.0). * indicates significant statistical difference, i.u. = instrument unit.

5.3 Discussion

Previous studies have demonstrated a defective skin barrier function in AD subjects compared to healthy controls, using measures such as TEWL and SC hydration [15, 242, 256]. In these earlier studies, the AD subjects recruited would have consisted of individuals with and without *FLG* mutations, since they were not specifically genotyped. The primary aim of this functional study was to determine if *FLG* loss-of-function alleles had any functional relevance

(determined by measures of skin barrier function). If this were the case, it might be possible to stratify AD phenotype by *FLG* genotype.

In this study, a total of 55 subjects with mild and moderate AD were recruited, as these categories of AD were representative of the majority of AD sufferers. These subjects were divided into filaggrin-related AD and wild-type AD groups based on their *FLG* genotype. The two groups were found to be comparable, with similar age, sex, history of asthma, family history of atopy, mean IgE level and AD severity (similar SASSAD scores). The only significant difference found when comparing their clinical data was a higher prevalence of hay fever in the filaggrin-related AD group. Hence, in general, the comparison of skin barrier function between the two groups was deemed to be valid.

In 2007, Hubiche *et al* [243] studied a French cohort of AD patients and confirmed the association of AD with *FLG* variants. Although they found a trend for higher TEWL values in AD subjects with *FLG* mutations, the association between *FLG* variants and TEWL was not statistically significant. They also did not find any association between *FLG* variants and AD severity. These findings were generally consistent with the results of this functional study reported here, although the higher TEWL in the filaggrin-related AD group reached statistical significance in this study. An explanation for this could be that while Hubiche *et al* only screened for two common *FLG* mutations (R501X and 2282del4), this study screened for the four *FLG* mutations that were most prevalent in European populations.

A second study on a small Japanese AD cohort by Nemoto-Hasebe *et al* [244] reported marginally lower SC hydration in filaggrin-related AD compared to wild-type AD, although this was not statistically significant. Similarly, this functional study reported in this thesis failed to show any significant difference in capacitance (which equates to SC hydration) between the filaggrin-related AD and wild-type AD groups. Paradoxically, Nemoto-Hasebe *et al* additionally reported that TEWL was significantly lower in filaggrin-related AD compared to

wild-type AD. They also measured SC thickness, and found that SC thickness was significantly greater in filaggrin-related AD. It is important to note that the *FLG* mutations found in the Japanese populations (Ser2554X, 3321del, Ser2889X and Ser3296X) were different from those prevalent in European populations, although the Japanese *FLG* variants were all similarly significantly associated with AD. The authors conjectured that this difference in *FLG* mutations might explain for their unexpected findings.

In addition to TEWL and skin capacitance, another measure of skin barrier function is the number of tape strips required to achieve TEWL > 20 $g/m^2/h$. This level of TEWL is generally accepted as the level where the SC is abrogated [146, 147]. Since filaggrin is generally considered an essential component of the cytoskeletal scaffolding that ultimately forms functional corneocytes, one would expect the number of tape strips required to reach TEWL > 20 $g/m^2/h$ to be less in filaggrin-related AD compared to wild-type AD skin. This was supported by the findings in this study. In an attempt to reconcile this with the greater SC thickness in filaggrin-related AD skin reported by Nemoto-Hasebe *et al* [244], it was hypothesized that the corneocytes were less adherent to one another, and therefore less densely packed in filaggrin-related AD skin. This should mean that although the SC in filaggrin-related AD skin might be thicker, their less-adherent corneocytes should be more easily removed, with a greater amount of corneocytes extracted by each tape. Testing this hypothesis was the secondary aim of this study and involved measuring the total protein (which should correlate with the amount of corneocytes) extracted from the tape strips from eight randomly selected subjects (four from the filaggrin-related AD group and four from the wild-type AD group). The mean amount of protein extracted from filaggrin-related AD skin was found to be significantly higher than that from the wild-type AD group (33.4 ± 8.1 vs 18.6 ± 6.4 $\mu g/cm^2$, $p = 0.028$), lending support to the hypothesis. However, in view of the small sample size (n = 8), this finding should be further validated by extending the protein quantification to a larger cohort.

In this study, *FLG* variants were not found to be significantly associated with AD severity, as evidenced by the similar SASSAD scores between filaggrin-related AD and wild-type AD groups (11.4 ± 7.5 vs 12.4 ± 9.1). However, this finding should be interpreted in the knowledge that only individuals with mild and moderate AD were recruited for this study. Nonetheless, this finding was consistent with that of Hubiche *et al* [243], although there have been suggestions from other studies that filaggrin-related AD may be associated with increased severity in childhood [22, 120], as well as AD with an early onset that persists into adulthood [31].

In summary, the results from this study suggest that it might be possible to stratify AD phenotype by *FLG* genotype, with filaggrin-related AD likely to exhibit poorer skin barrier and possibly run a more severe disease course. There is therefore potentially prognostic value in determine *FLG* status in AD patients. This study of AD phenotype was the most detailed yet on a European AD cohort, including as yet unreported studies on the ease of perturbation in filaggrin-related AD skin to a chemical irritant (sodium lauryl sulfate), the association between *FLG* variants with irritant and allergic contact dermatitis, and the effects of *FLG* mutations on epidermal dendritic cell populations. In addition, as there have been suggestions that measuring baseline skin barrier function may provide an incomplete assessment [257], future work will analyse acute perturbations of the SC with subsequent assessment of the kinetics of barrier recovery.

Chapter 6 Mass Spectrometric Analysis of Filaggrin

6.0 MASS SPECTROMETRIC ANALYSIS OF FILAGGRIN

To date, perhaps the most detailed mass spectrometric analyses of filaggrin was carried out by Walsh's group at the University of Washington almost 20 years ago. Using techniques such as MALDI-TOF MS and LC/MS, they studied rat and human filaggrin to characterise the protease processing sites during profilaggrin to filaggrin conversion [84], identify the amino terminus of filaggrin [253], analyse the phosphorylation sites of profilaggrin [258], and study the microheterogeneity of the protein [251].

In contrast to rat and mouse filaggrin, cDNA sequences for human filaggrin display marked variability (40% of the amino acid residues) [59, 61]. It has been shown that even within a single individual, filaggrin is a population of homologous but heterogeneous proteins [251]. Because of this extensive heterogeneity, structural studies of filaggrin have proven to be challenging.

The main aim of this structural study is to interrogate the structure-function relationship of filaggrin, specifically by comparing filaggrin extracted from AD and non-AD skin. With the use of long-range PCR, the entire DNA sequence of profilaggrin has finally been sequenced by the McLean group in Dundee [23]. However, genetics cannot completely inform about cell physiology for several reasons. For instance, it is known that a single gene (due to alternative splicing of primary transcripts) can generate several different proteins. Also, there are many post-translational modifications that can alter the structure and function of the final protein. Additionally, there are also dynamic processes of protein maturation and degradation that can alter the final active protein [245]. Therefore, although studying filaggrin at the protein level could pose significant challenges due to its extensive heterogeneity, this was believed to be essential in order to gain further insight into its role in diseases such as AD.

MS has been used for the analysis of proteins and peptides since 1989 with the development of 'soft' ionisation techniques for large, polar and highly-charged molecules [180, 189]. It is now the primary technique used for structural characterisation of proteins, including the determination of the amino acid sequence, studying the nature of post-translational modifications, and the verification of protein structure. Hence, to better understand the structure and function of filaggrin in AD and non-AD skin, MS techniques were employed, specifically MALDI-TOF MS and nano LC-MS/MS (see Chapter 1.6 for description of techniques).

The AD subjects recruited for this study was from the genotyped participants of the functional study (described in Chapter 5). Non-AD controls were healthy volunteers (without any history or clinical evidence of AD) recruited from the University of Edinburgh School of Chemistry, Department of Dermatology, as well as patients who underwent breast reduction surgery.

6.1 MALDI-TOF MS analysis of human filaggrin

The extraction and purification of filaggrin are detailed in Chapter 3. Filaggrin extracted from both breast tissues and tape strips were analysed, with the protein studied in both its intact and tryptic-digest states. Details of sample preparation and MS methodology are described in Chapter 2.9.

6.1.1 MALDI-TOF MS analysis of intact filaggrin protein

Intact purified filaggrin extracted from eight subjects (four AD and four non-AD) were analysed using MALDI-TOF MS. Filaggrin from two of the non-AD controls were extracted from breast reduction tissues, while the other two were from tape strips. All the filaggrin from the AD subjects were extracted using tape strips only.

MALDI-TOF MS of all non-AD samples, whether those extracted from breast reduction tissues or tape strips, produced similar mass spectra. The main peak was broad, centred at around *m/z* 35,000 ± 1400 at half-height (Figure 6.1). There was also a smaller peak at around *m/z* 17,000 that was likely a doubly-charged molecular ion of the *m/z* 35,000 species, and one at around *m/z* 70,000 which was thought to be a dimer of the dominant species.

MALDI-TOF MS analysis of intact filaggrin purified from all four AD subjects failed to yield any significant mass peaks, suggesting an inadequate amount or absence of filaggrin in the samples.

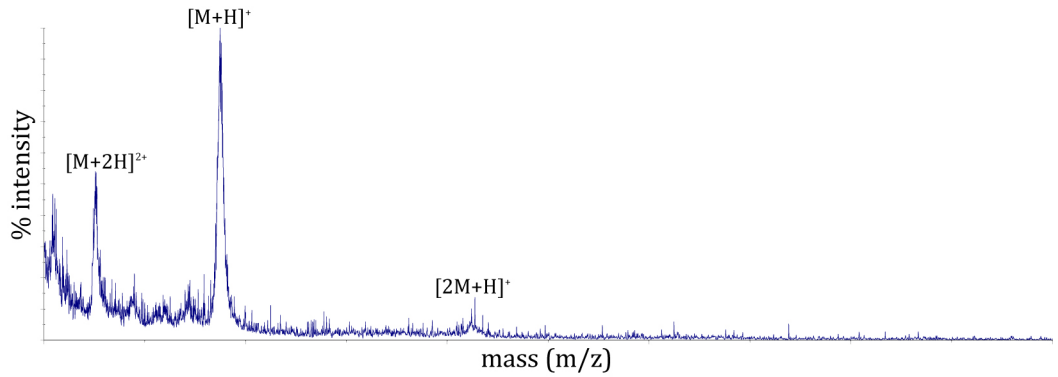

Figure 6.1. MALDI-TOF mass spectrum of intact filaggrin extracted from a non-AD subject. Mass spectra of all four non-AD samples were similar, showing a main broad peak $[M+H]^+$ centred at around *m/z* 35,000 ± 1400 at half-height. The broadness of the peak is consistent with the heterogeneity of filaggrin. The smaller peak at around *m/z* 17,000 was likely a doubly-charged molecular ion of the dominant *m/z* 34,000 species, while the small peak at around *m/z* 70,000 was possibly a dimer of the *m/z* 35,000 species. The small peaks at the beginning of the spectrum were matrix peaks.

6.1.2 MALDI-TOF analysis of filaggrin tryptic-digests

Filaggrin protein that was extracted and purified from 10 subjects were subjected to digestion with trypsin before being analysed using MALDI-TOF MS. The first eight of these subjects were the same as those described in Chapter 6.1.1. The additional two subjects were non-AD controls, with their filaggrin extracted from breast reduction tissues. In total, tryptic-digests from six non-AD and four AD subjects were analysed.

The MALDI-TOF mass spectra of two of the non-AD filaggrin tryptic-digests (one extracted from breast reduction tissues and one from tape strips) are shown in Figure 6.2. As was the case with the MALDI-TOF MS analysis of intact filaggrin, all six mass spectra of the non-AD tryptic-digest samples were similar, whether the filaggrin was extracted from breast tissues or tape strips.

a.

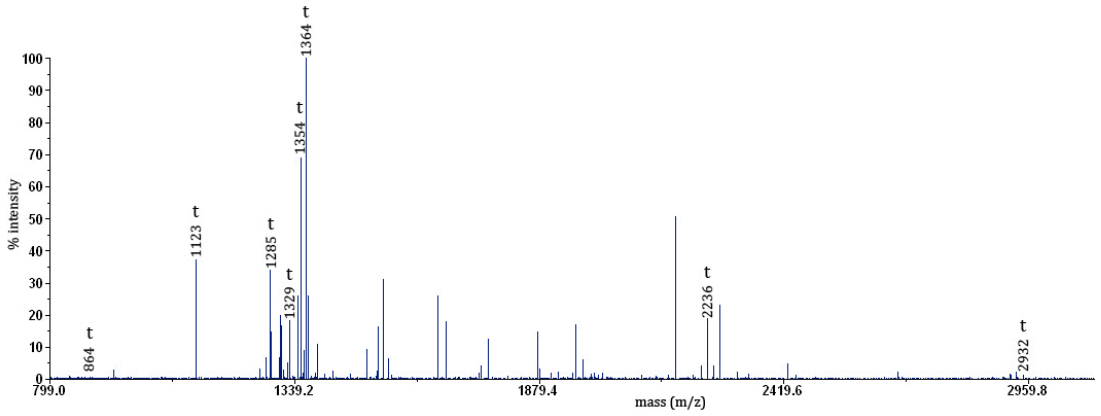

b.

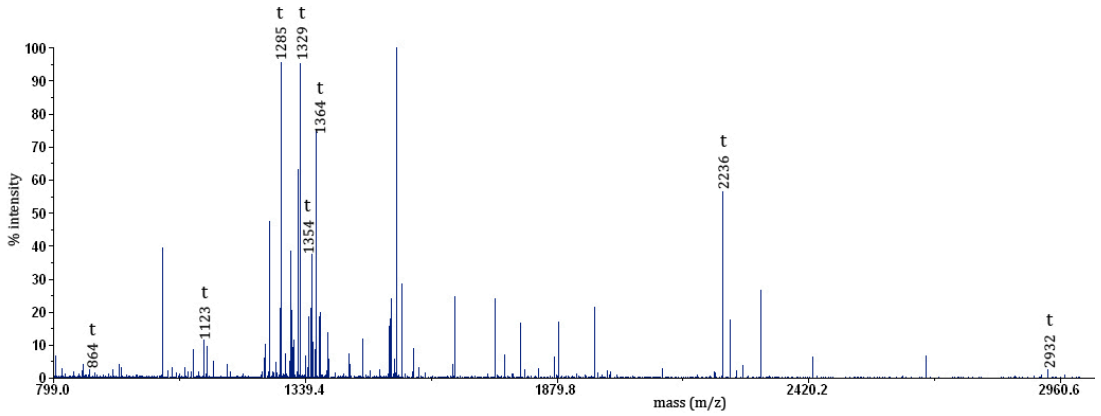

Figure 6.2. MALDI-TOF MS mass spectra of filaggrin tryptic-digests from (a) breast tissues and (b) tape strips, showing similarity in the mass spectra. In fact, the mass spectra from all the non-AD samples were very similar. Indicated are the *m/z* peaks observed in the mass spectra of all six non-AD samples (excluding those peaks from trypsin auto-digestion). The possible peptides corresponding to these peaks are shown in Table 6.1.

Using PMF (detailed in Chapter 1.6.4), the peptide masses obtained from each MALDI-TOF spectrum were matched against the theoretical peptide masses from *in silico*-digested proteins in the comprehensive NCBInr protein database. An online database search programme, MS-FIT, (http://prospector.ucsf.edu/prospector/cgi-bin/msform.cgi?form=msfitstandard) was used to facilitate this matching process. All the six non-AD samples were matched very well to filaggrin, with high MOWSE scores, despite the scores

being generally higher for the breast samples. Figure 6.3 shows the corresponding MS-FIT database search results for the mass spectra seen in Figure 6.2.

a.

Protein Hit Number	MOWSE Score	# pep # mat % mat 128 pks	% Cov	% TIC	Mean Err Da	Data Tol Da	# Hom Prot	MS-Digest Index #	Protein MW (Da)/pI	Accession #	Species	Protein Name
1	1.94e+28	57/56/44	61.7	43.8	-0.0137	0.0986	4	39829193982919	122645/9.1	119573768 119573768	HOMO SAPIENS filaggrin, isoform CRA_a	

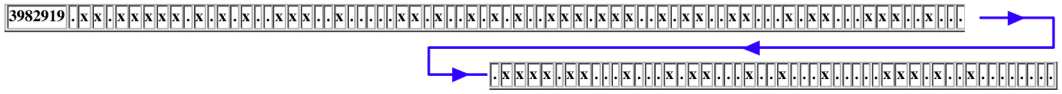

Similar Matches for Protein Hit 1

Protein Hit Number	MOWSE Score	# pep # mat % mat 128 pks	% Cov	% TIC	Mean Err Da	Data Tol Da	# Hom Prot	MS-Digest Index #	Protein MW (Da)/pI	Accession #	Species	Protein Name
1	1.94e+28	57/56/44	61.7	43.8	-0.0137	0.0986	4	39829193982919	122645/9.1	119573768 119573768	HOMO SAPIENS filaggrin, isoform CRA_a	

Protein Hit Number	MOWSE Score	# pep # mat % mat 128 pks	% Cov	% TIC	Mean Err Da	Data Tol Da	# Hom Pep	MS-Digest Index #	Protein MW (Da)/pI	Accession #	Species	Protein Name
2	2.17e+27	46/49/38	76.9	38.3	-0.00260	0.0156	28	39858803985880	94037/7.5	119573770 119573770	HOMO SAPIENS filaggrin, isoform CRA_c	
3	1.22e+22	42/45/35	64.6	35.2	-0.0189	0.114	38	39830643983064	80403/9.5	119573769 119573769	HOMO SAPIENS filaggrin, isoform CRA_b	
4	4.21e+18	35/39/30	62.8	30.5	-0.0221	0.123	34	23144162314416	66367/9.4	553621 553621	HOMO SAPIENS profilaggrin	
5	3.03e+18	32/35/27	42.3	27.3	7.72e-4	0.0328	11	23254852325485	115275/7.2	190394 190394	HOMO SAPIENS profilaggrin	

b.

Protein Hit Number	MOWSE Score	# pep # mat % mat 149 pks	% Cov	% TIC	Mean Err Da	Data Tol Da	# Hom Prot	MS-Digest Index #	Protein MW (Da)/pI	Accession #	Species	Protein Name
1	2.99e+15	37/37/25	46.2	24.8	-0.0191	0.231	4	39829193982919	122645/9.1	119573768 119573768	HOMO SAPIENS filaggrin, isoform CRA_a	

Similar Matches for Protein Hit 1

Protein Hit Number	MOWSE Score	# pep # mat % mat 149 pks	% Cov	% TIC	Mean Err Da	Data Tol Da	# Hom Prot	MS-Digest Index #	Protein MW (Da)/pI	Accession #	Species	Protein Name
1	2.99e+15	37/37/25	46.2	24.8	-0.0191	0.231	4	39829193982919	122645/9.1	119573768 119573768	HOMO SAPIENS filaggrin, isoform CRA_a	

Protein Hit Number	MOWSE Score	# pep # mat % mat 149 pks	% Cov	% TIC	Mean Err Da	Data Tol Da	# Hom Pep	MS-Digest Index #	Protein MW (Da)/pI	Accession #	Species	Protein Name
2	1.01e+13	25/25/17	44.1	16.8	-0.00867	0.111	21	39858803985880	94037/7.5	119573770 119573770	HOMO SAPIENS filaggrin, isoform CRA_c	
3	1.23e+10	24/24/16	44.4	16.1	-0.0234	0.268	21	39830643983064	80403/9.5	119573769 119573769	HOMO SAPIENS filaggrin, isoform CRA_b	
4	5.77e+9	20/18/12	35.3	12.1	-0.00928	0.0891	10	21938782193878	85177/7.6	190404 190404	HOMO SAPIENS profilaggrin	
5	7.21e+8	23/21/14	36.4	14.1	-0.0257	0.156	12	22717162271716	106453/10.4	190396 190396	HOMO SAPIENS profilaggrin	

Figure 6.3. Database search results using the online database search programme MS-FIT. (a) Search results using the peptide masses obtained from the mass spectrum in Figure 6.2a. (b) Search results corresponding to the mass spectrum in Figure 6.2b. All the tryptic-digest samples obtained from the six non-AD subjects matched well to filaggrin, with high MOWSE scores.

Several m/z peaks were observed in all the mass spectra of the six non-AD samples, disregarding those that were due to trypsin auto-digestion. Table 6.1 lists these m/z peaks and their corresponding peptide sequences as suggested by MS-FIT.

m/z	Corresponding peptides
864.4	GQSGESSGRGQSGESSGR
1122.6	KENLPISGHKKENLPISGHK
1284.6	NHLGSAWEQSRNHLGSAWEQSR
1328.6	HSASQEGQDTIRHSASQEGQDTIR
1353.6	HGSGHQQSADSSRHGSGHQQSADSSR
1363.7	HSGIGHGQASSAVRHSGIGHGQASSAVR
2235.9	NQGSSVSQDSDSQGHSEDSERNQGSSVSQDSDSQGHSEDSER
2932.4	VTNELYTVMKTYHMYHAESISAESKVTNELYTVMKTYHMYHAESISAESK

Table 6.1 List of *m/z* peaks observed in all the mass spectra of the non-AD filaggrin tryptic-digests, along with the corresponding peptides as suggested by MS-FIT.

As was the case with the intact filaggrin samples, MALDI-TOF MS analysis of the AD tryptic-digests yielded similarly poor mass spectra. The lack of any significant peptide m/z peaks once again suggests an inadequate amount or absence of filaggrin in the analysed samples.

6.2 Online nano LC-MS/MS of filaggrin tryptic-digests

In addition to MALDI-TOF MS, purified filaggrin samples from AD and non-AD subjects were also analysed using nano LC-MS/MS, which has the advantage of providing accurate sequence information.

Purified filaggrin samples from a total of 21 non-AD and AD subjects were digested with trypsin before being analysed by nano LC-MS/MS. These subjects included all those whose intact samples were analysed by MALDI-TOF

MS. As shown in Table 6.2, all the AD subjects were genotyped as being either *FLG* wild-type or heterozygous for the 2282del4 or R501X mutations. None of the subjects were homozygous for the *FLG* mutation.

Phenotype	Genotype	Number of subjects
Non-AD	*FLG* wild-type	6 (2 were extracted from breast tissues)
AD	*FLG* wild-type	9
	2282del4 heterozygote	5
	R501X heterozygote	1
	Total	21

Table 6.2 Phenotype and genotype of the subjects from which filaggrin were extracted and purified for nano LC-MS/MS analysis. Included among these were the 8 subjects whose purified filaggrin were analysed with MALDI-TOF MS. In two of the non-AD control subjects, filaggrin was extracted from breast reduction tissues. Filaggrin from the remaining four non-AD subjects, as well as from all the AD subjects, was extracted using tape strips.

As detailed in Chapter 2.9.5, the peptide fragmentation data obtained for each sample were matched against the NCBInr protein database using an in-house MASCOT search engine (Matrix Science). The tryptic-digests of all six non-AD protein samples were matched to filaggrin. Again, there was a difference in the matching scores between those samples extracted from breast reduction tissues and those from tape strips. The two breast tryptic-digests had higher MASCOT scores (ranged from 963 to 1736) compared to those from tape strips (ranged from 49 to 555). The full MASCOT search results for three tryptic-digests (one from breast reduction tissues, and two from tape strips) can be viewed from the attached data disc for comparison.

Analysis of the filaggrin tryptic-digests from the 15 AD subjects produced disappointing results. The initial base peak chromatograms of these samples suggested insufficient or absent protein and so instead of the usual 10 - 15 µl

sample loading volume, higher loading volumes (up to 250 µl) were used in an attempt to boost peptide detection. However, despite this, only two of these subjects (FW and MOK, both *FLG* wild-types) were matched weakly to filaggrin. Sample FW required a sample loading volume of 50 µl before a weak match to filaggrin with a MASCOT score of 53 was obtained. Increasing the sample volume to 250 µl did not improve the MASCOT score. Sample MOK produced a weak match to filaggrin with a loading volume of 50 µl (MASCOT score 69), but the match was slightly strengthened (MASCOT score 152) when the sample loading volume was increased to 250 µl. The attached data disc contains the full MASCOT search results for samples FW and MOK. This lack of any detectable filaggrin in the AD samples was confirmed by collecting fresh tape strips again from five of the AD subjects (including subject FW) to repeat the entire extraction and purification of their filaggrin. These replicated samples (again using up to 250 µl sample loading volumes) produced results similar to those of the initial samples.

As mentioned earlier, the main advantage of using nano LC-MS/MS is the ability to determine sequence information. Figure 6.4 shows the CID spectrum from one non-AD sample and its assignment to the filaggrin peptide HAETSSGGQAASSQEQAR (ion score of 148). It illustrates an example of MS/MS data and its interpretation. Indicated in the figure are the b and y ions. MASCOT produces a peptide summary report that groups peptide matches like this into protein hits, and derives a protein score (MASCOT score) from the combined ions scores. In this case, the combined MASCOT score is 1273.

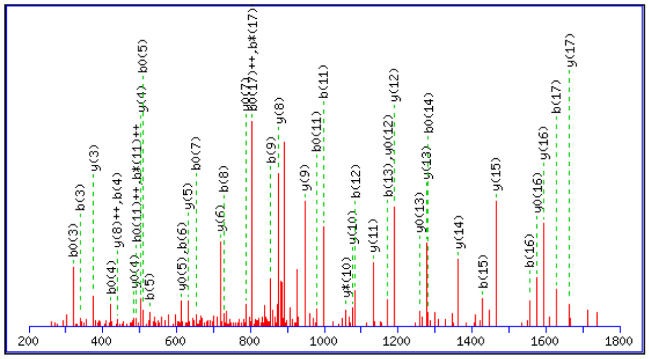

Monoisotopic mass of neutral peptide Mr(calc): 1800.7987
Ions Score: 148 **Expect:** 1.4e-012
Matches (Bold Red): 45/178 fragment ions using 47 most intense peaks

#	b	b^{++}	b*	b^{*++}	b^{0}	b^{0++}	Seq.	y	y^{++}	y*	y^{*++}	y^{0}	y^{0++}	#
1	138.0662	69.5367					H							18
2	209.1033	105.0553					A	**1664.7470**	832.8772	1647.7205	824.3639	1646.7365	823.8719	17
3	**338.1459**	169.5766			**320.1353**	160.5713	E	**1593.7099**	797.3586	1576.6834	788.8453	**1575.6994**	788.3533	16
4	**439.1936**	220.1004			**421.1830**	211.0951	T	**1464.6673**	732.8373	1447.6408	724.3240	1446.6568	723.8320	15
5	**526.2256**	263.6164			**508.2150**	254.6112	S	**1363.6197**	682.3135	1346.5931	673.8002	1345.6091	673.3082	14
6	**613.2576**	307.1325			595.2471	298.1272	S	**1276.5876**	638.7975	1259.5611	630.2842	**1258.5771**	629.7922	13
7	670.2791	335.6432			**652.2685**	326.6379	G	**1189.5556**	595.2814	1172.5291	586.7682	**1171.5450**	586.2762	12
8	**727.3006**	364.1539			709.2900	355.1486	G	**1132.5341**	566.7707	1115.5076	558.2574	1114.5236	557.7654	11
9	**855.3591**	428.1832	838.3326	419.6699	837.3486	419.1779	Q	**1075.5127**	538.2600	**1058.4861**	529.7467	1057.5021	529.2547	10
10	926.3963	463.7018	909.3697	455.1885	908.3857	454.6965	A	**947.4541**	474.2307	930.4276	465.7174	929.4435	465.2254	9
11	**997.4334**	499.2203	980.4068	**490.7070**	**979.4228**	**490.2150**	A	**876.4170**	**438.7121**	859.3904	430.1989	858.4064	429.7068	8
12	**1084.4654**	542.7363	1067.4388	534.2231	1066.4548	533.7311	S	**805.3799**	403.1936	788.3533	394.6803	**787.3693**	394.1883	7
13	**1171.4974**	586.2523	1154.4709	577.7391	1153.4869	577.2471	S	**718.3478**	359.6776	701.3213	351.1643	700.3373	350.6723	6
14	1299.5560	650.2816	1282.5294	641.7684	**1281.5454**	641.2764	Q	**631.3158**	316.1615	614.2893	307.6483	**613.3053**	307.1563	5
15	**1428.5986**	714.8029	1411.5720	706.2897	1410.5880	705.7977	E	**503.2572**	252.1323	486.2307	243.6190	**485.2467**	243.1270	4
16	**1556.6572**	778.8322	1539.6306	770.3189	1538.6466	769.8269	Q	**374.2146**	187.6110	357.1881	179.0977			3
17	**1627.6943**	814.3508	1610.6677	**805.8375**	1609.6837	**805.3455**	A	246.1561	123.5817	229.1295	115.0684			2
18							R	175.1190	88.0631	158.0924	79.5498			1

b ions: 0 1 2 3 4 5 6 7 8 9 10 11 12 13 14 15 16 17 18

H A E T S S G G Q A A S S Q E Q A R

y ions: 18 17 16 15 14 13 12 11 10 9 8 7 6 5 4 3 2 1 0

Figure 6.4 A CID spectrum for the filaggrin peptide HAETSSGGQAASSQEQAR, that is given an ion score of 148 by MASCOT. The b and y ions are indicated to illustrate how the data is interpreted. MASCOT groups peptide matches like this into protein hits and derives a protein score (MASCOT score) from the combined ion scores. In this case, the MASCOT score is 1273.

6.3 Immunoblotting

In order to further ascertain the presence (or absence) of filaggrin in the non-AD and AD samples, immunoblotting with a mouse monoclonal filaggrin antibody (ab17808, Abcam) was performed on all the initial SC extracts as well as the final purified protein samples. Immunoblots of the initial SC extracts of the non-AD subjects all produced a thick filaggrin bands (generally a thick smear from about 45 kDa upwards), while the immunoblots of the AD initial extracts were generally less prominent, regardless of whether the AD subjects were of *FLG* wild-type or heterozygous genotype. Figure 6.5 shows the band from the initial SC extract of a non-AD subject that was obtained by tape stripping, as well as those from all the non-AD subjects. As an equal volume of sample was loaded into each well, this difference in band thickness suggests that less filaggrin was present in the initial SC extract of the AD compared to the non-AD subjects. The final purified filaggrin samples were also analysed by immunoblotting. Immunoblots of the non-AD samples produced a prominent band at around 45 kDa, which was absent in any of the AD subjects, even in subjects FW and MOK (which were both weakly matched to filaggrin following nano LC-MS/MS analysis, albeit only after increasing their sample loading volumes).

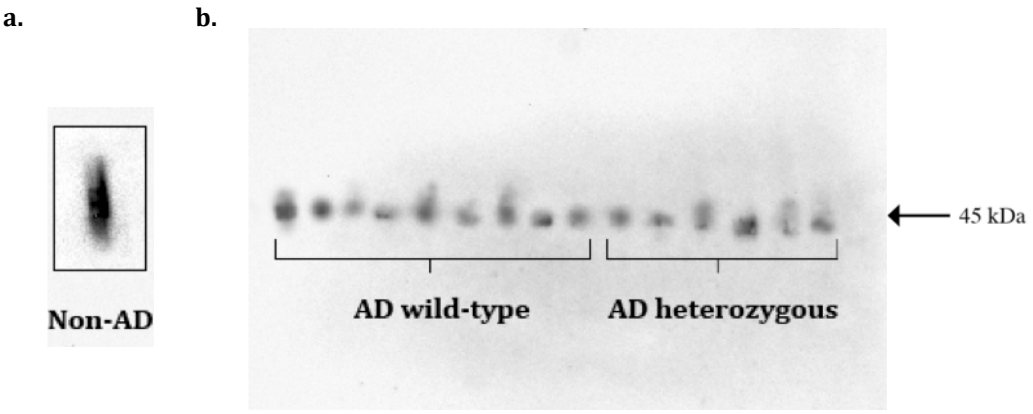

Figure 6.5 Comparison of immunoblots of initial SC extracts. (a) Immunoblot of the initial SC extract from one non-AD subject, showing the typical thick prominent filaggrin bands seen in the non-AD samples. (b) Immunoblot of the initial SC extracts from all the AD subjects. Regardless of the genotype, the AD subjects' immunoblots all showed less prominent filaggrin bands. Since each of these samples was extracted from 100 tape strips, and an identical volume of sample was loaded into each well, this suggests that there was less filaggrin in the initial SC extracts of the AD subjects compared to non-AD subjects. Ideally, a loading control could have been used to ensure that protein loading was the same in each well. The immunoblots of the final purified filaggrin of the non-AD samples all showed a filaggrin band at 45 kDa, while no bands were seen in the purified AD samples (data not shown).

6.4 Discussion

The main aim of this structural study was to interrogate the structure-function of filaggrin by comparing filaggrin from AD skin to non-AD skin using mass spectrometric techniques. Any differences found in filaggrin structure between the two groups could hopefully provide insight into the role of filaggrin in AD.

All the AD subjects recruited for this structural study were genotyped to detect the presence of the four commonest European *FLG* mutations (2282del4, R501X, R2247X and S3247X). It is certainly plausible that one or more of the AD subjects could have possessed a rarer *FLG* mutation, which would result in an underestimation of the number of heterozygotes or compound heterozygotes in the AD cohort. However, the likelihood of possessing these rarer mutations was relatively low since studies had shown that these four *FLG* mutations accounted for up to 95% of all known *FLG* mutations in European populations [248].

The non-AD subjects in this structural study were not genotyped, but since filaggrin was easily detected in all the non-AD samples, it was assumed that they all had the wild-type genotype. Previous biochemical and immunohistochemical studies had shown that a null mutation in the *FLG* allele resulted in an absence of filaggrin expression [23, 255], thereby supporting this assumption. Of course, one or more of the non-AD subjects could still be heterozygous for the *FLG* mutation, which would mean that they still expressed some filaggrin. However, this was unlikely to be the case for three reasons. First, the MS analysis of these samples gave uniformly strong signals; second, immunoblotting of these samples all showed thick filaggrin bands. Both these suggested the presence of a large amount of filaggrin present in all the non-AD samples. Third, *FLG* mutations had also been shown to be much less prevalent in non-AD individuals compared to AD sufferers [22]. Therefore for these three reasons, all the non-AD subjects were very likely to be *FLG* homozygous wild-types.

Purified filaggrin extracted from both AD subjects and non-AD controls were analysed using MALDI-TOF MS and nano LC-MS/MS to elicit structural information of filaggrin in both its intact and tryptic-digest states. MALDI-TOF analysis of intact filaggrin from non-AD subjects showed a dominant peak centred at approximately *m/z* 34,000 that was broad (*m/z* ± 1,400 at half-height). The width of the peak was consistent with the heterogeneic nature of filaggrin. There was also a smaller peak at around *m/z* 17,000 that likely represented a doubly-charged molecular ion of the dominant 34,000 species, and one at around *m/z* 70,000 which was thought to be a dimer of the dominant species. These data were similar to that reported by Thulin *et al* who reported a broad main peak centred at *m/z* 34,144 ± 1560 at half-height [251]. A smaller peak at *m/z* 17,071 was also seen in their intact filaggrin MALDI-TOF spectrum. They did not, however, comment on this peak, nor did they report the presence of any possible dimeric species. The latter could be due to the authors setting an upper *m/z* limit of 50,000 that was too low to detect this peak. These additional

peaks at half and double the *m/z* value of the dominant species were not unexpected as they are frequently observed in MALDI-TOF analyses performed in positive ionisation mode.

Analysis of filaggrin tryptic-digests from the non-AD subjects using either MALDI-TOF MS or nano LC-MS/MS yielded good data, with all samples matching well to filaggrin. In the case of MALDI-TOF MS, no significant difference in the mass spectra was noted between the filaggrin extracted from breast tissues and that from tape strips, although the MOWSE scores were higher in the breast samples. This difference was more pronounced in the nano LC-MS/MS results with the matching scores from the breast tissue samples being clearly better than those from tape strips, with more peptides matched. As extraction from breast tissues generally yielded more protein compared to tape stripping, this suggested that the amount of filaggrin extracted from tape strips could be further increased to allow for optimal nano LC-MS/MS analysis. Possible solutions would be to collect more tape strips from each subject, or increase the sample loading volume.

None of the MS analysis of filaggrin (both intact and tryptic-digests) from AD subjects yielded any interpretable results. The lack of any significant mass peaks in the MALDI-TOF mass spectra suggested that filaggrin was either absent or in too minute an amount for detection by MALDI-TOF MS. Nano LC-MS/MS also did not match any of the 15 AD tryptic-digest samples to filaggrin when the usual 15 µl sample loading volume was injected. However, after increasing the sample loading volume to a maximum of 250 µl, two AD samples (FW and MOK) were matched weakly to filaggrin. Once again, this was further evidence that the AD samples contained either no filaggrin, or in too small an amount for MS analysis.

Immunoblotting was used to ascertain the presence of filaggrin in the initial SC extracts as well as the final purified protein samples. Comparison of the immunoblots of the initial SC extracts showed that the filaggrin bands seen

in the non-AD samples were thicker and more intensely stained compared to those of the AD samples, indicating a greater amount of filaggrin in the former group. Also, while all the final purified protein samples of the non-AD subjects produced a distinct 45 kDa filaggrin band, this band was absent in all the AD samples. The immunoblotting results suggested that there was less filaggrin present in the AD initial tape strips, and with the subsequent protein loss through the purification process, there was too little filaggrin in the final purified samples for immunodetection. It is likely that if these samples were concentrated prior to immunoblotting, or if more tape strips were obtained from the AD subjects, filaggrin could have been detected. Certainly, at least for samples FW and MOK that were both eventually matched weakly to filaggrin after increasing their sample injection volumes, one would expect positive filaggrin immunodetection following further concentration of these samples.

It is interesting to note that all immunoblots in our study produced filaggrin bands at around 45 kDa, agreeing with the calculated molecular mass of human filaggrin (44.1 kDa) [259], but higher than the 37 kDa reported in recent studies [23]. Other authors have also reported different molecular weights for human filaggrin, such as 42-45 kDa [260] to as high as 51 kDa [113]. These differences are likely due to variation in purification procedures, resulting in different isoforms of the molecules.

Various modifications to the extraction and purification of filaggrin were attempted during this study in the hope of increasing the yield of filaggrin in the initial SC extracts and the final purified protein samples. These included trying various homogenisation methods, increasing the size of tape strips used (replacing the initial 14 mm-diameter tapes with larger 22 mm-diameter ones), extending the extraction time (from one day to two days), replacing an acetone protein precipitation step with an LC desalting step to reduce protein loss, trying different LC columns as well as deep cleaning and replacing the older columns. A flow chart detailing the various modifications made to the extraction and purification process is shown in Figure 3.4. Eventually, it was decided that

the process, as described in Chapter 3, could not be further optimised to increase protein yield.

There are at least two possible reasons for the comparatively less filaggrin found in the tape strips of AD subjects. Firstly, it could be that, for reasons as yet unknown, tape stripping of AD skin does not extract as much filaggrin compared to tape stripping non-AD skin. A second more likely explanation is that there is simply less filaggrin present in AD skin. This has been previously observed in at least two studies. In 1996, Seguchi *et al* obtained skin biopsies from 12 AD and 12 non-AD subjects and found that the amount of filaggrin was significantly less in the AD skin samples [113]. This study was conducted prior to the establishment of the association between AD and filaggrin, and also predated the ability to analyse for *FLG* mutations. As such, with the absence of any genotype information on the AD subjects, it is impossible to draw any firm conclusion from this study apart from the suggestion that filaggrin protein expression is generally reduced in AD individuals. More recently, Howell *et al* also studied filaggrin expression in AD individuals [115]. Importantly, all the subjects in this study were *FLG* genotyped. They demonstrated that both filaggrin protein and gene expressions were decreased in AD subjects compared to non-AD subjects. They subsequently showed, using primary keratinocytes *in vitro*, that this decrease in filaggrin could be partly attributed to the over-expression of T_H2 cytokines that act to down-regulate filaggrin expression. The authors did not specifically comment on the difference in filaggrin protein expression between the AD subgroups, but analysing their data revealed that filaggrin protein expression was significantly reduced in AD *FLG* wild-types compared to non-AD subjects, and also reduced in AD *FLG* heterozygotes compared to non-AD subjects. Interestingly, there was no significant difference noted in filaggrin protein expression between AD subjects who were *FLG* wild-type and *FLG* heterozygous. To date, there is already convincing evidence that individuals who are homozygous or compound heterozygous for the *FLG* mutation do not express functional filaggrin in their skin, and that individuals who are *FLG*

heterozygotes express less filaggrin [23, 73]. Results from this structural study and those from Howell *et al* show that AD individuals, even if they do not possess any *FLG* mutations, express less filaggrin protein in their skin. Although this rather unexpected finding was interesting, the consequence was the inability to extract sufficient filaggrin from the skin of AD subjects with tape stripping. This prevented any subsequent comparison of the filaggrin primary structure between AD and non-AD skin. Nonetheless, this finding of reduced filaggrin expression in AD skin could offer a possible explanation for why wild-type AD individuals develop AD while non-AD individuals do not. It raises the possibility that wild-type AD could have a primary immunological dysfunction that secondarily result in reduced filaggrin expression and impaired skin barrier. As such, the clinical phenotype of AD may result from different pathophysiological mechanisms - one initiated by a *FLG* defective barrier failure in which secondary immunological changes occur, and the other a predominantly immunologically-mediated disease in which cytokines released into the skin reduce barrier function.

The MS analysis of tryptic-digests rely on matching experimental peptide masses against theoretical peptide masses from *in silico*-digested filaggrin in a protein database. Within the NCBInr protein database that was used exclusively in this study, there is an entry for the human profilaggrin consensus sequence (RefSeq NP_002007, shown in Figure 6.6) that is inaccurately called 'filaggrin'. This contains the sequences for the N- and C-termini, and 10 full filaggrin repeats. The 10 filaggrin repeats are flanked by two partial filaggrin repeats (marked by blue font in Figure 6.6) that contain areas of high homology to the full filaggrin repeats. The linker peptide sequence RSGRSGSFLY is arbitrarily assigned as the start of each repeat [23, 64].

MSTLLENIFAIINLFKQYSKKDKNTDTLSKKELKELLEKEFRQILKNPDDPDMVDVFMDHLDIDHNKKID
FTEFLLMVFKLAQAYYESTRKENLPISGHKHRKHSHHDKHEDNKQEENKENRKRPSSLERRNNRKGNKGR
SKSPRETGGKRHESSSEKKERKGYSPTHREEEYGKNHHNSSKKEKNKTENTRLGDNRKRLSERLEEKEDN
EEGVYDYENTGRMTQKWIQSGHIATYYTIQDEAYDTTDSLLEENKIYERSRSSDGKSSSQVNRSRHENTS
QVPLQESRTRKRRGSRVSQDRDSEGHSEDSERHSGSASRNHHGSAWEQSRDGSRHPRSHDEDRASHGHSA
DSSRQSGTRHAETSSRGQTASSHEQARSSPGERHGSGHQQSADSSRHSATGRGQASSAVSDRGHRGSSGS
QASDSEGHSENSDTQSVSGHGKAGLRQQSHQESTRGRSGE**RSGRSGSSLYQVSTHEQPDSAHGRTGTSTG**
GRQGSHHEQARDSSRHSASQEGQDTIRGHPGSSRGGRQGSHHEQSVNRSGHSGSHHSHTTSQGRSDASHG
QSGSRSASRQTRNEEQSGDGTRHSGSRHHEASSQADSSRHSQVGQGQSSGPRTSRNQGSSVSQDSDSQGH
SEDSERWSGSASRNHHGSAQEQSRDGSRHPRSHHEDRAGHGHSADSSRKSGTRHTQNSSSGQAASSHEQA
RSSAGERHGSRHQLQSADSSRHSGTGHGQASSAVRDSGHRGSSGSQATDSEGHSEDSDTQSVSGHGQAGH
HQQSHQESARDRSGERSRRSGSFLYQVSTHKQSESSHGWTGPSTGVRQGSHHEQARDNSRHSASQDGQDT
IRGHPGSSRRGRQGSHHEQSVDRSGHSGSHHSHTTSQGRSDASRGQSGSRSASRTTRNEEQSRDGSRHSG
SRHHEASSHADISRHSQAGQGQSEGSRTSRRQGSSVSQDSDSEGHSEDSERWSGSASRNHRGSAQEQSRH
GSRHPRSHHEDRAGHGHSADSSRQSGTPHAETSSGGQAASSHEQARSSPGERHGSRHQQSADSSRHSGIP
RRQASSAVRDSGHWGSSGSQASDSEGHSEESDTQSVSGHGQDGPHQQSHQESARDWSGG**RSGRSGSFIYQ**
VSTHEQSESAHGRTRTSTGRRQGSHHEQARDSSRHSASQEGQDTIRAHPGSRRGGRQGSHHEQSVDRSGH
SGSHHSHTTSQGRSDASHGQSGSRSASRQTRKDKQSGDGSRHSGSRHHEAASWADSSRHSQVGQEQSSGS
RTSRHQGSSVSQDSDSERHSDDSERLSGSASRNHHGSSREQSRDGSRHPGFHQEDRASHGHSADSSRQSG
THHTESSSHGQAVSSHEQARSSPGERHGSRHQQSADSSRHSGIGHRQASSAVRDSGHRGSSGSQVTNSEG
HSEDSDTQSVSAHGQAGPHQQSHKESARGQSGESSGRSRSFLYQVSSHEQSESTHGQTAPSTGGRQGSRH
EQARNSSRHSASQDGQDTIRGHPGSSRGGRQGSYHEQSVDRSGHSGYHHSHTTPQGRSDASHGQSGPRSA
SRQTRNEEQSGDGSRHSGSRHHEPSTRAGSSRHSQVGQGESAGSKTSRRQGSSVSQDRDSEGHSEDSERR
SESASRNHYGSAREQSRHGSRNPRSHQEDRASHGHSAESSRQSGTRHAETSSGGQAASSQEQARSSPGER
HGSRHQQSADSSTDSGTGRRQDSSVVGDSGNRGSSGSQASDSEGHSEESDTQSVSAHGQAGPHQQSHQES
TRGQSGE**RSGRSGSFLYQVSTHEQSESAHGRTGPSTGGRQRSRHEQARDSSRHSASQEGQDTIRGHPGSS**
RGGRQGSHYEQSVDSSGHSGSHHSHTTSQERSDVSRGQSGSRSVSRQTRNEKQSGDGSRHSGSRHHEASS
RADSSRHSQVGQGQSSGPRTSRNQGSSVSQDSDSQGHSEDSERWSGSASRNHLGSAWEQSRDGSRHPGSH
HEDRAGHGHSADSSRQSGTRHTESSSRGQAASSHEQARSSAGERHGSHHQLQSADSSRHSGIGHGQASSA
VRDSGHRGYSGSQASDSEGHSEDSDTQSVSAQGKAGPHQQSHKESARGQSGESSGRSGSFLYQVSTHEQS
ESTHGQSAPSTGGRQGSHYDQAQDSSRHSASQEGQDTIRGHPGPSRGGRQGSHQEQSVDRSGHSGSHHSH
TTSQGRSDASRGQSGSRSASRKTYDKEQSGDGSRHSGSHHHEASSWADSSRHSLVGQGQSSGPRTSRPRG
SSVSQDSDSEGHSEDSERRSGSASRNHHGSAQEQSRDGSRHPRSHHEDRAGHGHSAESSRQSGTHHAENS
SGGQAASSHEQARSSAGERHGSHHQQSADSSRHSGIGHGQASSAVRDSGHRGSSGSQASDSEGHSEDSDT
QSVSAHGQAGPHQQSHQESTRGRSAG**RSGRSGSFLYQVSTHEQSESAHGRTGTSTGGRQGSHHKQARDSS**
RHSTSQEGQDTIHGHPGSSSGGRQGSHYEQLVDRSGHSGSHHSHTTSQGRSDASHGHSGSRSASRQTRND
EQSGDGSRHSGSRHHEASSRADSSGHSQVGQGQSEGPRTSRNWGSSFSQDSDSQGHSEDSERWSGSASRN
HHGSAQEQLRDGSRHPRSHQEDRAGHGHSADSSRQSGTRHTQTSSGGQAASSHEQARSSAGERHGSHHQQ
SADSSRHSGIGHGQASSAVRDSGHRGYSGSQASDNEGHSEDSDTQSVSAHGQAGSHQQSHQESARGRSGE
TSGHSGSFLYQVSTHEQSESSHGWTGPSTRGRQGSRHEQAQDSSRHSASQDGQDTIRGHPGSSRGGRQGY
HHEHSVDSSGHSGSHHSHTTSQGRSDASRGQSGSRSASRTTRNEEQSGDGSRHSGSRHHEASTHADISRH
SQAVQGQSEGSRRSRRQGSSVSQDSDSEGHSEDSERWSGSASRNHHGSAQEQLRDGSRHPRSHQEDRAGH
GHSADSSRQSGTRHTQTSSGGQAASSHEQARSSAGERHGSHHQQSADSSRHSGIGHGQASSAVRDSGHRG
YSGSQASDNEGHSEDSDTQSVSAHGQAGSHQQSHQESARGRSGE**TSGHSGSFLYQVSTHEQSESSHGWTG**
PSTRGRQGSRHEQAQDSSRHSASQYGQDTIRGHPGSSRGGRQGYHHEHSVDSSGHSGSHHSHTTSQGRSD
ASRGQSGSRSASRTTRNEEQSGDSSRHSVSRHHEASTHADISRHSQAVQGQSEGSRRSRRQGSSVSQDSD
SEGHSEDSERWSGSASRNHRGSVQEQSRHGSRHPRSHHEDRAGHGHSADRSRQSGTRHAETSSGGQAASS
HEQARSSPGERHGSRHQQSADSSRHSGIPRGQASSAVRDSRHWGSSGSQASDSEGHSEESDTQSVSGHGQ
AGPHQQSHQESARDRSGGRSGRSGSFLYQVSTHEQSESAHGRTRTSTGRRQGSHHEQARDSSRHSASQEG
QDTIRGHPGSSRRGRQGSHYEQSVDRSGHSGSHHSHTTSQGRSDASRGQSGSRSASRQTRNDEQSGDGSR
HSWSHHHEASTQADSSRHSQSGQGQSAGPRTSRNQGSSVSQDSDSQGHSEDSERWSGSASRNHRGSAQEQ
SRDGSRHPTSHHEDRAGHGHSAESSRQSGTHHAENSSGGQAASSHEQARSSAGERHGSHHQQSADSSRHS
GIGHGQASSAVRDSGHRGSSGSQASDSEGHSEDSDTQSVSAHGQAGPHQQSHQESTRGRSAGRSGRSGSF
LYQVSTHEQSESAHGRAGPSTGGRQGSRHEQARDSSRHSASQEGQDTIRGHPGSRRGGRQGSYHEQSVDR
SGHSGSHHSHTTSQGRSDASHGQSGSRSASRETRNEEQSGDGSRHSGSRHHEASTQADSSRHSQSGQGES
AGSRRSRRQGSSVSQDSDSEAYPEDSERRSESASRNHHGSSREQSRDGSRHPGSSHRDTASHVQSSPVQS
DSSTAKEHGHFSSLSQDSAYHSGIQSRGSPHSSSSYHYQSEGTERQKGQSGLVWRHGSYGSADYDYGESG
FRHSQHGSVSYNSNPVVFKERSDICKASAFGKDHPRYYATYINKDPGLCGHSSDISKQLGFSQSQRYYYY
E

Figure 6.6 Consensus sequence of human profilaggrin, based on RefSeq NP_002007. This shows 10 full filaggrin repeats (marked by alternate use of bold type and and regular type), flanked by two partial filaggrin sequences (marked by blue font) that contain areas of high homology to the full repeats 1-10. The linker peptide sequence RSGRSGSFLY is arbitrarily assigned as the start of each repeat.

Apart from the complete profilaggrin sequence RefSeq NP_002007, the NCBInr protein database also contains 16 other entries for 'profilaggrin' or 'filaggrin'. All these are truncated segments of the profilaggrin sequence, with most containing the sequence of either one incomplete filaggrin repeat, or several full filaggrin repeats. For instance, the entry 'filaggrin, isoform CRA_a' (NCBInr accession number EAW53383) contains the sequence for the N-terminus and almost the entire first and second filaggrin repeats. The presence of these various entries of 'profilaggrin' and 'filaggrin' in the protein databases frequently complicated the interpretation of MS search results. This was because samples were often matched to different truncated forms of profilaggrin, producing variable MOWSE/MASCOT scores with different percentage coverages. Logically, the tryptic-digest of a filaggrin sample that was matched to the complete profilaggrin sequence would have a lower score and lower percentage coverage than if it were matched to a shorter (and incomplete) profilaggrin sequence in the database. As a result, direct comparison of search results between samples were frequently not possible.

Another issue with the current protein databases stems from the significant heterogeneity of filaggrin. A comparison of the amino acid sequences of the 10 filaggrin repeats from RefSeq NP_002007 clearly reveals the significant heterogeneity of the protein. To illustrate this, Figure 6.7 shows the consensus sequence of a single filaggrin repeat together with all the alternative amino acids.

Figure 6.7 Amino acid sequence of human filaggrin which contains 324 amino acids. Alternative amino acids (in blue) noted from the comparison of the 10 full filaggrin repeats in RefSeq NP_002007 are displayed below the consensus sequence.

As the alternative amino acids noted in Figure 6.7 are from only one single individual, it is highly likely that other alternative amino acids exist that are not currently reflected in the protein databases. This may lead to experimental filaggrin peptides with alternative sequences either not being matched to filaggrin in the databases, or matched weakly. One possible solution is to sequence the *FLG* gene in a large cohort of individuals to assemble a more comprehensive database that better reflects the alternative sequences of filaggrin. However, the present technical difficulty in fully sequencing the *FLG* gene due to its large size and repetitive nature of the filaggrin units makes this currently impractical.

In summary, this structural study has demonstrated that it is possible to extract filaggrin using tape strips for structural studies using MS techniques. The use of tape stripping, which is a much less invasive method compared to

skin biopsies, will make it more feasible and practicable to study filaggrin protein directly from the SC. It is disappointing that an inadequate amount of filaggrin was obtained from all the AD samples to allow for any comparison of filaggrin structure between AD and non-AD samples. With the apparently limited amount of filaggrin present in AD skin, it seems that the only ways of obtaining sufficient filaggrin from AD individuals would be to either significantly increase the number of tape strips used, or to extract from the large amount of normal skin following breast reduction procedures or abdominoplasties. Our initial strategy was to use a data analysis programme called Progenesis LC-MS (NonLinear Dynamics) that can reliably quantify and compare the peaks in filaggrin tryptic-digest samples in order to see if there are any structural differences between filaggrin protein found in AD and non-AD individuals. Preliminary runs had shown that the programme could rapidly and reliably identify the peptide peaks in our samples, but there was insufficient MS data in any of the AD samples to allow for accurate comparison. Nonetheless, this study has confirmed the heterogeneity of filaggrin protein, even within a single individual, and has also shown that filaggrin protein is only minimally expressed in the skin of individuals with AD.

Chapter 7 General Discussion and Future Perspectives

7.0 GENERAL DISCUSSION AND FUTURE PERSPECTIVES

Clinically, the most striking features of AD are erythema, pruritus and inflammation, generally in association with elevated IgE. Correspondingly, most previous research on AD had postulated immunological dysfunction as the key underlying aetiological factor. However subsequent to the discovery of the exceptionally strong association between *FLG* mutations and AD, there was a significant shift in our understanding of the aetiology of the disease. McLean and colleagues hypothesize that the absence of filaggrin leads to a defect in the barrier function of the skin, and that this secondarily allows enhanced antigen presentation to the immune system. Therefore, according to this 'Barrier Hypothesis', the inflammation and immunological changes of AD (and possibly that of asthma and hay fever) are consequent upon this antigen exposure.

One of the main focuses of this thesis was a functional study aimed at determining whether *FLG* mutations correlated with altered skin barrier function in AD subjects. This study showed that *FLG* mutations correlated with higher TEWL and fewer number of tape strips required to abrogate skin barrier, thus providing strong evidence of an association between *FLG* variants and skin barrier dysfunction, although the clinical relevance of this was uncertain since *FLG* variants were not found to be associated with AD severity in this study. Nonetheless, as mentioned earlier, this lack of association between *FLG* mutations and AD severity could be due to the fact that only mild and moderate AD subjects were recruited for this study. Certainly, previous studies had suggested that filaggrin-related AD might be associated with increased severity in childhood [22, 120], as well as AD with an early onset that persists into adulthood [31]. In summary, the results from this study suggest that it might be possible to stratify AD phenotype by *FLG* genotype, with filaggrin-related AD likely to exhibit poorer skin barrier and possibly run a more severe disease course. Thus, there is potentially prognostic value in determining *FLG* status in AD patients.

There was also a secondary aim in this functional study, which was to test the hypothesis that corneocytes were less adherent to one another in filaggrin-related AD compared to wild-type AD skin. This was to test a hypothesis developed from an unexpected finding reported by Nemoto-Hasebe *et al* [244], who showed that SC thickness was greater in filaggrin-related AD compared to wild-type AD skin. To possibly explain this finding, it was hypothesised in this study that corneocytes in filaggrin-related AD skin were less adherent to one another (that is, less densely packed), which should translate to more corneocytes (and therefore more protein) being removed by each tape strip. Indeed, this study showed that significantly more protein was extracted from filaggrin-related AD compared to wild-type AD skin, lending support to this hypothesis. This was also consistent with another observation in this study showing that fewer tape strips were required to abrogate skin barrier in filaggrin-related AD skin, since less-adherent SC cells would mean that they would be easier to remove with subsequent loss of skin barrier. However, the sample size for this analysis was small, with only four filaggrin-related AD and four wild-type-AD samples analysed. Thus, this finding would benefit from further validation by extending the cohort size.

The second main focus of this thesis was a structural study aimed at interrogating the structure-function relation of filaggrin. Up to about half of individuals with AD do not possess *FLG* mutations and it is not known if filaggrin in these wild-type AD subjects is structurally similar to that in non-AD individuals. Any structural differences between the two groups may provide insight into why one group develops the disease while the other does not. This study utilised two MS techniques (MALDI-TOF MS and nano LC-MS/MS) to analyse filaggrin in both its intact and tryptic-digest states. Analysis of intact filaggrin from non-AD subjects confirmed the heterogeneic nature of filaggrin, even within a single individual; while MS analysis of non-AD filaggrin tryptic-digests yielded good mass spectra. However none of the MS analysis of filaggrin from AD subjects yielded any interpretable results, with the mass spectra obtained by both MS techniques suggesting that filaggrin was either absent or in

too minute an amount for detection. This was confirmed by immunoblotting of the initial SC extracts of all AD samples (regardless of their genotype) which showed less filaggrin extracted compared to non-AD samples. Additionally, no filaggrin was immunodetected in any of the final purified AD samples. A consequence of this reduced amount of filaggrin extracted from AD subjects was the inability to make any structural comparison between the protein from AD and non-AD skin. Nonetheless, this was an interesting finding in itself, and could offer an explanation for why wild-type AD individuals develop the disease. This reduced filaggrin in AD skin could partly be attributed to an over-expression of T_H2 cytokines that had previously been shown, *in vitro*, to down-regulate filaggrin expression [115]. Therefore, it is possible that wild-type AD could have a primary immunological dysfunction that secondarily result in reduced filaggrin expression and impaired skin barrier. As such, the clinical phenotype of AD may result from different pathophysiological mechanisms - one initiated by a *FLG* defective barrier failure in which secondary immunological changes occur, and the other a predominantly immunologically-mediated disease in which cytokines released into the skin reduce barrier function.

Part of this structural study also involved developing and optimising the extraction and purification of filaggrin, as sufficient amount of relatively pure filaggrin was required for MS analysis. Traditionally, discarded skin from procedures such as breast reduction surgery and abdominoplasty is used in skin research, since these provide a large amount of healthy skin. In this study, tape stripping was trialled for the first time as a mean of filaggrin extraction. This was a minimally-invasive and quick method of extracting SC cells, and has the great advantage of allowing for repeated extraction from the same individual.

Soon after commencing this study, it became clear that there were practical benefits to having a relatively quick screening test to detect and quantify filaggrin in the skin. One major benefit of such a test was the obviation of expensive and time-consuming genotype testing for individuals that were

unlikely to possess any *FLG* mutation. In the absence of any commercially-available filaggrin-specific ELISA at that time, a novel one was developed that could quantify filaggrin with a detection sensitivity of approximately 30 ng/ml. Given more time and resources, particularly with the commercial availability of many more new filaggrin antibodies, the 'sandwich' ELISA that was initially being developed could be made more specific, which should improve the detection sensitivity.

In summary, this study has provided greater insight into the role of filaggrin in skin barrier function and AD. The discovery of mutations in a single gene underlying up to around half of AD cases has been one of the most exciting recent genetic findings in dermatology. Unsurprisingly, this has generated a lot of research interest in filaggrin. Work is continuing in this lab to study the exceptionally strong link between filaggrin and AD. This includes analysing the effects of *FLG* mutations on epidermal dendritic cell populations as these cells initiate epidermal immune responses, and the susceptibility of *FLG* variants to irritant and allergic contact dermatitis. In addition, as there have been suggestions that measuring baseline skin barrier function may provide an incomplete assessment of barrier integrity [257], future work will analyse acute perturbations of the SC with subsequent assessment of the kinetics of barrier recovery.

Chapter 8 References

8.0 REFERENCES

1. Odland, G.F., *Physiology, Biochemistry, and Molecular Biology of the Skin*. 2 ed, ed. L.A. Goldsmith. 1991, New York: Oxford Univeristy Press.
2. Williams, H., et al., *Worldwide variations in the prevalence of symptoms of atopic eczema in the International Study of Asthma and Allergies in Childhood.* J Allergy Clin Immunol, 1999. **103**(1 Pt 1): p. 125-38.
3. Holgate, S.T., *The epidemic of allergy and asthma.* Nature, 1999. **402**(6760 Suppl): p. B2-4.
4. Larsen, F.S., N.V. Holm, and K. Henningsen, *Atopic dermatitis. A genetic-epidemiologic study in a population-based twin sample.* J Am Acad Dermatol, 1986. **15**(3): p. 487-94.
5. Schultz Larsen, F., *Atopic dermatitis: a genetic-epidemiologic study in a population-based twin sample.* J Am Acad Dermatol, 1993. **28**(5 Pt 1): p. 719-23.
6. Thomsen, S.F., et al., *Importance of genetic factors in the etiology of atopic dermatitis: a twin study.* Allergy Asthma Proc, 2007. **28**(5): p. 535-9.
7. Morar, N., et al., *The genetics of atopic dermatitis.* J Allergy Clin Immunol, 2006. **118**(1): p. 24-34; quiz 35-6.
8. Kaiser, H.B., *Risk factors in allergy/asthma.* Allergy Asthma Proc, 2004. **25**(1): p. 7-10.
9. Steinke, J.W., L. Borish, and L.J. Rosenwasser, *5. Genetics of hypersensitivity.* J Allergy Clin Immunol, 2003. **111**(2 Suppl): p. S495-501.
10. Cookson, W.O., et al., *Genetic linkage of childhood atopic dermatitis to psoriasis susceptibility loci.* Nat Genet, 2001. **27**(4): p. 372-3.
11. Ong, P.Y., et al., *Decreased IL-15 may contribute to elevated IgE and acute inflammation in atopic dermatitis.* J Immunol, 2002. **168**(1): p. 505-10.
12. Fiset, P.O., D.Y. Leung, and Q. Hamid, *Immunopathology of atopic dermatitis.* J Allergy Clin Immunol, 2006. **118**(1): p. 287-90.
13. Howell, M.D., et al., *Cytokine milieu of atopic dermatitis skin subverts the innate immune response to vaccinia virus.* Immunity, 2006. **24**(3): p. 341-8.
14. Seidenari, S. and G. Giusti, *Objective assessment of the skin of children affected by atopic dermatitis: a study of pH, capacitance and TEWL in eczematous and clinically uninvolved skin.* Acta Derm Venereol, 1995. **75**(6): p. 429-33.
15. Hon, K.L., et al., *Comparison of skin hydration evaluation sites and correlations among skin hydration, transepidermal water loss, SCORAD index, Nottingham Eczema Severity Score, and quality of life in patients with atopic dermatitis.* Am J Clin Dermatol, 2008. **9**(1): p. 45-50.
16. Proksch, E., R. Folster-Holst, and J.M. Jensen, *Skin barrier function, epidermal proliferation and differentiation in eczema.* J Dermatol Sci, 2006. **43**(3): p. 159-69.
17. Ogawa, H. and T. Yoshiike, *Atopic dermatitis: studies of skin permeability and effectiveness of topical PUVA treatment.* Pediatr Dermatol, 1992. **9**(4): p. 383-5.

18. Jakasa, I., et al., *Percutaneous penetration of sodium lauryl sulphate is increased in uninvolved skin of patients with atopic dermatitis compared with control subjects.* Br J Dermatol, 2006. **155**(1): p. 104-9.
19. Jakasa, I., et al., *Altered penetration of polyethylene glycols into uninvolved skin of atopic dermatitis patients.* J Invest Dermatol, 2007. **127**(1): p. 129-34.
20. Sugarman, J.L., et al., *The objective severity assessment of atopic dermatitis score: an objective measure using permeability barrier function and stratum corneum hydration with computer-assisted estimates for extent of disease.* Arch Dermatol, 2003. **139**(11): p. 1417-22.
21. Eberlein-Konig, B., et al., *Skin surface pH, stratum corneum hydration, trans-epidermal water loss and skin roughness related to atopic eczema and skin dryness in a population of primary school children.* Acta Derm Venereol, 2000. **80**(3): p. 188-91.
22. Palmer, C.N., et al., *Common loss-of-function variants of the epidermal barrier protein filaggrin are a major predisposing factor for atopic dermatitis.* Nat Genet, 2006. **38**(4): p. 441-6.
23. Sandilands, A., et al., *Comprehensive analysis of the gene encoding filaggrin uncovers prevalent and rare mutations in ichthyosis vulgaris and atopic eczema.* Nat Genet, 2007. **39**(5): p. 650-4.
24. Sybert, V.P., B.A. Dale, and K.A. Holbrook, *Ichthyosis vulgaris: identification of a defect in synthesis of filaggrin correlated with an absence of keratohyaline granules.* J Invest Dermatol, 1985. **84**(3): p. 191-4.
25. Smith, F.J., et al., *Loss-of-function mutations in the gene encoding filaggrin cause ichthyosis vulgaris.* Nat Genet, 2006. **38**(3): p. 337-42.
26. Irvine, A.D., *Fleshing out filaggrin phenotypes.* J Invest Dermatol, 2007. **127**(3): p. 504-7.
27. Weller, R. and W. McLean, *Filaggrin and Eczema.* J R Coll Physicians Edinb, 2008(38): p. 45-7.
28. Hudson, T.J., *Skin barrier function and allergic risk.* Nat Genet, 2006. **38**(4): p. 399-400.
29. Irvine, A.D. and W.H. McLean, *Breaking the (un)sound barrier: filaggrin is a major gene for atopic dermatitis.* J Invest Dermatol, 2006. **126**(6): p. 1200-2.
30. McGrath, J.A., *Filaggrin and the great epidermal barrier grief.* Australas J Dermatol, 2008. **49**(2): p. 67-73; quiz 73-4.
31. Barker, J.N., et al., *Null mutations in the filaggrin gene (FLG) determine major susceptibility to early-onset atopic dermatitis that persists into adulthood.* J Invest Dermatol, 2007. **127**(3): p. 564-7.
32. Marenholz, I., et al., *Filaggrin loss-of-function mutations predispose to phenotypes involved in the atopic march.* J Allergy Clin Immunol, 2006. **118**(4): p. 866-71.
33. Ruether, A., et al., *Filaggrin loss-of-function variant contributes to atopic dermatitis risk in the population of Northern Germany.* Br J Dermatol, 2006. **155**(5): p. 1093-4.

34. Stemmler, S., et al., *Two common loss-of-function mutations within the filaggrin gene predispose for early onset of atopic dermatitis.* J Invest Dermatol, 2007. **127**(3): p. 722-4.
35. Weidinger, S., et al., *Filaggrin mutations strongly predispose to early-onset and extrinsic atopic dermatitis.* J Invest Dermatol, 2007. **127**(3): p. 724-6.
36. Giardina, E., et al., *R501X and 2282del4 filaggrin mutations do not confer susceptibility to psoriasis and atopic dermatitis in Italian patients.* Dermatology, 2008. **216**(1): p. 83-4.
37. Zhang, H., et al., *Mutations in the filaggrin gene in Han Chinese patients with atopic dermatitis.* Allergy, 2010.
38. Sandilands, A., et al., *Prevalent and rare mutations in the gene encoding filaggrin cause ichthyosis vulgaris and predispose individuals to atopic dermatitis.* J Invest Dermatol, 2006. **126**(8): p. 1770-5.
39. Chen, H., et al., *Unique and recurrent mutations in the filaggrin gene in Singaporean Chinese patients with ichthyosis vulgaris.* J Invest Dermatol, 2008. **128**(7): p. 1669-75.
40. Nomura, T., et al., *Specific Filaggrin Mutations Cause Ichthyosis Vulgaris and Are Significantly Associated with Atopic Dermatitis in Japan.* J Invest Dermatol, 2008.
41. Sasaki, T., et al., *Sequence analysis of filaggrin gene by novel shotgun method in Japanese atopic dermatitis.* J Dermatol Sci, 2008. **51**(2): p. 113-20.
42. Weidinger, S., et al., *Filaggrin mutations, atopic eczema, hay fever, and asthma in children.* J Allergy Clin Immunol, 2008. **121**(5): p. 1203-1209 e1.
43. Henderson, J., et al., *The burden of disease associated with filaggrin mutations: a population-based, longitudinal birth cohort study.* J Allergy Clin Immunol, 2008. **121**(4): p. 872-7 e9.
44. Brown, S.J., et al., *Filaggrin null mutations and childhood atopic eczema: a population-based case-control study.* J Allergy Clin Immunol, 2008. **121**(4): p. 940-46 e3.
45. Brown, S.J., et al., *Prevalent and low-frequency null mutations in the filaggrin gene are associated with early-onset and persistent atopic eczema.* J Invest Dermatol, 2008. **128**(6): p. 1591-4.
46. Nomura, T., et al., *Unique mutations in the filaggrin gene in Japanese patients with ichthyosis vulgaris and atopic dermatitis.* J Allergy Clin Immunol, 2007. **119**(2): p. 434-40.
47. Hamada, T., et al., *De Novo Occurrence of the Filaggrin Mutation p.R501X with Prevalent Mutation c.3321delA in a Japanese Family with Ichthyosis Vulgaris Complicated by Atopic Dermatitis.* J Invest Dermatol, 2007.
48. Volz, A., et al., *Physical mapping of a functional cluster of epidermal differentiation genes on chromosome 1q21.* Genomics, 1993. **18**(1): p. 92-9.
49. Mischke, D., et al., *Genes encoding structural proteins of epidermal cornification and S100 calcium-binding proteins form a gene complex ("epidermal differentiation complex") on human chromosome 1q21.* J Invest Dermatol, 1996. **106**(5): p. 989-92.

50. Marenholz, I., et al., *Identification of human epidermal differentiation complex (EDC)-encoded genes by subtractive hybridization of entire YACs to a gridded keratinocyte cDNA library.* Genome Res, 2001. **11**(3): p. 341-55.
51. Steinert, P.M. and L.N. Marekov, *The proteins elafin, filaggrin, keratin intermediate filaments, loricrin, and small proline-rich proteins 1 and 2 are isodipeptide cross-linked components of the human epidermal cornified cell envelope.* J Biol Chem, 1995. **270**(30): p. 17702-11.
52. Steinert, P.M., *Structural-mechanical integration of keratin intermediate filaments with cell peripheral structures in the cornified epidermal keratinocyte.* Biol Bull, 1998. **194**(3): p. 367-8; discussion 369-70.
53. Dale, B.A., et al., *Identification of filaggrin in cultured mouse keratinocytes and its regulation by calcium.* J Invest Dermatol, 1983. **81**(1 Suppl): p. 90s-5s.
54. Steven, A.C., et al., *Biosynthetic pathways of filaggrin and loricrin--two major proteins expressed by terminally differentiated epidermal keratinocytes.* J Struct Biol, 1990. **104**(1-3): p. 150-62.
55. Manabe, M., et al., *Interaction of filaggrin with keratin filaments during advanced stages of normal human epidermal differentiation and in ichthyosis vulgaris.* Differentiation, 1991. **48**(1): p. 43-50.
56. Harding, C.R. and I.R. Scott, *Histidine-rich proteins (filaggrins): structural and functional heterogeneity during epidermal differentiation.* J Mol Biol, 1983. **170**(3): p. 651-73.
57. Presland, R.B., et al., *Characterization of the human epidermal profilaggrin gene. Genomic organization and identification of an S-100-like calcium binding domain at the amino terminus.* J Biol Chem, 1992. **267**(33): p. 23772-81.
58. Markova, N.G., et al., *Profilaggrin is a major epidermal calcium-binding protein.* Mol Cell Biol, 1993. **13**(1): p. 613-25.
59. Gan, S.Q., et al., *Organization, structure, and polymorphisms of the human profilaggrin gene.* Biochemistry, 1990. **29**(40): p. 9432-40.
60. Resing, K.A., et al., *Identification of proteolytic cleavage sites in the conversion of profilaggrin to filaggrin in mammalian epidermis.* J Biol Chem, 1989. **264**(3): p. 1837-45.
61. McKinley-Grant, L.J., et al., *Characterization of a cDNA clone encoding human filaggrin and localization of the gene to chromosome region 1q21.* Proc Natl Acad Sci U S A, 1989. **86**(13): p. 4848-52.
62. Rothnagel, J.A. and P.M. Steinert, *The structure of the gene for mouse filaggrin and a comparison of the repeating units.* J Biol Chem, 1990. **265**(4): p. 1862-5.
63. Dale, B.A., et al., *Characterization of two monoclonal antibodies to human epidermal keratohyalin: reactivity with filaggrin and related proteins.* J Invest Dermatol, 1987. **88**(3): p. 306-13.
64. Kuechle, M.K., et al., *Profilaggrin requires both linker and filaggrin peptide sequences to form granules: implications for profilaggrin processing in vivo.* J Invest Dermatol, 1999. **112**(6): p. 843-52.

65. Presland, R.B., et al., *Regulated expression of human filaggrin in keratinocytes results in cytoskeletal disruption, loss of cell-cell adhesion, and cell cycle arrest.* Exp Cell Res, 2001. **270**(2): p. 199-213.
66. Pearton, D.J., B.A. Dale, and R.B. Presland, *Functional analysis of the profilaggrin N-terminal peptide: identification of domains that regulate nuclear and cytoplasmic distribution.* J Invest Dermatol, 2002. **119**(3): p. 661-9.
67. Presland, R.B., et al., *Characterization of two distinct calcium-binding sites in the amino-terminus of human profilaggrin.* J Invest Dermatol, 1995. **104**(2): p. 218-23.
68. Ishida-Yamamoto, A., et al., *Translocation of profilaggrin N-terminal domain into keratinocyte nuclei with fragmented DNA in normal human skin and loricrin keratoderma.* Lab Invest, 1998. **78**(10): p. 1245-53.
69. Zhang, D., et al., *Characterization of mouse profilaggrin: evidence for nuclear engulfment and translocation of the profilaggrin B-domain during epidermal differentiation.* J Invest Dermatol, 2002. **119**(4): p. 905-12.
70. Presland, R.B., et al., *Regulation of human profilaggrin promoter activity in cultured epithelial cells by retinoic acid and glucocorticoids.* J Dermatol Sci, 2001. **27**(3): p. 192-205.
71. Rothnagel, J.A., et al., *The gene for mouse epidermal filaggrin precursor. Its partial characterization, expression, and sequence of a repeating filaggrin unit.* J Biol Chem, 1987. **262**(32): p. 15643-8.
72. Haydock, P.V. and B.A. Dale, *The repetitive structure of the profilaggrin gene as demonstrated using epidermal profilaggrin cDNA.* J Biol Chem, 1986. **261**(27): p. 12520-5.
73. Presland, R.B., et al., *Loss of normal profilaggrin and filaggrin in flaky tail (ft/ft) mice: an animal model for the filaggrin-deficient skin disease ichthyosis vulgaris.* J Invest Dermatol, 2000. **115**(6): p. 1072-81.
74. Lonsdale-Eccles, J.D., D.C. Teller, and B.A. Dale, *Characterization of a phosphorylated form of the intermediate filament-aggregating protein filaggrin.* Biochemistry, 1982. **21**(23): p. 5940-8.
75. Resing, K.A., K.A. Walsh, and B.A. Dale, *Identification of two intermediates during processing of profilaggrin to filaggrin in neonatal mouse epidermis.* J Cell Biol, 1984. **99**(4 Pt 1): p. 1372-8.
76. Kam, E., et al., *Identification of rat epidermal profilaggrin phosphatase as a member of the protein phosphatase 2A family.* J Cell Sci, 1993. **106 (Pt 1)**: p. 219-26.
77. Ohno, J., et al., *Immuno- and enzyme-histochemical detection of phosphoprotein phosphatase in rat epidermis.* J Histochem Cytochem, 1989. **37**(5): p. 629-34.
78. Pelech, S. and P. Cohen, *The protein phosphatases involved in cellular regulation. 1. Modulation of protein phosphatases-1 and 2A by histone H1, protamine, polylysine and heparin.* Eur J Biochem, 1985. **148**(2): p. 245-51.
79. Lonsdale-Eccles, J.D., A.M. Lynley, and B.A. Dale, *Cyanogen bromide cleavage of proteins in sodium dodecyl sulphate/polyacrylamide gels.*

Diagonal peptide mapping of proteins from epidermis. Biochem J, 1981. **197**(3): p. 591-7.
80. Scott, I.R. and C.R. Harding, *Studies on the synthesis and degradation of a high molecular weight, histidine-rich phosphoprotein from mammalian epidermis.* Biochim Biophys Acta, 1981. **669**(1): p. 65-78.
81. Resing, K.A., et al., *Characterization of profilaggrin endoproteinase 1. A regulated cytoplasmic endoproteinase of epidermis.* J Biol Chem, 1995. **270**(47): p. 28193-8.
82. Dale, B.A., et al., *Transient expression of epidermal filaggrin in cultured cells causes collapse of intermediate filament networks with alteration of cell shape and nuclear integrity.* J Invest Dermatol, 1997. **108**(2): p. 179-87.
83. Pearton, D.J., et al., *Proprotein convertase expression and localization in epidermis: evidence for multiple roles and substrates.* Exp Dermatol, 2001. **10**(3): p. 193-203.
84. Resing, K.A., R.S. Johnson, and K.A. Walsh, *Characterization of protease processing sites during conversion of rat profilaggrin to filaggrin.* Biochemistry, 1993. **32**(38): p. 10036-45.
85. Yamazaki, M., et al., *Cytoplasmic processing of human profilaggrin by active mu-calpain.* Biochem Biophys Res Commun, 1997. **235**(3): p. 652-6.
86. List, K., et al., *Loss of proteolytically processed filaggrin caused by epidermal deletion of Matriptase/MT-SP1.* J Cell Biol, 2003. **163**(4): p. 901-10.
87. Leyvraz, C., et al., *The epidermal barrier function is dependent on the serine protease CAP1/Prss8.* J Cell Biol, 2005. **170**(3): p. 487-96.
88. Descargues, P., et al., *Spink5-deficient mice mimic Netherton syndrome through degradation of desmoglein 1 by epidermal protease hyperactivity.* Nat Genet, 2005. **37**(1): p. 56-65.
89. Hewett, D.R., et al., *Lethal, neonatal ichthyosis with increased proteolytic processing of filaggrin in a mouse model of Netherton syndrome.* Hum Mol Genet, 2005. **14**(2): p. 335-46.
90. Brash, A.R., et al., *The hepoxilin connection in the epidermis.* FEBS J, 2007. **274**(14): p. 3494-502.
91. Krieg, P., et al., *Epidermis-type lipoxygenases.* Adv Exp Med Biol, 2002. **507**: p. 165-70.
92. Steinert, P.M., et al., *Characterization of a class of cationic proteins that specifically interact with intermediate filaments.* Proc Natl Acad Sci U S A, 1981. **78**(7): p. 4097-101.
93. Dale, B.A., K.A. Holbrook, and P.M. Steinert, *Assembly of stratum corneum basic protein and keratin filaments in macrofibrils.* Nature, 1978. **276**(5689): p. 729-31.
94. Lynley, A.M. and B.A. Dale, *The characterization of human epidermal filaggrin. A histidine-rich, keratin filament-aggregating protein.* Biochim Biophys Acta, 1983. **744**(1): p. 28-35.

95. Mack, J.W., A.C. Steven, and P.M. Steinert, *The mechanism of interaction of filaggrin with intermediate filaments. The ionic zipper hypothesis.* J Mol Biol, 1993. **232**(1): p. 50-66.
96. Candi, E., R. Schmidt, and G. Melino, *The cornified envelope: a model of cell death in the skin.* Nat Rev Mol Cell Biol, 2005. **6**(4): p. 328-40.
97. Presland, R.B., et al., *Barrier function in transgenic mice overexpressing K16, involucrin, and filaggrin in the suprabasal epidermis.* J Invest Dermatol, 2004. **123**(3): p. 603-6.
98. Rawlings, A.V. and C.R. Harding, *Moisturization and skin barrier function.* Dermatol Ther, 2004. **17 Suppl 1**: p. 43-8.
99. Katagiri, C., et al., *Changes in environmental humidity affect the water-holding property of the stratum corneum and its free amino acid content, and the expression of filaggrin in the epidermis of hairless mice.* J Dermatol Sci, 2003. **31**(1): p. 29-35.
100. Tarcsa, E., et al., *Protein unfolding by peptidylarginine deiminase. Substrate specificity and structural relationships of the natural substrates trichohyalin and filaggrin.* J Biol Chem, 1996. **271**(48): p. 30709-16.
101. Mechin, M.C., et al., *The peptidylarginine deiminases expressed in human epidermis differ in their substrate specificities and subcellular locations.* Cell Mol Life Sci, 2005. **62**(17): p. 1984-95.
102. Nachat, R., et al., *Peptidylarginine deiminase isoforms 1-3 are expressed in the epidermis and involved in the deimination of K1 and filaggrin.* J Invest Dermatol, 2005. **124**(2): p. 384-93.
103. Ishida-Yamamoto, A., et al., *Sequential reorganization of cornified cell keratin filaments involving filaggrin-mediated compaction and keratin 1 deimination.* J Invest Dermatol, 2002. **118**(2): p. 282-7.
104. Denecker, G., et al., *Caspase-14 protects against epidermal UVB photodamage and water loss.* Nat Cell Biol, 2007. **9**(6): p. 666-74.
105. Kamata, Y., et al., *Neutral cysteine protease bleomycin hydrolase is essential for the breakdown of deiminated filaggrin into amino acids.* J Biol Chem, 2009. **284**(19): p. 12829-36.
106. O'Regan, G.M., et al., *Filaggrin in atopic dermatitis.* J Allergy Clin Immunol, 2008. **122**(4): p. 689-93.
107. Brown, S.J. and W.H. McLean, *Eczema genetics: current state of knowledge and future goals.* J Invest Dermatol, 2009. **129**(3): p. 543-52.
108. Wells, R.S. and C.B. Kerr, *Clinical features of autosomal dominant and sex-linked ichthyosis in an English population.* Br Med J, 1966. **1**(5493): p. 947-50.
109. Fleckman, P. and S. Brumbaugh, *Absence of the granular layer and keratohyalin define a morphologically distinct subset of individuals with ichthyosis vulgaris.* Exp Dermatol, 2002. **11**(4): p. 327-36.
110. Nirunsuksiri, W., et al., *Decreased profilaggrin expression in ichthyosis vulgaris is a result of selectively impaired posttranscriptional control.* J Biol Chem, 1995. **270**(2): p. 871-6.
111. Zhong, W., et al., *Linkage analysis suggests a locus of ichthyosis vulgaris on 1q22.* J Hum Genet, 2003. **48**(7): p. 390-2.

112. Gruber, R., et al., *Filaggrin mutations p.R501X and c.2282del4 in ichthyosis vulgaris.* Eur J Hum Genet, 2007. **15**(2): p. 179-84.
113. Seguchi, T., et al., *Decreased expression of filaggrin in atopic skin.* Arch Dermatol Res, 1996. **288**(8): p. 442-6.
114. Ginger, R.S., et al., *Filaggrin repeat number polymorphism is associated with a dry skin phenotype.* Arch Dermatol Res, 2005. **297**(6): p. 235-41.
115. Howell, M.D., et al., *Cytokine modulation of atopic dermatitis filaggrin skin expression.* J Allergy Clin Immunol, 2007. **120**(1): p. 150-5.
116. McGrath, J.A. and J. Uitto, *The filaggrin story: novel insights into skin-barrier function and disease.* Trends Mol Med, 2008. **14**(1): p. 20-7.
117. Palmer, C.N., et al., *Filaggrin null mutations are associated with increased asthma severity in children and young adults.* J Allergy Clin Immunol, 2007. **120**(1): p. 64-8.
118. Callard, R.E. and J.I. Harper, *The skin barrier, atopic dermatitis and allergy: a role for Langerhans cells?* Trends Immunol, 2007. **28**(7): p. 294-8.
119. Ying, S., et al., *Lack of filaggrin expression in the human bronchial mucosa.* J Allergy Clin Immunol, 2006. **118**(6): p. 1386-8.
120. Weidinger, S., et al., *Loss-of-function variations within the filaggrin gene predispose for atopic dermatitis with allergic sensitizations.* J Allergy Clin Immunol, 2006. **118**(1): p. 214-9.
121. Safavi, K.H., et al., *Incidence of alopecia areata in Olmsted County, Minnesota, 1975 through 1989.* Mayo Clin Proc, 1995. **70**(7): p. 628-33.
122. Ikeda, T., *A new classification of alopecia areata.* Dermatologica, 1965. **131**(6): p. 421-45.
123. Young, E., H.M. Bruns, and L. Berrens, *Alopecia areata and atopy [proceedings].* Dermatologica, 1978. **156**(5): p. 306-8.
124. Tan, E., et al., *The pattern and profile of alopecia areata in Singapore--a study of 219 Asians.* Int J Dermatol, 2002. **41**(11): p. 748-53.
125. Goh, C., et al., *Profile of 513 patients with alopecia areata: associations of disease subtypes with atopy, autoimmune disease and positive family history.* J Eur Acad Dermatol Venereol, 2006. **20**(9): p. 1055-60.
126. Betz, R.C., et al., *Loss-of-function mutations in the filaggrin gene and alopecia areata: strong risk factor for a severe course of disease in patients comorbid for atopic disease.* J Invest Dermatol, 2007. **127**(11): p. 2539-43.
127. Liao, H., et al., *Filaggrin mutations are genetic modifying factors exacerbating X-linked ichthyosis.* J Invest Dermatol, 2007. **127**(12): p. 2795-8.
128. Agner, T. and J. Serup, *Sodium lauryl sulphate for irritant patch testing--a dose-response study using bioengineering methods for determination of skin irritation.* J Invest Dermatol, 1990. **95**(5): p. 543-7.
129. Fluhr, J.W., K.R. Feingold, and P.M. Elias, *Transepidermal water loss reflects permeability barrier status: validation in human and rodent in vivo and ex vivo models.* Exp Dermatol, 2006. **15**(7): p. 483-92.

130. Elias, P.M. and K.R. Feingold, *Coordinate regulation of epidermal differentiation and barrier homeostasis.* Skin Pharmacol Appl Skin Physiol, 2001. **14 Suppl 1**: p. 28-34.
131. Chuong, C.M., et al., *What is the 'true' function of skin?* Exp Dermatol, 2002. **11**(2): p. 159-87.
132. Tagami, H., H. Kobayashi, and K. Kikuchi, *A portable device using a closed chamber system for measuring transepidermal water loss: comparison with the conventional method.* Skin Res Technol, 2002. **8**(1): p. 7-12.
133. De Paepe, K., et al., *Validation of the VapoMeter, a closed unventilated chamber system to assess transepidermal water loss vs. the open chamber Tewameter.* Skin Res Technol, 2005. **11**(1): p. 61-9.
134. Barel, A.O. and P. Clarys, *Study of the stratum corneum barrier function by transepidermal water loss measurements: comparison between two commercial instruments: Evaporimeter and Tewameter.* Skin Pharmacol, 1995. **8**(4): p. 186-95.
135. Pinnagoda, J., et al., *The intra- and inter-individual variability and reliability of transepidermal water loss measurements.* Contact Dermatitis, 1989. **21**(4): p. 255-9.
136. Scott, R.C., et al., *A comparison of techniques for the measurement of transepidermal water loss.* Arch Dermatol Res, 1982. **274**(1-2): p. 57-64.
137. Pinnagoda, J., et al., *Guidelines for transepidermal water loss (TEWL) measurement. A report from the Standardization Group of the European Society of Contact Dermatitis.* Contact Dermatitis, 1990. **22**(3): p. 164-78.
138. Rawlings, A.V., *Ethnic skin types: are there differences in skin structure and function?* Int J Cosmet Sci, 2006. **28**(2): p. 79-93.
139. Rogiers, V., *EEMCO guidance for the assessment of transepidermal water loss in cosmetic sciences.* Skin Pharmacol Appl Skin Physiol, 2001. **14**(2): p. 117-28.
140. Rawlings, A., et al., *The effect of glycerol and humidity on desmosome degradation in stratum corneum.* Arch Dermatol Res, 1995. **287**(5): p. 457-64.
141. Chrit, L., et al., *An in vivo randomized study of human skin moisturization by a new confocal Raman fiber-optic microprobe: assessment of a glycerol-based hydration cream.* Skin Pharmacol Physiol, 2006. **19**(4): p. 207-15.
142. Tupker, R.A., et al., *Susceptibility to irritants: role of barrier function, skin dryness and history of atopic dermatitis.* Br J Dermatol, 1990. **123**(2): p. 199-205.
143. Verdier-Sevrain, S. and F. Bonte, *Skin hydration: a review on its molecular mechanisms.* J Cosmet Dermatol, 2007. **6**(2): p. 75-82.
144. Berardesca, E., *EEMCO guidance for the assessment of stratum corneum hydration: electrical methods.* Skin Res Technol, 1997. **3**(2): p. 126-132.
145. Breternitz, M., et al., *Acute barrier disruption by adhesive tapes is influenced by pressure, time and anatomical location: integrity and cohesion assessed by sequential tape stripping. A randomized, controlled study.* Br J Dermatol, 2007. **156**(2): p. 231-40.

146. Ghadially, R., et al., *The aged epidermal permeability barrier. Structural, functional, and lipid biochemical abnormalities in humans and a senescent murine model.* J Clin Invest, 1995. **95**(5): p. 2281-90.
147. Yosipovitch, G., et al., *Skin barrier structure and function and their relationship to pruritus in end-stage renal disease.* Nephrol Dial Transplant, 2007. **22**(11): p. 3268-72.
148. Fluhr, J.W., et al., *Additive impairment of the barrier function by mechanical irritation, occlusion and sodium lauryl sulphate in vivo.* Br J Dermatol, 2005. **153**(1): p. 125-31.
149. Bommannan, D., R.O. Potts, and R.H. Guy, *Examination of stratum corneum barrier function in vivo by infrared spectroscopy.* J Invest Dermatol, 1990. **95**(4): p. 403-8.
150. Higo, N., et al., *Validation of reflectance infrared spectroscopy as a quantitative method to measure percutaneous absorption in vivo.* Pharm Res, 1993. **10**(10): p. 1500-6.
151. Lotte, C., et al., *Racial differences in the in vivo percutaneous absorption of some organic compounds: a comparison between black, Caucasian and Asian subjects.* Arch Dermatol Res, 1993. **284**(8): p. 456-9.
152. Pershing, L.K., et al., *Feasibility of measuring the bioavailability of topical betamethasone dipropionate in commercial formulations using drug content in skin and a skin blanching bioassay.* Pharm Res, 1992. **9**(1): p. 45-51.
153. Rougier, A., et al., *Regional variation in percutaneous absorption in man: measurement by the stripping method.* Arch Dermatol Res, 1986. **278**(6): p. 465-9.
154. Tojo, K. and A.C. Lee, *A method for predicting steady-state rate of skin penetration in vivo.* J Invest Dermatol, 1989. **92**(1): p. 105-8.
155. Escobar-Chavez, J.J., D. Quintanar-Guerrero, and A. Ganem-Quintanar, *In vivo skin permeation of sodium naproxen formulated in pluronic F-127 gels: effect of Azone and Transcutol.* Drug Dev Ind Pharm, 2005. **31**(4-5): p. 447-54.
156. van der Valk, P.G. and H.I. Maibach, *A functional study of the skin barrier to evaporative water loss by means of repeated cellophane-tape stripping.* Clin Exp Dermatol, 1990. **15**(3): p. 180-2.
157. Kalia, Y.N., F. Pirot, and R.H. Guy, *Homogeneous transport in a heterogeneous membrane: water diffusion across human stratum corneum in vivo.* Biophys J, 1996. **71**(5): p. 2692-700.
158. Fluhr, J.W., et al., *Testing for irritation with a multifactorial approach: comparison of eight non-invasive measuring techniques on five different irritation types.* Br J Dermatol, 2001. **145**(5): p. 696-703.
159. Hostynek, J.J., et al., *Human stratum corneum penetration by nickel. In vivo study of depth distribution after occlusive application of the metal as powder.* Acta Derm Venereol Suppl (Stockh), 2001(212): p. 5-10.
160. Lademann, J., et al., *Investigation of follicular penetration of topically applied substances.* Skin Pharmacol Appl Skin Physiol, 2001. **14 Suppl 1**: p. 17-22.

161. Sheth, N.V., M.B. McKeough, and S.L. Spruance, *Measurement of the stratum corneum drug reservoir to predict the therapeutic efficacy of topical iododeoxyuridine for herpes simplex virus infection.* J Invest Dermatol, 1987. **89**(6): p. 598-602.
162. Wilhelm, K.P., C. Surber, and H.I. Maibach, *Effect of sodium lauryl sulfate-induced skin irritation on in vivo percutaneous penetration of four drugs.* J Invest Dermatol, 1991. **97**(5): p. 927-32.
163. Pechere, M., et al., *Malassezia spp carriage in patients with seborrheic dermatitis.* J Dermatol, 1999. **26**(9): p. 558-61.
164. Pechere, M., et al., *A simple quantitative culture of Malassezia spp. in HIV-positive persons.* Dermatology, 1995. **191**(4): p. 348-9.
165. Nangia, A., et al., *Influence of skin irritants on percutaneous absorption.* Pharm Res, 1993. **10**(12): p. 1756-9.
166. van Voorst Vader, P.C., et al., *Patch tests with house dust mite antigens in atopic dermatitis patients: methodological problems.* Acta Derm Venereol, 1991. **71**(4): p. 301-5.
167. Surakka, J., et al., *A method for measuring dermal exposure to multifunctional acrylates.* J Environ Monit, 1999. **1**(6): p. 533-40.
168. Kondo, H., Y. Ichikawa, and G. Imokawa, *Percutaneous sensitization with allergens through barrier-disrupted skin elicits a Th2-dominant cytokine response.* Eur J Immunol, 1998. **28**(3): p. 769-79.
169. Fluhr, J.W., et al., *Glycerol accelerates recovery of barrier function in vivo.* Acta Derm Venereol, 1999. **79**(6): p. 418-21.
170. Blank, I.H., *Further observations on factors which influence the water content of the stratum corneum.* J Invest Dermatol, 1953. **21**(4): p. 259-71.
171. Reed, J.T., R. Ghadially, and P.M. Elias, *Skin type, but neither race nor gender, influence epidermal permeability barrier function.* Arch Dermatol, 1995. **131**(10): p. 1134-8.
172. Ohman, H. and A. Vahlquist, *In vivo studies concerning a pH gradient in human stratum corneum and upper epidermis.* Acta Derm Venereol, 1994. **74**(5): p. 375-9.
173. Dreher, F., et al., *Quantification of stratum corneum removal by adhesive tape stripping by total protein assay in 96-well microplates.* Skin Res Technol, 2005. **11**(2): p. 97-101.
174. Dreher, F., et al., *Colorimetric method for quantifying human Stratum corneum removed by adhesive-tape stripping.* Acta Derm Venereol, 1998. **78**(3): p. 186-9.
175. Bashir, S.J., et al., *Physical and physiological effects of stratum corneum tape stripping.* Skin Res Technol, 2001. **7**(1): p. 40-8.
176. Schwindt, D.A., et al., *Cumulative irritation in older and younger skin: a comparison.* Acta Derm Venereol, 1998. **78**(4): p. 279-83.
177. Halkier-Sorensen, L., et al., *Cutaneous barrier function after cold exposure in hairless mice: a model to demonstrate how cold interferes with barrier homeostasis among workers in the fish-processing industry.* Br J Dermatol, 1995. **132**(3): p. 391-401.

178. Fluhr, J.W., et al., *Sequential application of cold and sodium lauryl sulphate decreases irritation and barrier disruption in vivo in humans.* Br J Dermatol, 2005. **152**(4): p. 702-8.
179. Marttin, E., et al., *A critical comparison of methods to quantify stratum corneum removed by tape stripping.* Skin Pharmacol, 1996. **9**(1): p. 69-77.
180. Fenn, J.B., et al., *Electrospray ionization for mass spectrometry of large biomolecules.* Science, 1989. **246**(4926): p. 64-71.
181. Yamashita, M. and J.B. Fenn, *Negative ion production with the electrospray ion source.* J Phys Chem, 1984(88): p. 4671-4675.
182. Yamashita, M. and F. J.B., *Electrospray ion source. Another variation on the free-jet theme.* J Phys Chem, 1984. **88**: p. 4451-4459.
183. Karas, M. and F. Hillenkamp, *Laser desorption ionization of proteins with molecular masses exceeding 10,000 daltons.* Anal Chem, 1988. **60**(20): p. 2299-301.
184. Griffiths, W.J., et al., *Electrospray and tandem mass spectrometry in biochemistry.* Biochem J, 2001. **355**(Pt 3): p. 545-61.
185. Shevchenko, A., et al., *Mass spectrometric sequencing of proteins silver-stained polyacrylamide gels.* Anal Chem, 1996. **68**(5): p. 850-8.
186. Wilm, M., et al., *Femtomole sequencing of proteins from polyacrylamide gels by nano-electrospray mass spectrometry.* Nature, 1996. **379**(6564): p. 466-9.
187. Andren, P.E., et al., *Blood-brain barrier penetration of 3-aminopropyl-n-butylphosphinic acid (CGP 36742) in rat brain by microdialysis/mass spectrometry.* J Mass Spectrom, 1998. **33**(3): p. 281-7.
188. Domon, B. and R. Aebersold, *Mass spectrometry and protein analysis.* Science, 2006. **312**(5771): p. 212-7.
189. Karas, M., D. Bachmann, and F. Hillenkamp, *Influence of the wavelength in high-irradiance ultraviolet laser desorption mass spectrometry of organic molecules.* Anal Chem, 1985. **57**: p. 2935-9.
190. Knochenmuss, R., *A quantitative model of ultraviolet matrix-assisted laser desorption/ionization.* J Mass Spectrom, 2002. **37**(8): p. 867-77.
191. Karas, M. and R. Kruger, *Ion formation in MALDI: the cluster ionization mechanism.* Chem Rev, 2003. **103**(2): p. 427-40.
192. Dreisewerd, K., *The desorption process in MALDI.* Chem Rev, 2003. **103**(2): p. 395-426.
193. Knochenmuss, R. and R. Zenobi, *MALDI ionization: the role of in-plume processes.* Chem Rev, 2003. **103**(2): p. 441-52.
194. Hillenkamp, F. and J. Peter-Katalinic, *MALDI-MS: A practical guide to instrumentation, methods and applications*. 1 ed. 2007, Darmstadt: Wiley VCH. 362.
195. Hoffmann, E.d. and V. Stroobant, *Mass spectrometry: Principles and applications*. 3 ed. 2009, Chichester: John Wiley & Sons Ltd.
196. Zenobi, R. and R. Knochenmuss, *Ion formation in MALDI mass spectrometry.* Mass Spectrometry Reviews, 1998. **17**(5): p. 337-366.
197. Pan, C., et al., *Recent developments in methods and technology for analysis of biological samples by MALDI-TOF-MS.* Anal Bioanal Chem, 2007. **387**(1): p. 193-204.

198. Roepstorff, P., *MALDI-TOF mass spectrometry in protein chemistry.* EXS, 2000. **88**: p. 81-97.
199. Henzel, W.J., et al., *Identifying proteins from two-dimensional gels by molecular mass searching of peptide fragments in protein sequence databases.* Proc Natl Acad Sci U S A, 1993. **90**(11): p. 5011-5.
200. Mann, M., P. Hojrup, and P. Roepstorff, *Use of mass spectrometric molecular weight information to identify proteins in sequence databases.* Biol. Mass Spectrom., 1993. **22**: p. 338-345.
201. Pappin, D.J., P. Hojrup, and A.J. Bleasby, *Rapid identification of proteins by peptide-mass fingerprinting.* Curr Biol, 1993. **3**(6): p. 327-32.
202. James, P., et al., *Protein identification by mass profile fingerprinting.* Biochem Biophys Res Commun, 1993. **195**(1): p. 58-64.
203. Yates, J.R., 3rd, et al., *Peptide mass maps: a highly informative approach to protein identification.* Anal Biochem, 1993. **214**(2): p. 397-408.
204. Mann, M., C.K. Meng, and J.B. Fenn, *Interpreting mass spectra of multiply charged ions.* Anal Chem, 1989. **61**(15): p. 1702-1708.
205. Taylor, G.I., *The stability of horizontal fluid interface in a vertical electric field.* J Fluid Mech, 1965. **2**: p. 1-15.
206. Fernandez, M.J.d.l., *The fluid dynamics of Taylor cones.* J Annu Rev Fluid Mech, 2007. **39**: p. 217-243.
207. Cloupeau, M., *Recipes for use of EHD spraying in cone-jet mode and notes on corona discharge.* J Aerosol Sci, 1994. **25**: p. 1143-1157.
208. Cloupeau, M. and B. Prunet-Foch, *Electrohydrodynamic spraying functioning modes: A critical review.* J Aerosol Sci, 1994. **25**: p. 1021-1036.
209. Gaskell, S.J., *Electrospray: principles and practice.* J Mass Spectrom, 1997. **32**: p. 677-688.
210. Kebarle, P. and Y. Ho, *On the mechanism of electrospray mass spectrometry. In electrospray ionization mass spectrometry: Fundamentals, instrumentation and applications* ed. R.B. Eole. 1997, New York: John Wiley & Sons.
211. Iribarne, J.V. and B.A. Thomson, *On the evaporation of small ions from charged droplets.* J Chem Phys, 1976. **64**: p. 2287-2294.
212. Thomson, B.A. and J.V. Iribarne, *Field induced ion evaporation from liquid surfaces at atmospheric pressure.* J Chem Phys, 1979. **71**: p. 4451-4463.
213. Kebarle, P., *A brief overview of the present status of the mechanisms involved in electrospray mass spectrometry.* J Mass Spectrom, 2000. **35**(7): p. 804-17.
214. Tang, L. and P. Kebarle, *Effect of the conductivity of the electrosprayed solution on the electrospray current. Factors determining analyte sensitivity in electrospray mass spectrometry.* Anal Chem, 1991. **63**: p. 2709-2715.
215. Kebarle, P. and L. Tang, *From ions in solution to ions in the gas phase.* Anal Chem, 1993. **65**: p. 972A-986A.
216. Wilm, M. and M. Mann, *Electrospray and Taylor-cone theory: Dole's beam of macromolecules at last?* Int J Mass Spectrom Ion Processes, 1994. **136**: p. 167-180.

217. Kebarle, P. and U.H. Verberk, *Electrospray: From ions in solution to ions in the gas phase, what we know now.* Mass Spectrometry Reviews, 2009. **28**(6): p. 898-917.
218. Merchant, M. and S.R. Weinberger, *Recent advancements in surface-enhanced laser desorption/ionization-time of flight-mass spectrometry.* Electrophoresis, 2000. **21**(6): p. 1164-77.
219. Chen, Y.C., J. Shiea, and J. Sunner, *Thin-layer chromatography-mass spectrometry using activated carbon, surface-assisted laser desorption/ionization.* J Chromatogr A, 1998. **826**(1): p. 77-86.
220. Shen, Z., et al., *Porous silicon as a versatile platform for laser desorption/ionization mass spectrometry.* Anal Chem, 2001. **73**(3): p. 612-9.
221. Laiko, V.V., M.A. Baldwin, and A.L. Burlingame, *Atmospheric pressure matrix-assisted laser desorption/ionization mass spectrometry.* Anal Chem, 2000. **72**(4): p. 652-7.
222. Brown, R.S. and J.J. Lennon, *Mass resolution improvement by incorporation of pulsed ion extraction in a matrix-assisted laser desorption/ionization linear time-of-flight mass spectrometer.* Anal Chem, 1995. **67**(13): p. 1998-2003.
223. Kaufmann, R., B. Spengler, and F. Lutzenkirchen, *Mass spectrometric sequencing of linear peptides by product-ion analysis in a reflectron time-of-flight mass spectrometer using matrix-assisted laser desorption ionization.* Rapid Commun Mass Spectrom, 1993. **7**(10): p. 902-10.
224. Paul, W. and H. Steinwedel, *Apparatus for Separating Charged Particles of Different Specific Charges*. 1960: German Patent 944,900,1956, US Patent 2,939,952.
225. Stafford, J., et al., *Recent improvements in and analytical applications of advanced ion trap technology.* Int J Mass Spectrom Ion Processes, 1984. **60**(1): p. 85-98.
226. Yoshinari, K., *Theoretical and numerical analysis of the behavior of ions injected into a quadrupole ion trap mass spectrometer.* Rapid Commun Mass Spectrom, 2000. **14**(4): p. 215-23.
227. Bruker-Daltonik, *HCT Series User Manual Version 1.3*. 2008.
228. Cooks, R.G., et al., *Metastable ions*. 1973, Amsterdam: Elsevier.
229. Johnson, R.S., et al., *Novel fragmentation process of peptides by collision-induced decomposition in a tandem mass spectrometer: differentiation of leucine and isoleucine.* Anal Chem, 1987. **59**(21): p. 2621-5.
230. Roepstorff, P. and J. Fohlman, *Proposal for a common nomenclature for sequence ions in mass spectra of peptides.* Biomed Mass Spectrom, 1984. **11**(11): p. 601.
231. Yates, J.R., 3rd, *Mass spectrometry and the age of the proteome.* J Mass Spectrom, 1998. **33**(1): p. 1-19.
232. Patterson, S.D. and R. Aebersold, *Mass spectrometric approaches for the identification of gel-separated proteins.* Electrophoresis, 1995. **16**(10): p. 1791-814.
233. Biemann, K., *Contributions of mass spectrometry to peptide and protein structure.* Biomed Environ Mass Spectrom, 1988. **16**(1-12): p. 99-111.

234. Wells, J.M. and S.A. McLuckey, *Collision-induced dissociation (CID) of peptides and proteins.* Methods Enzymol, 2005. **402**: p. 148-85.
235. Aebersold, R. and D.R. Goodlett, *Mass spectrometry in proteomics.* Chem Rev, 2001. **101**(2): p. 269-95.
236. Faull, P., *Exploring Gas-Phase Protein Conformations by Ion Mobility-Mass Spectrometry*. 2009, PhD Thesis The University of Edinburgh.
237. Dancik, V., et al., *De novo peptide sequencing via tandem mass spectrometry.* J Comput Biol, 1999. **6**(3-4): p. 327-42.
238. Steen, H. and M. Mann, *The ABC's (and XYZ's) of peptide sequencing.* Nat Rev Mol Cell Biol, 2004. **5**(9): p. 699-711.
239. Brent, R., *Genomic biology.* Cell, 2000. **100**(1): p. 169-83.
240. Mortz, E., et al., *Sequence tag identification of intact proteins by matching tanden mass spectral data against sequence data bases.* Proc Natl Acad Sci U S A, 1996. **93**(16): p. 8264-7.
241. Mann, M. and M. Wilm, *Error-tolerant identification of peptides in sequence databases by peptide sequence tags.* Anal Chem, 1994. **66**(24): p. 4390-9.
242. Aalto-Korte, K., *Improvement of skin barrier function during treatment of atopic dermatitis.* J Am Acad Dermatol, 1995. **33**(6): p. 969-72.
243. Hubiche, T., et al., *Analysis of SPINK 5, KLK 7 and FLG genotypes in a French atopic dermatitis cohort.* Acta Derm Venereol, 2007. **87**(6): p. 499-505.
244. Nemoto-Hasebe, I., et al., *Clinical severity correlates with impaired barrier in filaggrin-related eczema.* J Invest Dermatol, 2009. **129**(3): p. 682-9.
245. James, P.E., *Proteome Research: Mass Spectrometry*. 2001: Springer-Verlag Berlin Heidelbeberg.
246. Williams, H.C., et al., *Validation of the U.K. diagnostic criteria for atopic dermatitis in a population setting. U.K. Diagnostic Criteria for Atopic Dermatitis Working Party.* Br J Dermatol, 1996. **135**(1): p. 12-7.
247. Berth-Jones, J., *Six area, six sign atopic dermatitis (SASSAD) severity score: a simple system for monitoring disease activity in atopic dermatitis.* Br J Dermatol, 1996. **135 Suppl 48**: p. 25-30.
248. Brown, S.J., et al., *Loss-of-function variants in the filaggrin gene are a significant risk factor for peanut allergy.* J Allergy Clin Immunol, 2011. **127**(3): p. 661-7.
249. Sergeant, A., et al., *Heterozygous null alleles in filaggrin contribute to clinical dry skin in young adults and the elderly.* J Invest Dermatol, 2009. **129**(4): p. 1042-5.
250. Loffler, H., F. Dreher, and H.I. Maibach, *Stratum corneum adhesive tape stripping: influence of anatomical site, application pressure, duration and removal.* Br J Dermatol, 2004. **151**(4): p. 746-52.
251. Thulin, C.D., J.A. Taylor, and K.A. Walsh, *Microheterogeneity of human filaggrin: analysis of a complex peptide mixture using mass spectrometry.* Protein Sci, 1996. **5**(6): p. 1157-64.
252. Simon, M., et al., *The cytokeratin filament-aggregating protein filaggrin is the target of the so-called "antikeratin antibodies," autoantibodies specific for rheumatoid arthritis.* J Clin Invest, 1993. **92**(3): p. 1387-93.

253. Thulin, C.D. and K.A. Walsh, *Identification of the amino terminus of human filaggrin using differential LC/MS techniques: implications for profilaggrin processing.* Biochemistry, 1995. **34**(27): p. 8687-92.
254. Steinert, P.M., et al., *In vitro assembly of homopolymer and copolymer filaments from intermediate filament subunits of muscle and fibroblastic cells.* Proc Natl Acad Sci U S A, 1981. **78**(6): p. 3692-6.
255. Sandilands, A., et al., *Filaggrin in the frontline: role in skin barrier function and disease.* J Cell Sci, 2009. **122**(Pt 9): p. 1285-94.
256. Leung, D.Y., et al., *New insights into atopic dermatitis.* J Clin Invest, 2004. **113**(5): p. 651-7.
257. Fluhr, J.W., et al., *Impact of anatomical location on barrier recovery, surface pH and stratum corneum hydration after acute barrier disruption.* Br J Dermatol, 2002. **146**(5): p. 770-6.
258. Resing, K.A., R.S. Johnson, and K.A. Walsh, *Mass spectrometric analysis of 21 phosphorylation sites in the internal repeat of rat profilaggrin, precursor of an intermediate filament associated protein.* Biochemistry, 1995. **34**(29): p. 9477-87.
259. Feltkamp, T.E., et al., *Interlaboratory variability of the antiperinuclear factor (APF) test for rheumatoid arthritis.* Clin Exp Rheumatol, 1993. **11**(1): p. 57-9.
260. Palosuo, T., et al., *Purification of filaggrin from human epidermis and measurement of antifilaggrin autoantibodies in sera from patients with rheumatoid arthritis by an enzyme-linked immunosorbent assay.* Int Arch Allergy Immunol, 1998. **115**(4): p. 294-302.